



**FACULTY OF ELECTRICAL ENGINEERING
UNIVERSITI TEKNIKAL MALAYSIA MELAKA**



**FINAL YEAR
PROJECT REPORT (FYP 2)**

اونيورسيتي تيكنيكل مليسيا ملاك

UNIVERSITI TEKNIKAL MALAYSIA MELAKA

**TWO-LINK MUSCULOSKELETAL STRUCTURE
WORKSPACE FORCE CONTROL**

Muhamad Yusazlan Bin Yusof

Bachelor of Mechatronics Engineering

Jun 2014

SUPERVISOR ENDORSEMENT

“I hereby declare that I have read through this report entitle “Two-Link Musculoskeletal Structure Workspace Force Control” and found that it has comply the partial fulfillment for awarding the degree of Bachelor of Electrical Engineering (Mechatronics Engineering)”

Signature :
اونيزرسي تيكنيكل مليسيا ملاك

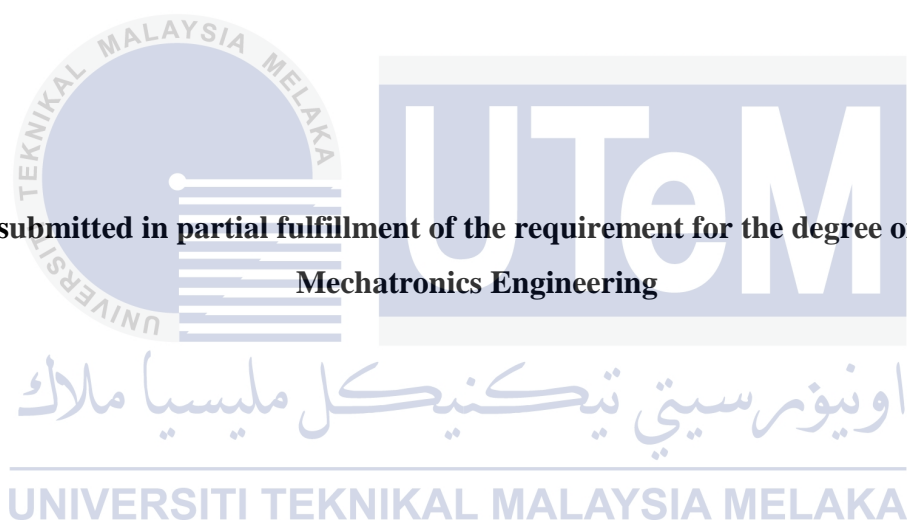
Supervisor's Name :
UNIVERSITI TEKNIKAL MALAYSIA MELAKA

Date :

**TWO-LINK MUSCULOSKELETAL STRUCTURE
WORKSPACE FORCE CONTROL**

MUHAMAD YUSAZLAN BIIN YUSOF

**A report submitted in partial fulfillment of the requirement for the degree of Bachelor in
Mechatronics Engineering**



**Faculty of Electrical Engineering
UNIVERSITI TEKNIKAL MALAYSIA MELAKA**

2013/2014

“I declare this report entitle “Two-Link Musculoskeletal Structure Workspace Force Control” is the result of my own research except as cited in the references. The report has been not accepted for any degree and is not concurrently submitted in candidature of any other degree”

Signature :
اونيورسيٲى ٲيكنيكل ماليسيا ملاك

Name :
UNIVERSITI TEKNIKAL MALAYSIA MELAKA

Date :

ACKNOWLEDGEMENT

I am grateful and would like to express my sincere gratitude to my supervisor Dr. Ahmad Zaki Hj Shukor for his invaluable guidance, continuous encouragement and constant support in making this research possible. I really appreciate his guidance from the initial to the final level that enabled me to develop an understanding of this research thoroughly. Without his advice and assistance it would be a lot tougher to completion. I also sincerely thank him for the time spent proofreading and correcting my mistakes.

My sincere thanks go to all lecturers and members of the staff of the Electrical Engineering Department, UTeM, who helped me in many ways and made my education journey at UTeM pleasant and unforgettable. Many thanks go to my entire class member for their excellent co-operation, inspirations and supports during this study. This four year experience with all you guys will be remembered as important memory for me.

I acknowledge my sincere indebtedness and gratitude to my parents for their love, dream and sacrifice throughout my life. I am really thankful for their sacrifice, patience, and understanding that were inevitable to make this work possible. Their sacrifice had inspired me from the day I learned how to read and write until what I have become now. I cannot find the appropriate words that could properly describe my appreciation for their devotion, support and faith in my ability to achieve my dreams.

Lastly I would like to thanks any person which contributes to my final year project directly on indirectly. I would like to acknowledge their comments and suggestions, which was crucial for the successful completion of this study.

ABSTRACT

This project presents the force control for two-link musculoskeletal manipulator modeling where force control had been used to control the force at end-effectors while end effector of the manipulator touching the environment. Proper force control algorithm for two-link musculoskeletal manipulator had been developed and simulated by using a robotic dynamics simulator. All the kinematic and dynamic properties are shown to address the presence of environmental contact with the manipulator. From this contact, the force control algorithm were explored, by comparing the performance of the manipulator in term of settling time and accuracy when different force references have been given. Force control algorithm were divided into two types which is independent muscle control and end effector muscle control. The results for independent muscle control show the increment of force references will make the force applied to the end effector and muscles increased. Meanwhile, for end effector muscle control, the result shows the maximum force applied to the manipulator increased if the reference forces increased but through this it will also improve the settling time of force that had been applied to each muscles in the manipulator.

ABSTRAK

Projek ini membentangkan mengenai kawalan daya untuk model robot dua hubungan yang dipacu oleh penggerak selari yang bertindak sebagai otot kepada model robot. Di mana kawalan kuasa telah digunakan untuk mengawal daya pada pengesan hujung pengolah semasa pengesan hujung pengolah menyentuh alam sekitar. Algoritma kawalan daya yang betul untuk robot dua hubungan yang dipacu oleh penggerak selari telah dibangunkan dan disimulasikan dengan menggunakan simulator robot dinamik. Semua sifat-sifat kinematik dan dinamik ditunjukkan untuk menghubungkan kehadiran alam sekitar dengan pengolah. Dari hubungan ini, algoritma kawalan daya telah diteroka, dengan membandingkan prestasi model robot melalui tempoh masa dan ketepatan apabila rujukan kuasa yang berbeza telah diberikan. Algoritma kawalan daya telah dibahagikan kepada dua jenis iaitu kawalan otot bebas dan kawalan otot pengesan hujung pengolah. Keputusan menunjukkan kenaikan rujukan kuasa akan menjadikan daya yang dikenakan kepada pengesan hujung pengolah dan otot meningkat. Sementara itu, untuk kawalan otot pengesan hujung pengolah, keputusan menunjukkan daya maksimum digunakan untuk robot meningkat jika daya rujukan meningkat tetapi melalui ini ia juga akan menambah baik masa untuk setiap daya yang dikenakan pada otot menjadi stabil.

UNIVERSITI TEKNIKAL MALAYSIA MELAKA

TABLE OF CONTENTS

CHAPTER	TITLE	PAGE
	ACKNOWLEDGEMENT	iv
	ABSTRACT	v
	TABLE OF CONTENTS	vii
	LIST OF TABLE	xi
	LIST OF FIGURE	xiii
	LIST OF ABBREVIATIONS	xv
	LIST OF APPENDICES	xvi
1	INTRODUCTION	
	1.1 Introduction	1
	1.2 Motivation	1
	1.3 Problem Statement	2
	1.4 Objective	4
	1.5 Scope	5
	1.6 Organization of Report	5
2	LITERATURE REVIEW	
	2.1 Introduction	6
	2.2 Robot	6
	2.2.1 Industrial Robot	7

2.2.2 Rigid-Flexible Robot Manipulator	8
2.1.3 Musculoskeletal Robot Manipulator	9
2.3 Robot Simulation Modelling	10
2.4 Previous Research on Force Control For Robot Manipulator	11
2.5 Summary Of Review	15
2.6 Conclusion	16

3 METHODOLOGY

3.1 Introduction	17
3.2 Overall Process Flow of Project	18
3.3 Phase 1	
3.3.1 Step 1	19
3.3.2 Step 2	20
3.3.3 Step 3	21
3.3.4 Step 4	23
3.4 Phase 2	
3.4.1 Step 1	28
3.4.2 Step 2	29
3.4.3 Step 3	31
3.5 Phase 3	31
3.6 Reliability of Data	31

4 RESULT AND ANALYSIS

4.1 Introduction	33
4.2 Two-Link Musculoskeletal Manipulator Modelling	33

4.3	Force Control Algorithm	34
4.4	Simulation 1 (Independent Muscle Control)	
4.4.1	Simulation setup and Result	35
4.4.2	Comparison Between Same Type of Muscle With Different Type of Reference Forces	38
4.4.3	Synthesise of Data	43
4.4.4	Conclusion	45
4.5	Simulation 2 (End Effector Muscle Control)	
4.5.1	Simulation setup and Result	45
4.5.2	Comparison Between Same Type of Muscle With Different Type of Reference Forces	50
4.5.3	Conclusion	56
5	CONCLUSION AND RECOMMENDATION	
5.1	Introduction	57
5.2	Conclusion	57
5.3	Recommendation	58

REFERENCES	59
-------------------	-----------

APPENDICES

APPENDIX A	62
APPENDIX B	67
APPENDIX C	72
APPENDIX D	75
APPENDIX E	77

APPENDIX F	82
APPENDIX G	87
APPENDIX H	90
APPENDIX I	91
APPENDIX J	104



اونيورسيتي تیکنیکل ملیسیا ملاک

UNIVERSITI TEKNIKAL MALAYSIA MELAKA

LIST OF TABLE

TABLE	TITLE	PAGE
2.1	Synthesise of data from previous research	15
3.1	Research variables description	22
3.2	Differentiation of trigonometric functions	28
4.1	Simulation 1 maximum and minimum force at end effector (X-direction)	41
4.2	Simulation 1 maximum and minimum force at end effector (Y-direction)	42
4.3	Simulation 1 settling time (muscles)	43
4.4	Simulation 1 settling time (end effector)	44
4.5	Simulation 1 final force applied to muscles	44
4.6	Simulation 2 maximum and minimum shoulder mono-articular muscle force (F_{lm1})	47
4.7	Simulation 2 maximum and minimum elbow mono-articular muscle force (F_{lm2})	48
4.8	Simulation 2 maximum and minimum biar-articular muscle force (F_{lm3})	49
4.9	Simulation 2 maximum and minimum end effector in X-direction force (F_{endx})	49
4.10	Simulation 2 maximum and minimum end effector in Y-direction force (F_{endy})	50
4.11	Simulation 2 settling time and final force value for shoulder mono-articular muscle	52

4.12	Simulation 2 settling time and final force value for elbow mono-articular muscle	53
4.13	Simulation 2 settling time and final force value for biar-articular muscle	55



LIST OF FIGURES

FIGURE	TITLE	PAGE
1.1	3 Link robot with variables	3
2.1	KUKA KR 210	7
2.2	Two-link rigid flexible manipulator with tip mass sketch	8
2.3	Musculoskeletal robot manipulator system based on human arm	9
2.4	Two-link lab-scale FSMM	11
2.5	Two-link parallel manipulator	12
2.6	Sketch of biar-articular structure	14
2.7	Spiral motor illustration	14
3.1	Research Methodology	18
3.2	Mono-Articular Biar-Articular Link Constraint	19
3.3	ROCOS environment	20
3.4	Conceptual design of the research	21
3.5	Parameter declaration	23
3.6	Contact point declaration	24
3.7	Contact point for polygon L1	25
3.8	Centre of gravity declaration	25
3.9	Polygon centre of gravity declaration	26

3.10	Polygon data declaration	27
3.11	Robot manipulator force direction	32
3.12	Robot manipulator ideal and actual force direction	32
4.1	Two link musculoskeletal manipulator modelling	33
4.2	Force control block diagram for biar-articular manipulator	34
4.3	Sample of simulation 1 muscles force result	36
4.4	Sample of simulation 1 end effector force result	37
4.5	Simulation 1 all shoulder mono-articular muscle force (F_{lm1})	38
4.6	Simulation 1 all elbow mono-articular muscle force (F_{lm2})	39
4.7	Simulation 1 all biar-articular muscle force (F_{lm3})	40
4.8	Simulation 1 all end effector force (X-direction)	40
4.9	Simulation 1 all end effector forces (Y-direction)	42
4.10	Sample of simulation 2 muscles force result	46
4.11	Sample of simulation 2 end effector force result	47
4.12	Simulation 2 all shoulder mono-articular muscle force (F_{lm1})	51
4.13	Simulation 2 all elbow mono-articular muscle force (F_{lm2})	53
4.14	Simulation 2 all biar-articular muscle force (F_{lm3})	54
4.15	Simulation 2 all end effector forces (Y-direction)	55

LIST OF SYMBOLS

l_{m1}	-	Shoulder mono-articular muscle
l_{m2}	-	Elbow mono-articular muscle
l_{m3}	-	Biar-articular muscle
F_{lm1}	-	Force applied at shoulder mono-articular muscle
F_{lm2}	-	Force applied at elbow mono-articular muscle
F_{lm3}	-	Force applied at biar-articular muscle
F_{endy}	-	Force applied at end effector in y-direction
F_{endx}	-	Force applied at end effector in x-direction
F_{ref}	-	Force reference at muscle
$F_{ref(endy)}$	-	Force reference at end effector in y-direction
$F_{ref(endx)}$	-	Force reference at end effector in x-direction
t	-	Time
s	-	Second
N	-	Newton

LIST OF APPENDICES

APPENDIX	TITLE	PAGE
A	Simulation 1 muscle force results	
B	Simulation 1 end effector force results	
C	Simulation 1 muscle comparison results	
D	Simulation 1 end effector comparison results	
E	Simulation 2 muscle force results	
F	Simulation 2 end effector force results	
G	Simulation 2 muscle comparison results	
H	Simulation 2 end effector comparison results	
I	Two-link musculoskeletal manipulator modelling coding	
J	Force control algorithm coding	

CHAPTER 1

INTRODUCTION

1.1 Introduction

In this chapter, the purpose of this research will be described. Begin with the current issues in the real world environment and then the problem statement for this research will be translated. The objectives of the research are made to overcome the problem statement. The scopes of the research are defined to make the limitation of the research.

1.2 Motivation

Nowadays, robot have been widely used in industrial environment because it capability to do work that dangerous to human. Moreover, robot can do task without getting tired. With this, the production of the product will be more consistent and the quality of the product will be improved. This is proven by Robotics Industries Association (RIA) where the overall industrial robot order from all over the world was increased by 49 percent during 2005. Most of the order was coming from Asian nation such as China, Malaysia, Philippines, Indonesia, Singapore and India with about 125 percent of industrial robot order [21]. For example, the plant at PROTON SDN. BHD. TANJUNG MALIM operate on 60 percent automation with a total of 180 robots, of which 138 units are employed in the Body Shop, 31 units in the Paint Shop and 11 units in the Trim & Final Assembly. Overall automation levels of each shop are body 60%, Painting 32% and final assembly 2% [1].

Generally, most industrial robot use position control scheme to control the robot

movement. Theoretically, the position control scheme is a method of control where the robot tool follows a prescribed trajectory in space which has been pre-programmed or “taught” before run-time. However, for some applications, it is more important to precisely control the force applied by end-effectors rather than controlling the robots positioning to produce a better product. Furthermore, by using position controlled robot system in industry will endanger humans or objects surrounding it during operation. This is because when position control scheme is being used, the robot will follow the instruction in the program until it completes its task regardless of its surrounding. This can cause injury or harm to anything within its working space.

This have proven when there are workplace accident in 2009 at Golden State Foods bakery in California that caused by worker’s lack of precaution. According to the inspection report. “At approximately 7:55 a.m. on July 21, 2009, Employee #1 was operating a robotic palletizer for Golden State Foods, Inc., a food processor and packager for fast food restaurants. She entered the caged robotic palletizer cell while the robotic palletizer was running. She had not de-energized the equipment. Her torso was crushed by the arms of the robotic palletizer as it attempted to pick up boxes on the roller conveyor. She was killed.” [21].

Lately, researches focus on new methods to control the robot which is force control method. Through this method, the problem that was caused by position control method can be solved. However, force control method is still new and has many shortages in terms of robot control static and dynamic characteristics. Because of this problem, the force control method is still on early development and not widely used in industrial environment.

1.3 Problem Statement

Generally, force control scheme is a method where force at end-effectors is being controlled and this will decide its next movement, either it need to stop, continue, or do next task that have programmed to the robot. To make the robot works perfectly, the robot controller algorithm for force control method is more complex compared to the position control method.

This is because by using force control method, it will consider the surrounding environment before the controller makes decision on the robots next move. Compared to position control method, it only considers the position on the end-effectors of the robot without considering the surrounding environment. So, the complex controller needs to be developed to make sure the robot work perfectly and is safe to its surrounding.

Furthermore, to make a force control method work, there are several important variables that need to be considered. One of the important variables is the force axis that applies to the robot end-effector. This can be either or a combination of X-axis, Y-axis and Z-axis if the robot is modelled in 3 Dimensions. Other important variable for the robot to function well is the rotational angle or displacement of the joint compared to the previous joint. For example, if the robot is two-link robot and have two degree of freedom, there are two angles that need to be considered which is the rotational angles or displacement between base of the robot and first joint of the robot, and rotational angles or displacement between first and second joint of the robot. Figure 1.0 show the three link robot with it variables.

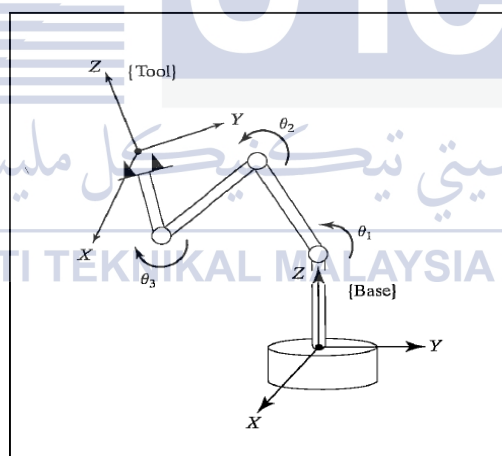


Figure 1.1: 3 Link robot with variables [22]

Lastly, to develop the force control method it requires the fundamental engineering knowledge. One of the engineering knowledge that needs to be considered is the mathematical relations between torque and forces. This fundamental knowledge is important where it will be used to determine the force at muscle and end-effectors. Knowledge on torque is needed to determine the torque that will be applied to each joint. Virtual work theory also needs to be

considered because the purpose of force control method is to use it for industrial environment and household. Thus, the specific force control algorithm needs to be developed to make sure the robot can work properly.

In response to this problem, this research purpose is to study and develop the way to control the robot by using force control. This research will also consider the performance of the robot when using force control method.

1.4 Objective

The objectives were refined and developed to be more specific achievable. As such, these achievable objectives for this research are:

1. To design two-link musculoskeletal manipulator driven by linear actuator using robotics dynamics simulator.
2. To derive force control algorithm based on virtual work principle and simulate two-link musculoskeletal manipulator with force control algorithm using robotics dynamics simulator.
3. To analyse and compare the relationship between speed and accuracy from force control data in term of force tracking.

1.5 Scope

Research scope are the limitations for each research that have been conduct. One of the scope for this research is the modelling of two-link musculoskeletal will be represented in the form of two dimension modelling. This two-link musculoskeletal manipulator will be modelling in rigid form two-link manipulator and the length of each arm joint will be 0.4m.

Another scope that have been set for this research is the centrifugal/coriolis force (C terms) is being neglect and force that will be apply to the linear actuator and end-effector of the robot will be in range of 0 Newton to 100 Newton. This tracking force is applied to the end-effectors of the manipulator, where the direction of the force is considered in one direction only.

Lastly, this research will conduct using robot software simulator which is ROCOS software, where the time taken for the robot manipulator end-effector to achieve the desired force when it make a contact with the wall will be considered. Other than that, this research also will consider the accuracy of the robot manipulator to maintain the desired force at end-effector when it make a contact with the wall.

1.6 Organization of Report

This report is organized as follows; Chapter 2 describes about the literature review where some of previous work that related to this research have been review. Chapter 3 is a methodology for the research. In this chapter, the method to complete this research have been described. Chapter 4 is mention about the result and analysis for this research where it show the result from the independent muscle control and end effector muscle control simulation. Lastly, chapter 5 is described about the conclusion and recommendation for this research.

CHAPTER 2

LITERATURE REVIEW

2.1 Introduction

This chapter will provide the review from previous research that is related to this research. There are previous researches on force control robot manipulator using different controller type and experiment design to obtain the accurate and fast settling time force at robot end-effectors. Other than that, the industrial robot, rigid-flexible manipulator, musculoskeletal manipulator and robotic experiment are discussed in this chapter.

2.2 Robot

There are plenty type of robot have been proposed by researcher to test and improved the robot performance by applied force control method. Some of research was applied to actual robot and some of research was on robot manipulator. Some of robot type that have been proposed by researcher is:

- Industrial robot.
- Rigid-flexible robot manipulator.
- Musculoskeletal robot manipulator.

2.2.1 Industrial Robot

Industrial robot as defined by ISO 8373 is an automatically controlled, reprogrammable, multipurpose manipulator programmable in three or more axes, which may be either fixed in place or mobile for use in industrial automation applications.

One of the common industrial robot that have been widely use in research is KUKA robot. Basically, KUKA is derived from the initial letters of the company name “Keller und Knappich Augsburg” where this company is focusing in develop and produce an automation industrial robot [2].

Nowadays, KUKA company already have develop many industrial robot for many industry sector such as automotive manufactures, food and beverages, rubber and plastics, metal products, automotive suppliers, wood and furniture, and lastly foundry sector[2]. One research that have been done by [3] is using a 6 DOF KUKA KR210 industrial robot with an ATI DELTA force sensor. 6 DOF KUKA KR210 is a industrial robot arm with high payload and often used for grinding purpose [2].



Figure 2.1: KUKA KR 210 [2]

2.2.2 Rigid-Flexible Robot Manipulator

Rigid is a characteristic of the object that enables the object to can't bend or be forced out of shape. While, flexible is a contrast characteristic of object with rigid, where it allow the object to bend or change shape. So, the rigid-flexible robot manipulator is a combination of one link of joint with rigid arm and one link of joint with flexible arm where this manipulator is a two-link manipulator. There are also a two-link manipulator that using a flexible actuator at the joint of arm one and two [4]. By using the rigid-flexible robot manipulator, the system performance can be affected with interaction between the joint motion and the angular motion of the constrained surface. Therefore, the better dynamic system performance is necessary so that the motion profiles can judge the surface rotation and the joint motion since there are two motions involved [5].

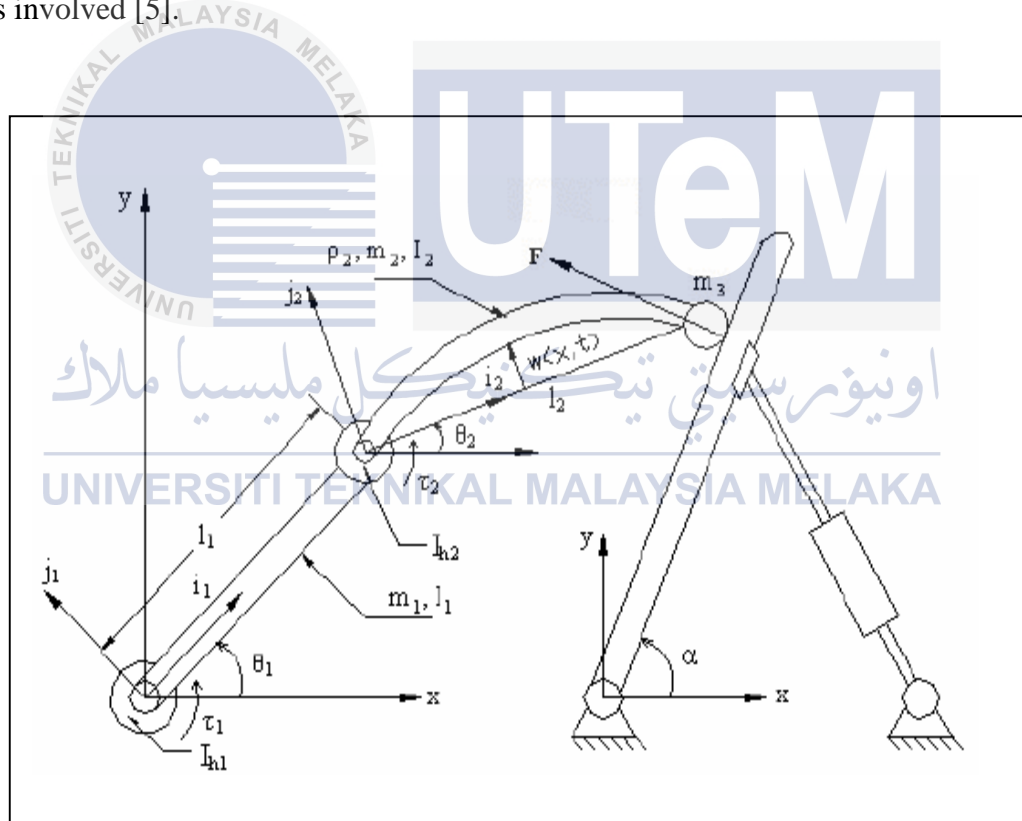


Figure 2.2: Two-link rigid flexible manipulator with tip mass sketch [5]

2.2.3 Musculoskeletal Robot Manipulator

Robotic system and application is rapidly grown and now many researcher have been focusing to develop a robot based on human body motion. This is because robots based on human body motion are much sophisticated compared with present robot [6]. [6-10] have been done research on musculoskeletal robot manipulator. Most of the research has been focusing to human arm robot because most all present robots are based on human arm.

According to [10], the musculoskeletal manipulator give faster responses in the independent muscle force control, reduced force overshoot in step force command and efficient force distribution in the end effectors step force commands and muscular viscoelasticity control compare to present robot.

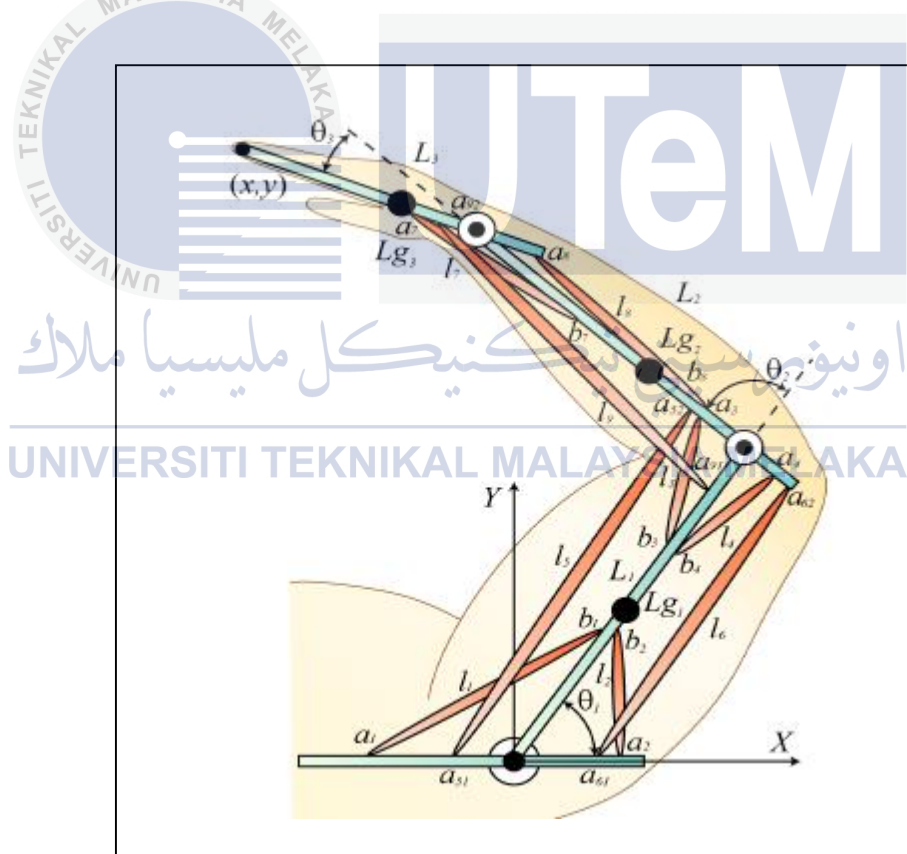


Figure 2.3: Musculoskeletal robot manipulator system based on human arm [7]

2.3 Robot Simulation Modelling

There are plenty ways to do research on robot such as simulation modelling and experiment setup on actual robot or robot manipulator. One most common and regularly uses for robotic research is by using simulation modelling. Simulation modelling is regularly uses for robotic research because it gives many benefits.

One benefit by using simulation modelling is it low barrier to entry which is mean by using simulation researcher able develop very interesting robots in short time. At the same time, it constrains researcher in ways similar to physical robots, so researcher can focus in something that can be realized [11]. Simulation modelling also can save cost of the research because simulation modelling doesn't need experiment setup. Moreover by using simulation modelling, researcher can get many type of data in short time with just change the variable in the modelling.

Solid Work and MATLAB/Simulink are one of common software that can be uses for simulation modelling. Solid Work is a 3 Dimensions mechanical Computer Aided-Design (CAD) program that runs on Microsoft Windows where it widely use to modelling design such as mechanical design and electrical design [12].

Meanwhile, MATLAB/Simulink is a numerical computing environment and fourth-generation programming language. MATLAB/Simulink is developed by Math Works, MATLAB allows matrix manipulations, plotting of functions and data, implementation of algorithms, creation of user interfaces, and interfacing with programs written in other languages, including C,C++,Java and Fortran [13]. This 2 software is needed to use together in order to complete a research where the MATLAB/Simulink is use for check the theory and Solid Work is use for robot motion simulation [14].

2.4 Previous Research on Force Control For Robot Manipulator

In order to modelling force control for robot manipulator, several methods had been used in previous research. *Theeraphong Wongratanaphisan (2009)* [15] has done analysis on robot robustness and propose the suitable force controller for the robot to performed contact tasks. For this purposes, [15] using a two-link flexible structure mounted manipulator (FSMM) as research modeling. FSMM is a robotic system that consists of a rigid manipulator mounted on a nonrigid supporting structure. Figure 2.4 show the robot manipulator that have been use by [15].

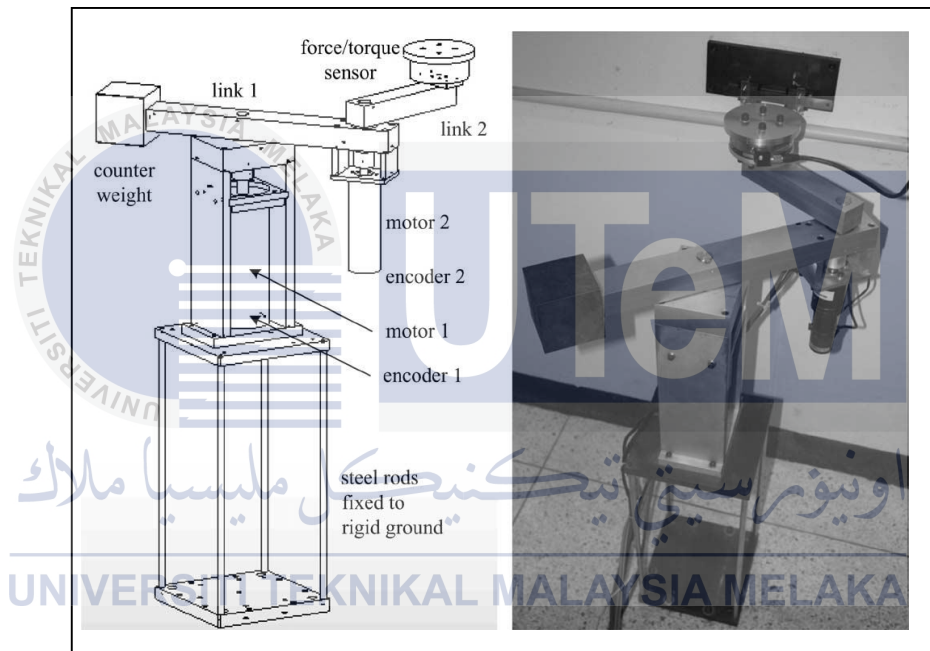


Figure 2.4: Two-link lab-scale FSMM[15]

The robust impedance control has been use by [15] as it forces controller system. By using robust impedance control, FSMM performed well on a two-link FSMM.

Ryo Kikuuwe (2008) [16] has designed a low-force robotic manipulator to guide a human user's movement to place a tool (or the user's hand) at a predetermined position or move it along a predetermined trajectory. Two-link Degree of Freedom (DOF) planar parallel manipulator was selected as robot modelling for [16] research. This two-link parallel manipulator is shown in Figure 2.5.

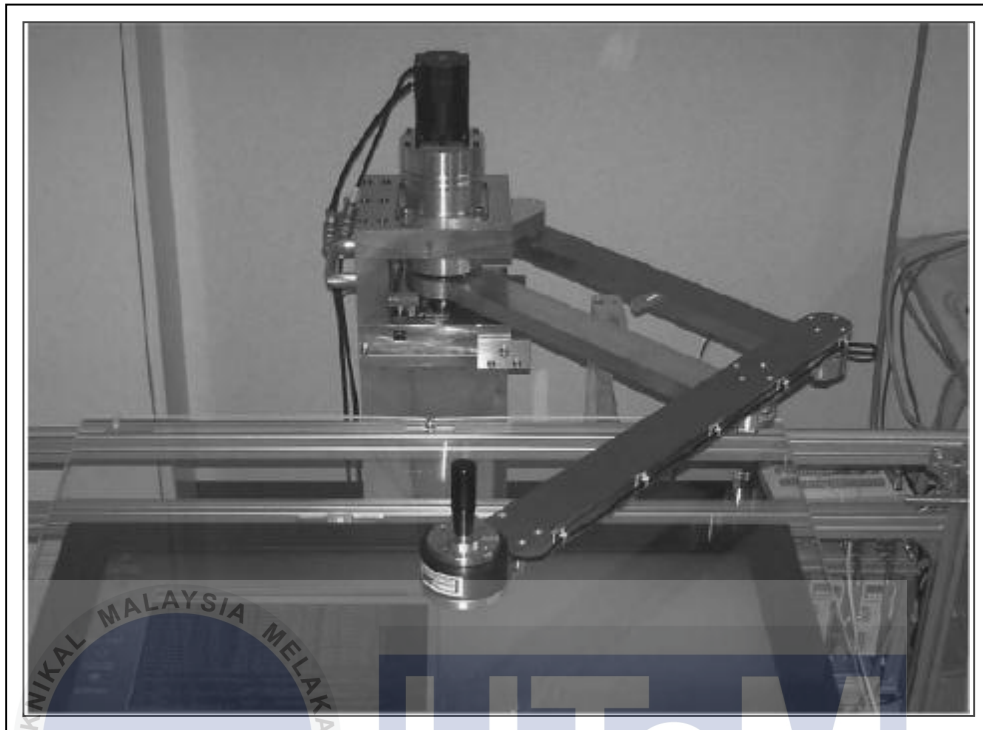


Figure 2.5: Two-link parallel manipulator [16]

In the beginning, this robot have been run using PD force control method but in final stage of this research, [16] change the controller from PD force controller into Proxy-Based Sliding Mode Control (PSMC) because PD force controller requires direct high-gain velocity feedback while [16] manipulator is a low force application. By using PSMC as a controller for [16] manipulator, it show the manipulator perform well with constant time 0.1 second compare to 0.01 second and 0.5 second in most cases.

Meanwhile, *Ye Bosheng (2012)* [17] has proposed an adaptive control method for a robot's end-effectors while slides steadily on an arbitrarily inclined panel. The robot modelling for [17] research is based on a 5-DOF industrial robot with a Wuhan company numerical control HNC-210B controller and a HSV-18 servo-drive as the hardware platform for the robot control system. The adaptive impedance control by using fuzzy control method is a controller that have been proposed by [17] for this manipulator to complete it task. As a result, the controller is compatible with the manipulator to perform the task.

In addition, paper written by **Nabil Zemiti (2010)** [18] has develop a suitable controller to control the force feedback of one robot manipulator. Kinematically Defective Manipulator (KDMs) is a robot manipulator that [18] has been try to develop a new force controller. KDMs are robot manipulators that have fewer joints than the dimension of the space in which their end-effectors moves. For this research, [18] used a MC²E (French acronym for compact manipulator for endoscopic surgery) as a modelling where this robot provides 4-DOF at the instrument tip. The damping control has been applied to the model and it show that the robot can't follow the reference force that have given by the controller.

Next, the paper written by **Rajni V. Patel (2009)** [19] has focusing to develop a controller to control the robust position and contact force control for robot arms. The Mitsubishi PA 10-7C is a robot that has been used by [19] as a modelling manipulator for the research. Mitsubishi PA 10-7C is a two-link robot with 7-DOF that been communicates with the servo controller of the Mitsubishi arm at a sampling rate of 333Hz over a pair of optical cables. The controller that has been develops by [19] for this research is impedance control scheme based on PD controller method. By applied this controller to Mitsubishi PA 10-7C, the force regulation for Mitsubishi PA 10-7C almost perfect if no motion on the surface.

Lastly, the paper written by **Ahmad Zaki (2013)** [20], it's mentioned about the force control of musculoskeletal manipulator driven by spiral motor. The purpose of the study is to develop a force control scheme for the musculoskeletal manipulator. The Biar-Articular structure is used as a manipulator modelling for this study. The Biar-Articular structure is design based on human arm where it consist a Mono-Articular and Biar-Articular muscle attached to certain points of the arm bones. Figure 2.6 show the design sketch of Biar-Articular structure for this study.

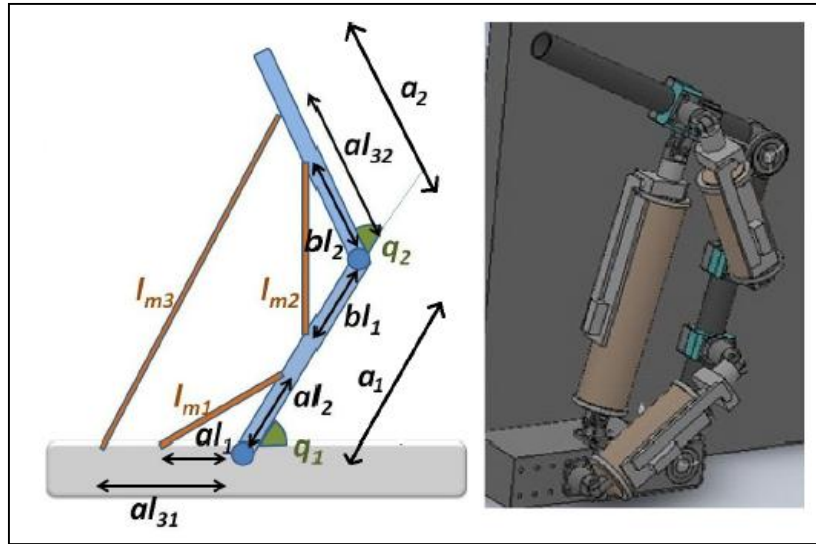


Figure 2.6: Sketch of biar-articular structure [20]

The spiral motor have been chosen by [20] as an actuator to drive the cylinder that act as a muscle for the manipulator. The spiral motor is a novel high thrust force actuator with high back drivability. The spiral motor consists of a helical structure mover and stator with permanent magnet. The mover moves spirally in the stator, and the linear motion is extracted to drive the load. Thus, the motor realizes direct drive motion. Moreover, the motor has high thrust-force characteristics because the flux is effectively utilized in its 3-D structure.

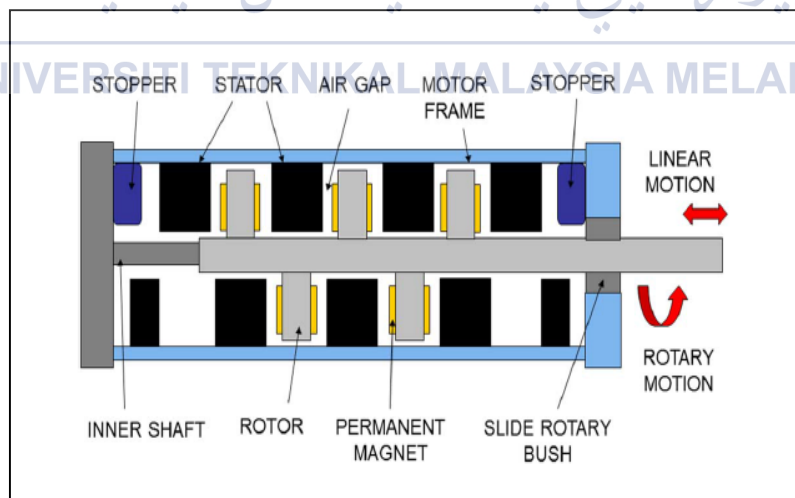


Figure 2.7: Spiral motor illustration [20]

The PD with Disturbance Observers (DOB) that designed in workspace and muscle-space is been used by [20] as the Biar-Articular manipulator controller and the Simulation on

Biar-Articular manipulator have been conducted. The force controls were simulated in three different schemes which is independent muscle control, step force command and muscular viscoelasticity control. Through the Simulation, the controller performed well with the manipulator and its show the Biar-Articular structure provided some significant advantages compare to present robot. The advantage of Biar-Articular manipulator were the faster responses in the independent muscle force control, reduced force overshoot in step force command and efficient force distribution (reduction of Mono-Articular muscle burden) in the end-effectors step force commands and muscular viscoelasticity control.

2.5 Summary of Review

Table 2.1: Synthesise of data from previous research

Author of Paper	[15]	[16]	[17]	[18]	[19]	[20]
Modelling Structure	2 -DOF	2-DOF	5-DOF	4-DOF	7-DOF	2-DOF
Modelling Controller	Impedance control	Sliding Mode	Fuzzy Logic	Pure damping and force control	PD	PD with DOB
Limitation of Tracking Force for End Effector	< 50 N	< 50N	< 2.5N	< 5N	< 25N	< 25N
Tracking Force Axis	X	X and Y	X,Y and Z	X,Y and Z	X,Y and Z	X and Y
Settling Time	< 2 sec	-	< 0.1sec	< 0.5sec	< 14sec	< 1sec

2.6 Conclusion

From all the previous research that have been review, there are many type of robot that been tested using force control scheme. Generally, there are two type of test for force control scheme that researcher focusing until now. The two type of test are the force tracking test and force reference test. The force tracking test is a test that focusing on how fast the time take for the robot to achieve the desired force while the force reference test is a test that focusing on how accurate the robot following the reference force that given by the user.

All the robot required a different force control scheme, where it depend on the robot structure and the desired movement by the user. Robot structure is a mechanical part of the robot such as the length of each robot joint, the type of actuator use to drive the robot and the design of the robot. Meanwhile, the desired movement by the user mean the movement of the robot according to the user desired where it can be prismatic movement (linear movement) or rotational movement. Mostly the robot movement is depending on the task that the robot will do.

According to the paper that have been review, it show the musculoskeletal robot manipulator give the best result for force control scheme test. This is because the musculoskeletal robot manipulator give a faster settling time which is less than 1 second for the force less than 25N by only using PD controller. However, the common robot manipulator also can achieve the faster settling time like musculoskeletal robot manipulator, but it need an advance controller system to achieve the same result such as Fuzzy Logic controller.

CHAPTER 3

METHODOLOGY

3.1 Introduction

This chapter will show the method that will apply in this research. Generally, there are 3 main phase of methodology to complete this research. The first phase to complete this research is to design two-link musculoskeletal manipulator driven by linear actuator using robotics dynamics simulator. The second phase of this research is to derive force control algorithm based on virtual work principle and simulate two-link musculoskeletal manipulator with force control algorithm using robotics dynamics simulator. The robotics dynamics simulator that been use for this research is ROCOS software. Lastly, the third phase which is about to analyse and compare the relationship between speed and accuracy from force control data in term of force tracking will be conducted to complete this research.

3.2 Overall Research Methodology

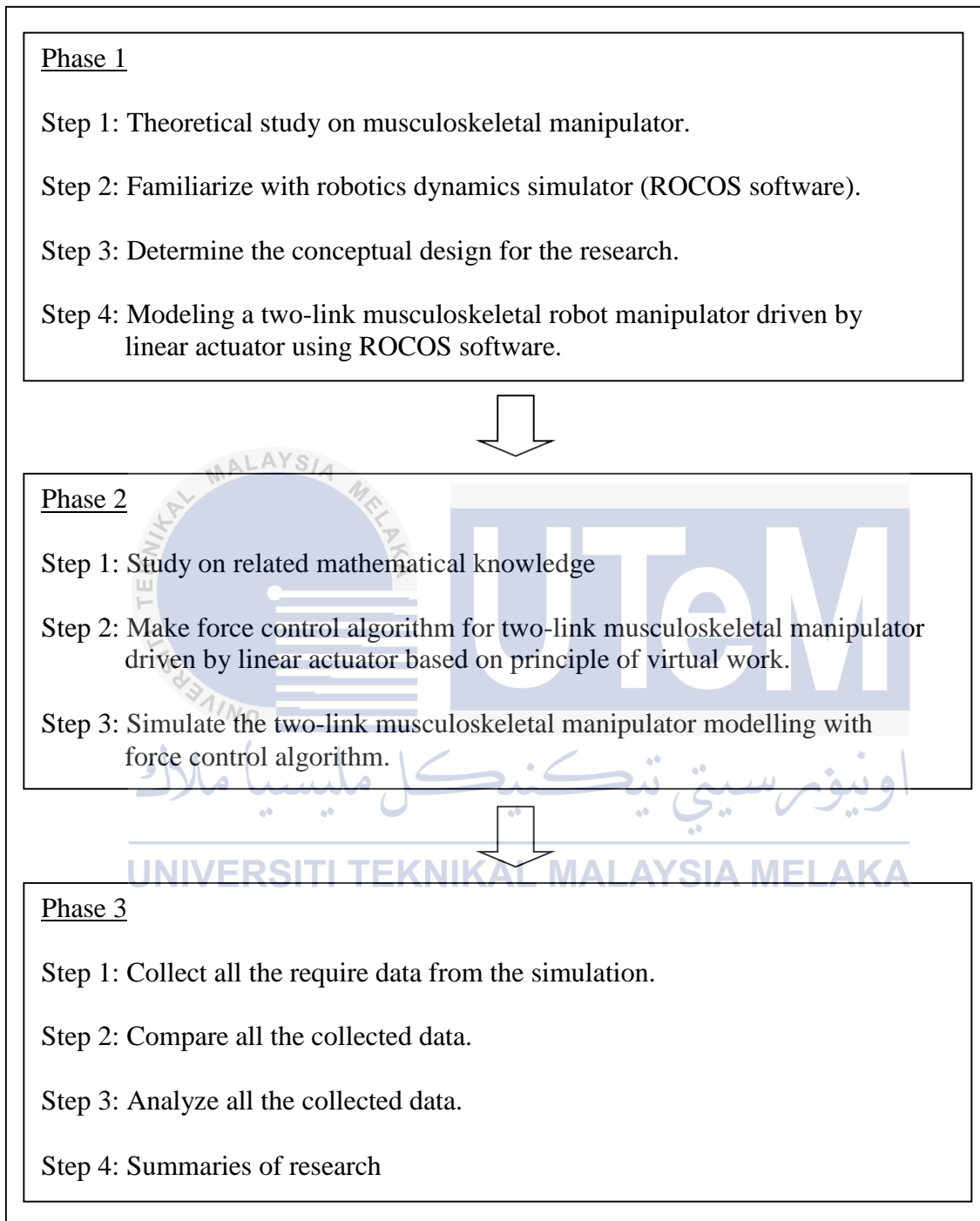


Figure 3.1: Research methodology

3.3 Phase 1

3.3.1 Step 1 (Theoretical study on musculoskeletal manipulator)

There are two type of musculoskeletal manipulator that have been widely used for robotic design which is mono-articular link constraint and biar-articular link constraint.

Mono-articular link constraint is a robotic design that apply the linear actuator that cross one joint while the biar-articular link constraint is a robotic design that apply the linear actuator that cross two joint rather than just one joint. Figure 3.3 show the mono-articular and biar-articular link constraint.

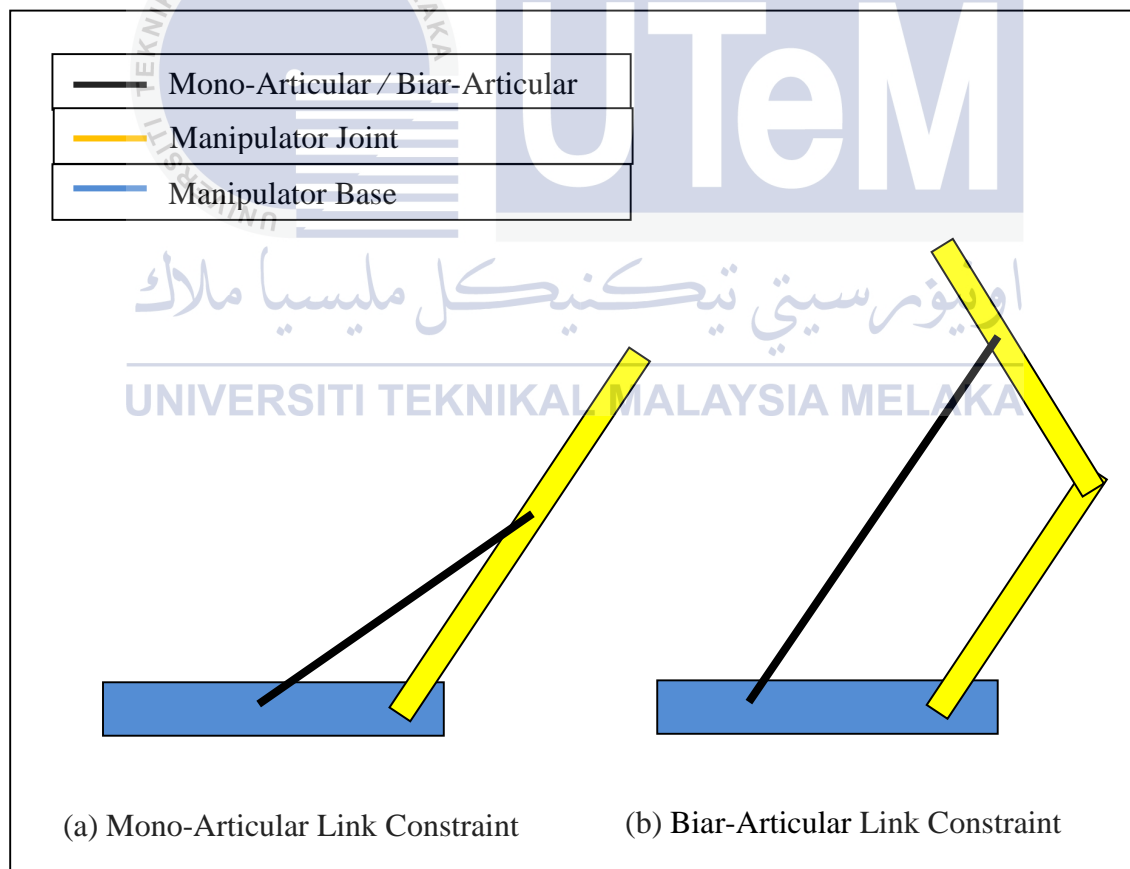


Figure 3.2: Mono-articular biar-articular link constraint

3.3.2 Step 2 (Familiarize with Robotic Simulator)

For this research, the modelling of two-link musculoskeletal robot manipulator and all the research will be conducted in simulation form by using one of robotic dynamic simulator software which is ROCOS Software. Basically, ROCOS is a software that using coding method to generate the modelling of two-link musculoskeletal robot manipulator. There are many variable such as parameter, contact point, centre of gravity, mass, and polygon data for each polygon that need to be declared inside ROCOS software to make sure the two-link musculoskeletal robot manipulator modelling work perfectly. Lastly, the only wall that available inside ROCOS software is at the floor. This situation also needed to be considered since the force control scheme required the external force such as force from the wall to analysis the behaviour of force control scheme. Figure 3.3 shows the example of ROCOS environment.

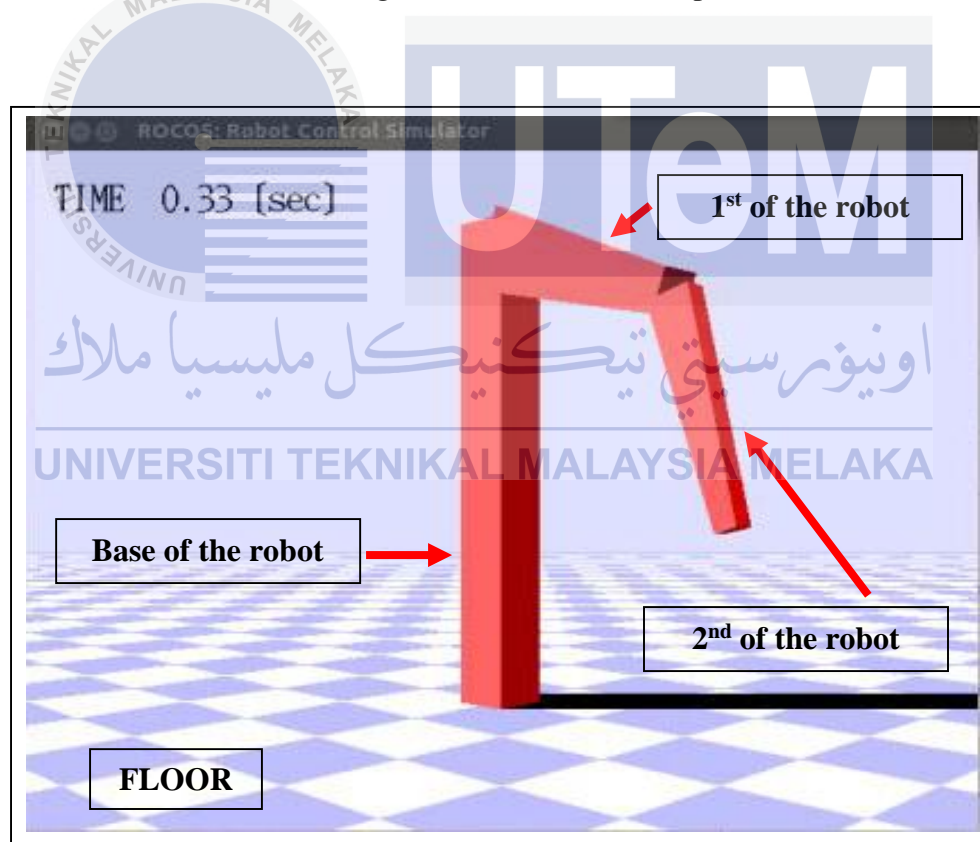


Figure 3.3: ROCOS environment

3.3.3 Step 3 (Determine the Conceptual Design for Research)

After totally understand step 1 and step 2, the conceptual design for the research be conducted. In this process, the length of each joint, the linear actuator extend and retract limit angle of rotation, axis frame for the manipulator and the centre of mass for each joint will be decide. Figure 3.4 shown the conceptual design for the research and Table 3.1 shows the modelling variable description.

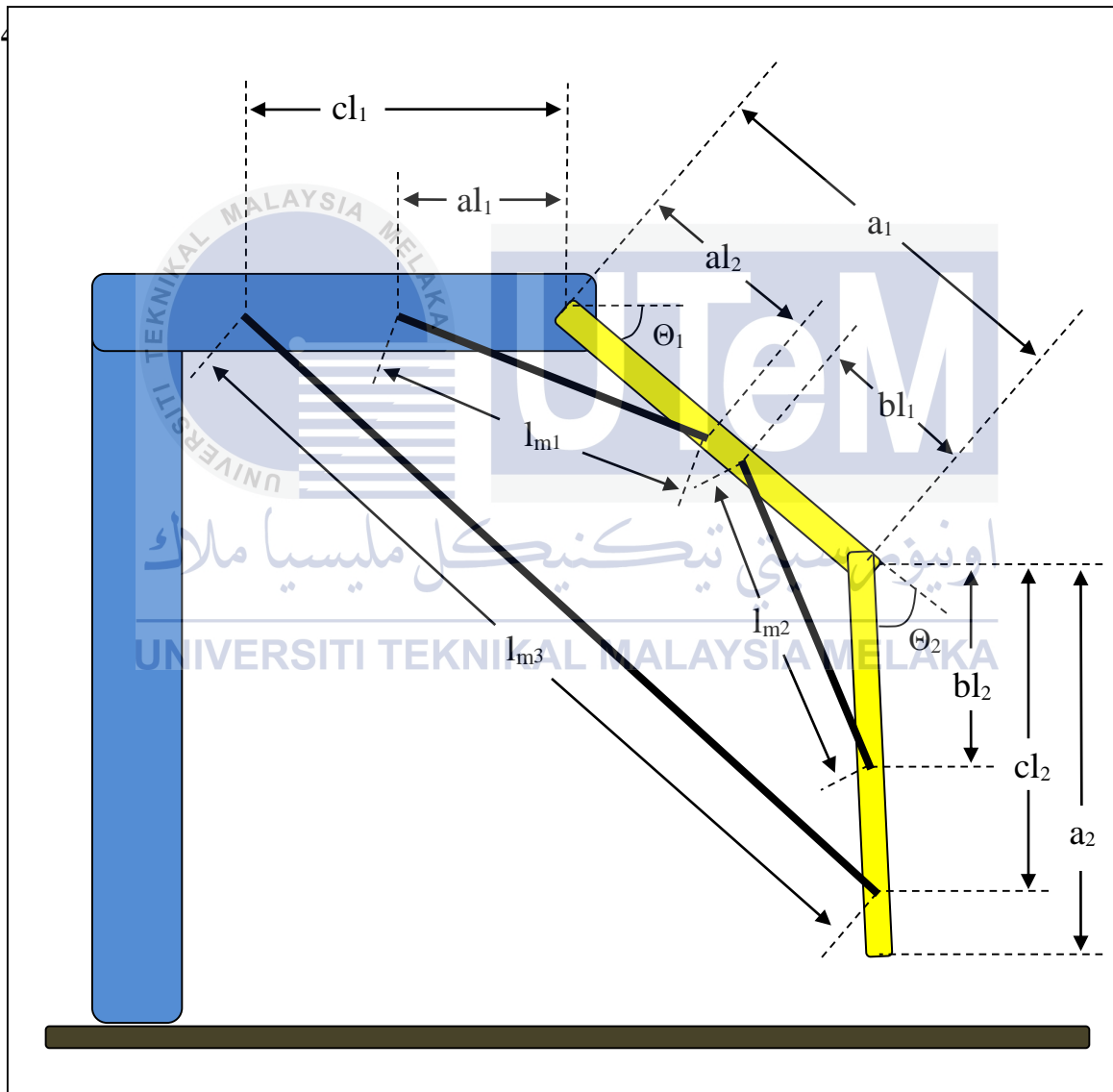






Figure 3.4: Conceptual design of the research

Table 3.1: Modelling variables description

No.	Variable	Description
1.		Manipulator link
2.		Manipulator base
3.		Ground
4.		Linear actuator act as manipulator muscle
5.	l_{m1}	Length of manipulator muscle that connect from base to first link
6.	a_{l1}	Length between the point where the manipulator muscle l_{m1} connect to the base with the joint of first link and base
7.	a_{l2}	Length between the point where the manipulator muscle l_{m1} connect to the first link with the joint of first link and base
8.	l_{m2}	Length of manipulator muscle that connect from first link to second link
9.	b_{l1}	Length between the point where the manipulator muscle l_{m2} connect to the second link with the joint of first link and second link
10.	b_{l2}	Length between the point where the manipulator muscle l_{m2} connect to the first link with joint of first link and second link
11.	l_{m3}	Length of manipulator muscle that connect from manipulator base to second link
12.	cl_1	Length between the point where the manipulator muscle C_1 connect to the base with the joint of first link and base
13.	cl_2	Length between the point where the manipulator muscle C_1 connect to the second link with joint of first link and second link
14.	a_1	Length of manipulator first link
15.	a_2	Length of manipulator second link

3.3.4 Step 4 (Modelling conceptual design using ROCOS)

Modelling conceptual design using ROCOS software required all the variable that have been mentioned at phase 1 (step 2). Explanation for the declaration process of all the variable inside ROCOS software will be explained further.

A. Parameter Declaration

Parameter declaration is the declaration for the length of the polygon in the terms of X-axis, Y-axis and Z-axis. This declaration is needed since the modelling is in the 3 dimension modelling. Figure 3.5 show the coding for parameter declaration in ROCOS.

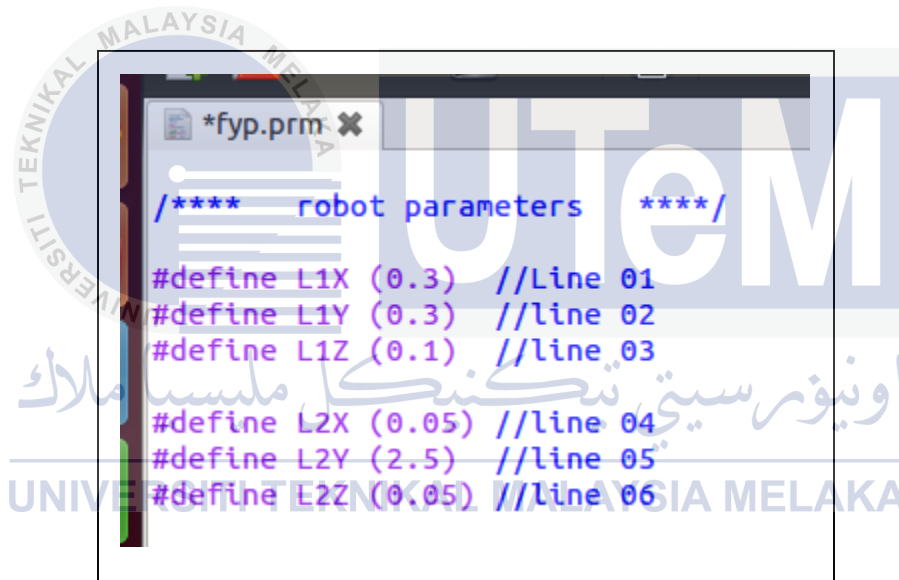


Figure 3.5: Parameter declaration

Figure 3.5 shown the declaration for two parameter that is polygon L1 and polygon L2. Line 01 is a declaration for the width of the polygon L1 and line 02 is a declaration for the length of the polygon L1. Other than that, line 03 also needed, where it is a declaration for the height of the polygon L1. The same concept also apply for the polygon L2.

B. Contact Point Declaration

Contact point declaration is a declaration of the point in terms of X, Y and Z-axis where line of the polygon intersect. This also known as the edge point for the polygon. Figure 3.6 show contact point declaration coding inside ROCOS.

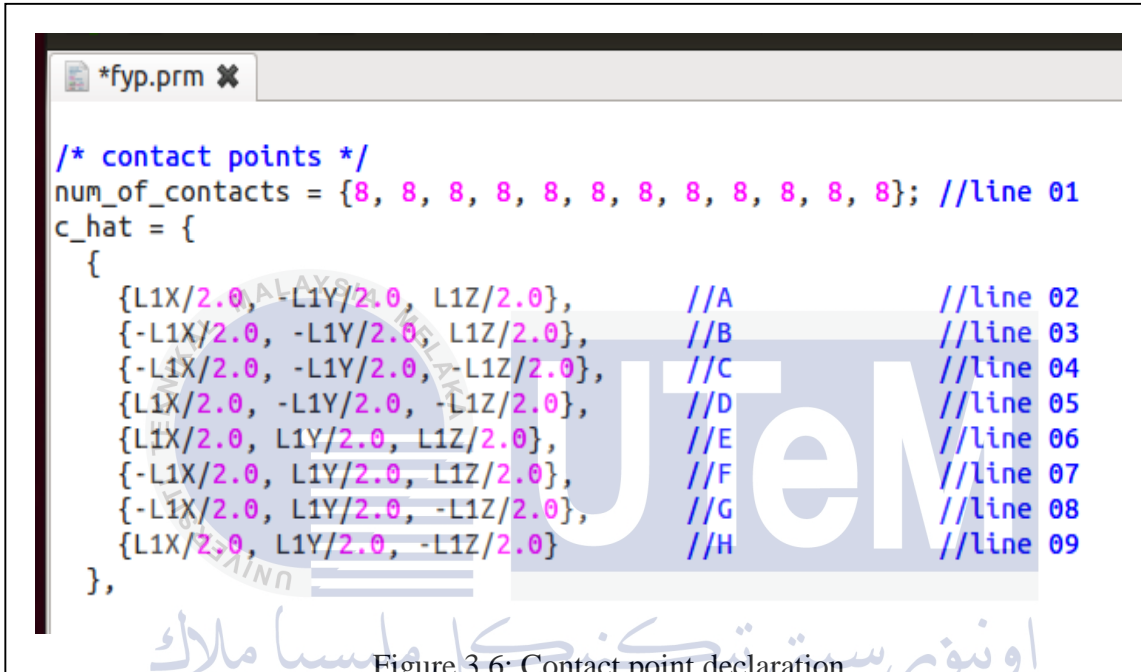


Figure 3.6: Contact point declaration

Figure 3.6 shown the contact point declaration coding for the polygon L1. Line 01 show the total contact number for each polygon block. Since for this research has 12 block of polygon, so there are 12 parameter at line 01. If the research has 5 block of polygon, then the parameter at line 01 will have 5 parameter. Other than that, coding form line 02 until line 09 is a contact point that available at polygon L1. Figure 3.7 show the position of the contact point for the polygon L1.

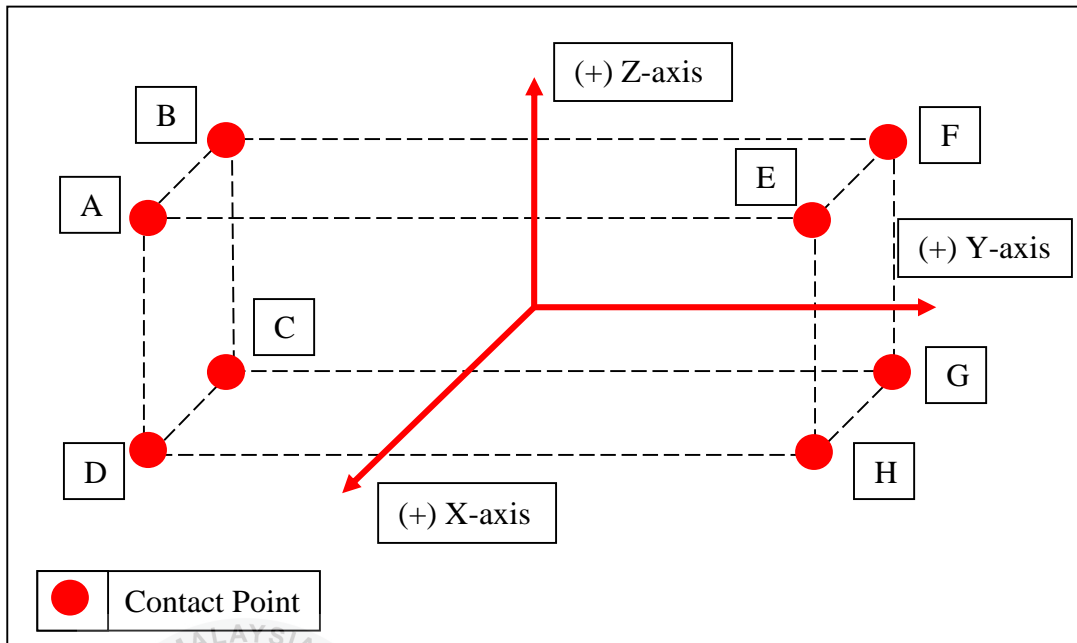


Figure 3.7: Contact point for polygon L1

C. Centre of Gravity Declaration

Centre of gravity declaration is a declaration to set a point where the center of mass of an object is the point at which the whole mass of the body is considered to act. Line 01 from Figure 3.8 is the declaration center of gravity point for polygon L1.

```

*fyp.prm x
/* link[i]'s center of gravity in its coordinates */
s_hat = {
{0.0, 0.0, 0.0},           //line 01
{0.0, 0.0, 0.0},           //line 02
{L3Y/2.0, 0.0, 0.0},       //line 03
{0.0, 0.0, L4Z/2},         //line 04
{0.0, 0.0, 0.0},           //line 05
{L6Y/2.0, 0.0, 0.0},       //line 06
{0.0, 0.0, L7Z/2},         //line 07
{ L8Y/2.0, 0.0, 0.0},       //line 08
{ L9Y/2.0, 0.0, 0.0},       //line 09
{0.0, 0.0, 0.0},           //line 10
{L11Y/2, 0.0, 0.0},         //line 11
{0.0, 0.0, L12Z/2.0}       //line 12
};

```

Figure 3.8: Centre of gravity declaration

D. Mass of Polygon Declaration

Mass of polygon declaration is a declaration that the weight of each polygon is being declared. For the simulation process, the weight of each polygon not very important but for the laboratory experimental setup, weight of each polygon need to be precise. For the simulation process, the weight of the base of the manipulator needed to be multiple times heavier from the any manipulator link to prevent the modelling flip over.

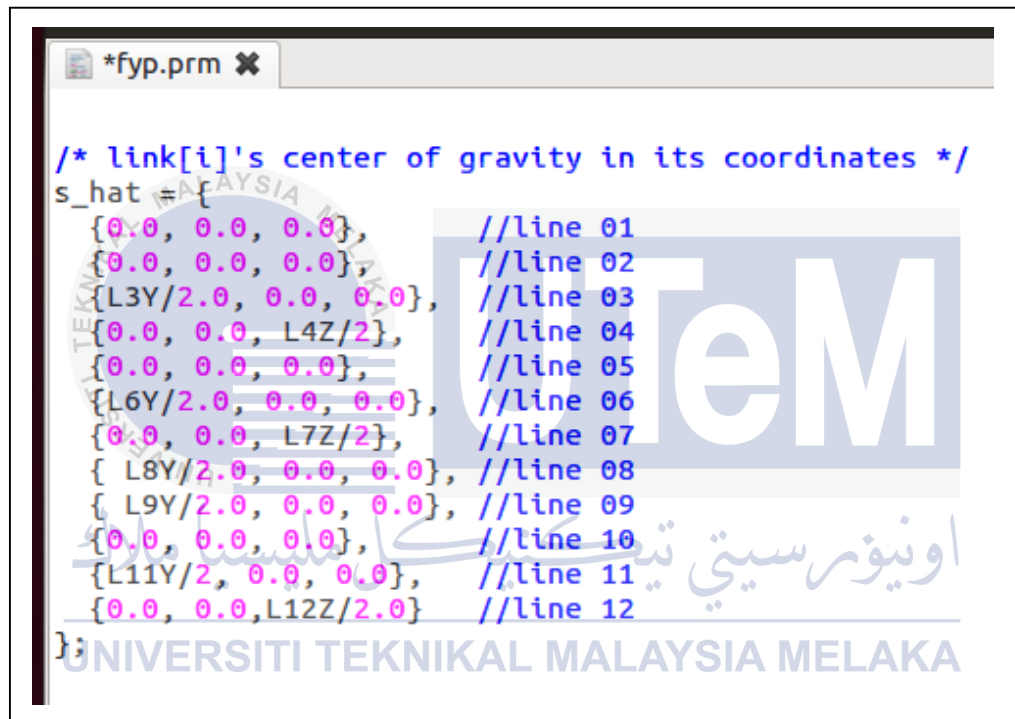
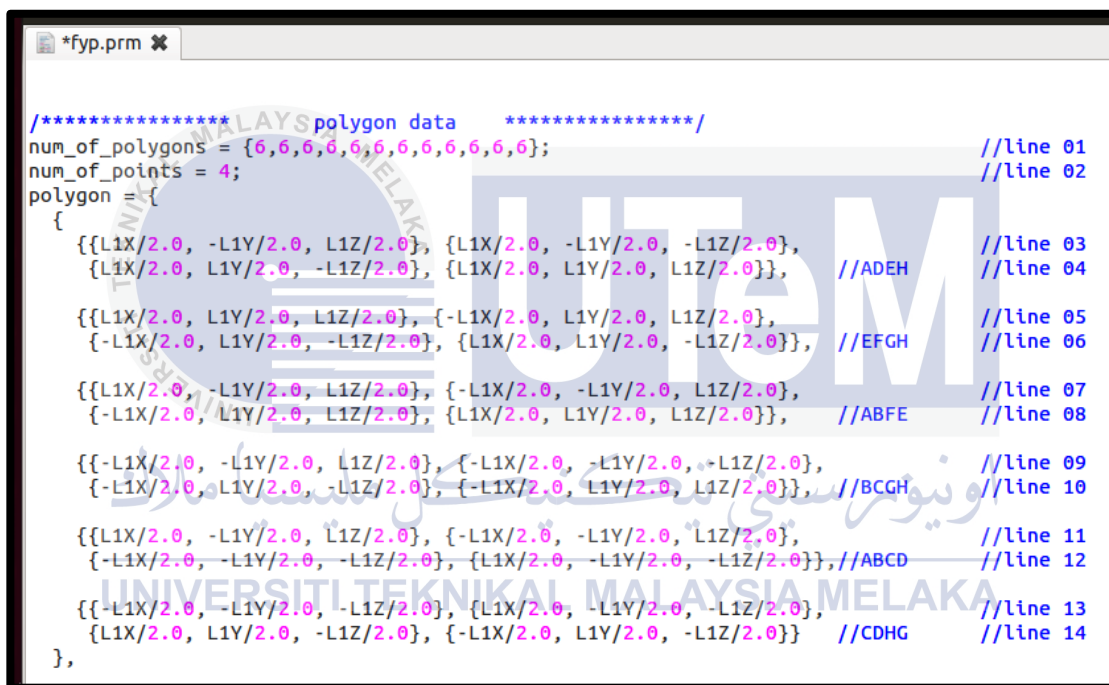


Figure 3.9: Polygon centre of gravity declaration

Figure 3.9 shown the centre of gravity point for each of the polygon block. The polygon L1 centre of gravity is declared at coding line 01 where it coordinate is being set in term of (X-axis, Y-axis, Z-axis). Coding line 02 until line 12 is used to declare the coordinate for the other polygon block since this research has 12 block of polygon in total.

E. Polygon Data Declaration

Polygon data declaration is a declaration where all the contact point that available at each polygon block surface being combine. Then all the polygon block surface is combined to make a complete polygon block. The quantity of the combining point is depend on the shape of the polygon block surface. If the polygon block is rectangular shape, then each of the polygon block surface contain 4 contact to be combined. After that, all 6 surface of the rectangular will be combined to make a complete rectangular shape.



```

/***** polygon data *****/
num_of_polygons = {6,6,6,6,6,6,6,6,6,6,6,6}; //line 01
num_of_points = 4; //line 02
polygon = {
{
  {{L1X/2.0, -L1Y/2.0, L1Z/2.0}, {L1X/2.0, -L1Y/2.0, -L1Z/2.0}, //line 03
   {L1X/2.0, L1Y/2.0, -L1Z/2.0}, {L1X/2.0, L1Y/2.0, L1Z/2.0}}, //line 04
  //ADEH
  {{L1X/2.0, L1Y/2.0, L1Z/2.0}, {-L1X/2.0, L1Y/2.0, L1Z/2.0}, //line 05
   {-L1X/2.0, L1Y/2.0, -L1Z/2.0}, {L1X/2.0, L1Y/2.0, -L1Z/2.0}}, //line 06
  //EFGH
  {{L1X/2.0, -L1Y/2.0, L1Z/2.0}, {-L1X/2.0, -L1Y/2.0, L1Z/2.0}, //line 07
   {-L1X/2.0, -L1Y/2.0, -L1Z/2.0}, {L1X/2.0, -L1Y/2.0, -L1Z/2.0}}, //line 08
  //ABFE
  {{-L1X/2.0, -L1Y/2.0, L1Z/2.0}, {-L1X/2.0, -L1Y/2.0, -L1Z/2.0}, //line 09
   {-L1X/2.0, L1Y/2.0, -L1Z/2.0}, {-L1X/2.0, L1Y/2.0, L1Z/2.0}}, //line 10
  //BCGH
  {{L1X/2.0, -L1Y/2.0, L1Z/2.0}, {-L1X/2.0, -L1Y/2.0, L1Z/2.0}, //line 11
   {-L1X/2.0, -L1Y/2.0, -L1Z/2.0}, {L1X/2.0, -L1Y/2.0, -L1Z/2.0}}, //line 12
  //ABCD
  {{-L1X/2.0, -L1Y/2.0, -L1Z/2.0}, {L1X/2.0, -L1Y/2.0, -L1Z/2.0}, //line 13
   {L1X/2.0, L1Y/2.0, -L1Z/2.0}, {-L1X/2.0, L1Y/2.0, -L1Z/2.0}}, //line 14
  //CDHG
},
},

```

Figure 3.10: Polygon data declaration

Figure 3.10 shown the polygon data declaration coding inside ROCOS software where line 01 is a declaration for a total polygon that had inside in this research. Other than that, line 02 is a declaration for number of point that available inside one polygon surface. Line 03 and line 04 is declaration which is used to combine 4 contact point which is point A, D, E and H to make one polygon surface. Then, all the line from line 03 until line 14 is been combined to make a complete block of polygon L1.

3.4 Phase 2

3.4.1 Step 1 (Study on related mathematical knowledge)

There is some mathematical knowledge that needs to be understood. By understanding mathematical knowledge it will help the derivation of force control algorithm for this research. The mathematical knowledge involved for this research force control derivation is differential equation, matrix, and trigonometry identities.

Differential equation is a mathematical equation for an unknown function of one or several variable that relates the values of the function itself and its derivatives of various orders. For this research, the most important orders that need to be understand is first order differential equation that consist sine and cosine. Table 3.2 shows the differentiation of trigonometric functions.

Table 3.2: Differentiation of trigonometric functions

Function	Derivative
$\cos(x)$	$-\sin(x)$
$\sin(x)$	$\cos(x)$
$\tan(x)$	$\sec^2(x)$

Matrix is a rectangular array to represent the data. It arranged in rows and columns. By using a matrix to represent the data, it makes the derivation of data become easier. For this research, there are several matrix form that involved which is 3x3, 3x2, 2x3, and 2x2 matrix. Jacobian matrix, inverse matrix and matrix transpose also involved for this research.

3.4.2 Step 2 (Making force control algorithm)

Based on Figure 3.4 and using trigonometric identities, the relationship of muscle length, l_m with the joint angles, θ is derived as in (1).

$$l_m = \begin{bmatrix} l_{m1} \\ l_{m2} \\ l_{m3} \end{bmatrix} \quad (3.1)$$

Where:

$$\begin{aligned} l_{m1} &= \sqrt{a l_1^2 + a l_2^2 + 2 a l_1 a l_2 \cos \theta_1} \\ l_{m2} &= \sqrt{b l_1^2 + b l_2^2 + 2 b l_1 b l_2 \cos \theta_2} \\ l_{m3} &= \sqrt{c l_1^2 + c l_2^2 + a_1^2 + 2 c l_1 a_1 \cos \theta_1 + 2 c l_2 a_1 \cos \theta_2 + 2 c l_1 c l_2 \cos(\theta_1 + \theta_2)} \end{aligned} \quad (3.2)$$

It is apparent that the extension or contraction of mono-articular muscles affects the respective joint angles to which they attach. However, the bi-articular muscle is redundant, because it affects both joint angles.

UNIVERSITI TEKNIKAL MALAYSIA MELAKA

Based on Equation (3.1) and (3.2), the relationship between muscle velocity and joint velocity is given as in Equation (3.3).

$$\dot{l}_m = J_{lm\theta} + \dot{\theta} \quad (3.3)$$

Where $J_{lm\theta}$ the Jacobian matrix between muscle and joint space and contains the following elements.

$$J_{lm\theta} = \begin{bmatrix} \frac{\partial l_{m1}}{\partial \theta_1} & \frac{\partial l_{m1}}{\partial \theta_2} \\ \frac{\partial l_{m2}}{\partial \theta_1} & \frac{\partial l_{m2}}{\partial \theta_2} \\ \frac{\partial l_{m3}}{\partial \theta_1} & \frac{\partial l_{m3}}{\partial \theta_2} \end{bmatrix} \quad (3.4)$$

Where:

$$\begin{aligned} \frac{\partial l_{m1}}{\partial \theta_1} &= -\frac{al_2al_2\sin\theta_1}{l_{m1}} & \frac{\partial l_{m1}}{\partial \theta_2} &= 0 \\ \frac{\partial l_{m2}}{\partial \theta_1} &= 0 & \frac{\partial l_{m2}}{\partial \theta_2} &= -\frac{bl_1bl_2\sin\theta_2}{l_{m2}} \\ \frac{\partial l_{m3}}{\partial \theta_1} &= \frac{-cl_1a_1\sin\theta_1-cl_1cl_2\sin(\theta_1+\theta_2)}{l_{m3}} \\ \frac{\partial l_{m3}}{\partial \theta_2} &= \frac{-cl_2a_1\sin\theta_2-cl_1cl_2\sin(\theta_1+\theta_2)}{l_{m3}} \end{aligned} \quad (3.5)$$

Thus, the equation relating joint torques τ (vector of θ_1 and θ_2) and muscle forces F_{lm} (vector of l_{m1} , l_{m2} and l_{m3}) can be described.

$$\tau = J_{lm\theta}^T F_{lm} \quad (3.6)$$

Also, the equation relating the joint torque and the end effector force, F_e (vector of cartesian forces) for a two link planar rotary manipulator is shown in (3.7).

$$\tau = J^T F_e \quad (3.7)$$

where J is the Jacobian matrix from the task space to the joint space and contains the elements as shown in (3.8).

$$\begin{bmatrix} -a_1 \sin(\theta_1) - a_2 \sin(\theta_1 + \theta_2) & -a_2 \sin(\theta_1 + \theta_2) \\ a_1 \cos(\theta_1) + a_2 \cos(\theta_1 + \theta_2) & a_2 \cos(\theta_1 + \theta_2) \end{bmatrix} \quad (3.8)$$

The relationship between the end effector forces and the muscle forces can be determined as follows.

$$F_e = [J^t]^{-1} J_{lm\theta}^T F_{lm\theta} \quad (3.9)$$

3.4.3 Step 3 (Simulate modelling with force control algorithm)

Lastly, the simulation process can be conducted to test the validity and reliability of the force control algorithm that have been made. For the simulation process, there are two type of simulation that have been conducted which is independent muscle control and end effector force control simulation.

Basically, the independent muscle control is a method where the system will maintains the force that apply at muscle according to the references forces that have been given. Meanwhile, the end effector force control is a method where the system will maintains the force that apply at the end effector according to the references forces.

3.5 Phase 3

Basically, phase 3 is a process where analysis for this research will be conducted. So, further explanation for this process will be provided at chapter 4.

3.6 Reliability of Data

The data from this research is reliable because this research is using a 2 dimension modelling where the force tracking at end-effector only apply in 1 direction of axis only. Figure 3.11 show the axis direction for force tracking at end-effector of the robot manipulator when it make a contact with the wall.

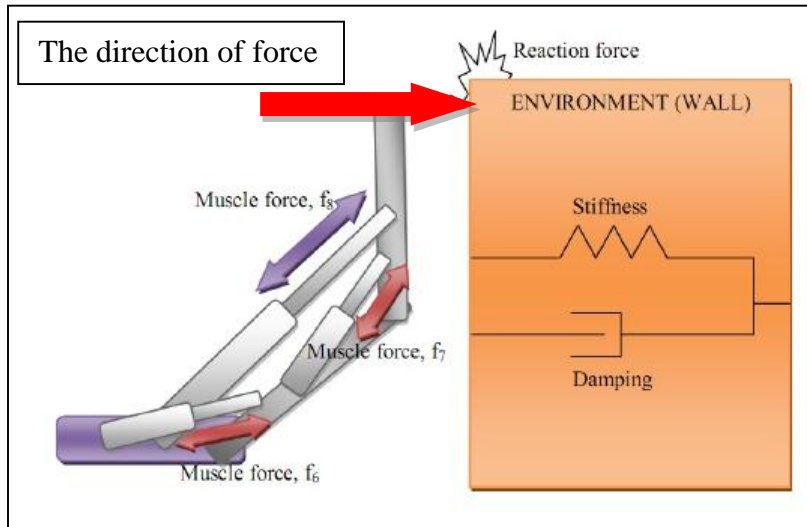


Figure 3.11: Robot manipulator force direction [20]

However, for the actual environment or 3 dimensional modelling, there are possibility the data collected from the simulation got some error due to the force acting at end-effector of the robot not actually in 1 direction. This error is due to the mechanical design of the robot. Figure 3.12 show the illustration for this error.

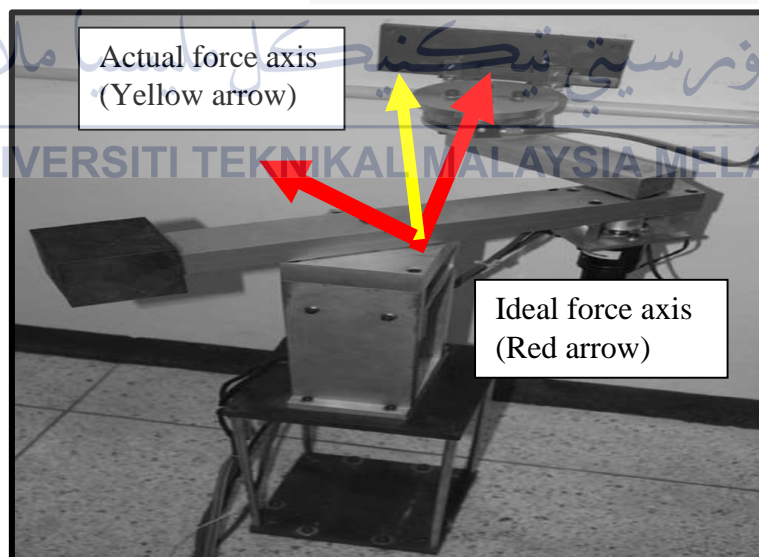


Figure 3.12: Robot manipulator ideal and actual force direction [15]

CHAPTER 4

RESULT AND ANALYSIS

4.1 Introduction

This chapter will indicate and provide information about the finding of the research, and all the finding will be analyzed and discussed. This chapter will discuss more on the process of analyzing the result from the stage of how the simulation had been conducted until the process of data comparison and validation process.

4.2 Two Link Musculoskeletal Manipulator Modelling

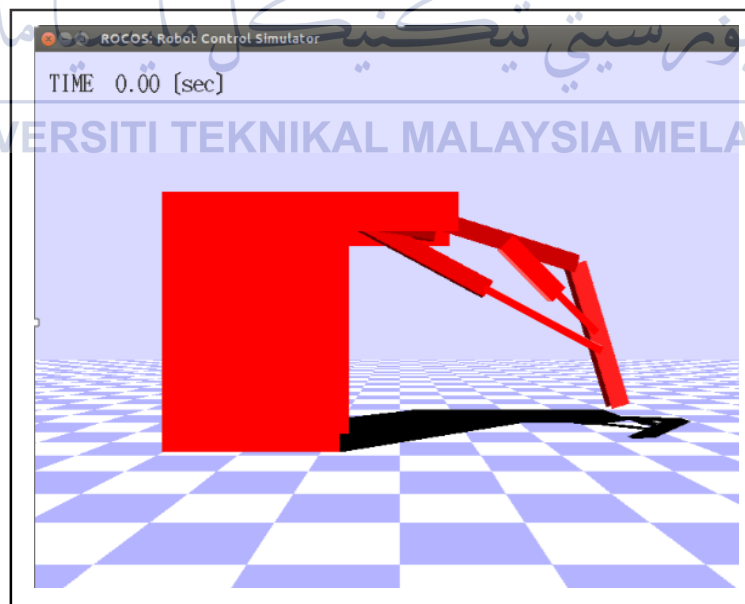


Figure 4.1: Two link musculoskeletal manipulator modelling

Figure 4.1 represented the two link musculoskeletal manipulator modelling that had been used in this research. By using this modelling, force control algorithm for the actuation-redundant biar-articular manipulator have been derived.

4.3 Force Control Algorithm

For a robotic manipulator, the forces that need to be controlled are the end effector or tool position. This research also focusing on controlling the end effector forces in Cartesian space and then the forces in cartesian is converted to forces in muscle actuation. Although the forces controlled are in the muscle domain, the equivalent virtual forces in the shoulder and elbow could be obtained by using the muscle to joint jacobian.

The force control algorithm for the actuation-redundant biar-articular manipulator could be represented as in Figure 4.2. It can be seen that the disturbance observer had been involved in force control algorithm, where disturbance observer is used to estimate the reaction forces in the Cartesian domain. The Cartesian velocities could be obtained from virtual joint velocities using conventional jacobian terms. Force reference command is labelled as F_{lm} , a vector of x-direction and y-direction force references for each muscle. K_e is the vector of force control gain for x and y.

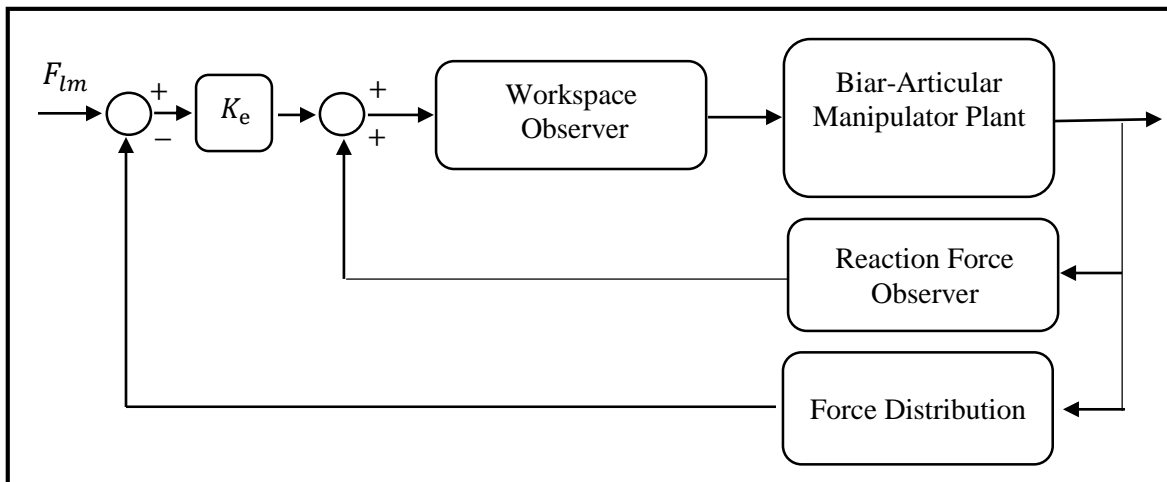


Figure 4.2: Force control block diagram for biar-articular manipulator

In figure 4.2, force distribution block is shown in the control. This is because the end effector forces (in x and y-direction) need to be converted to the muscle forces for shoulder mono-articular, elbow mono-articular and biar-articular muscle which will be tracked by muscle level control. In short, the force control equation can be represent by Equation (4.1).

$$F_{lm} = K_e(F_{ref} - F_{reac}) + F_{act} \quad (4.1)$$

where:

K_e = Force control gain.

F_{lm1} = Force apply at each muscle.

F_{ref} = Force references for each muscle.

F_{reac} = Environment force in term of each muscle.

F_{act} = Environment force(C term) in term of each muscle.

4.4 Simulation 1 (Independent Muscle Control)

4.4.1 Simulation Setup and Result

For independent force control of each muscles, the interaction with the environment will be investigated. In this simulation, the initial position of the end effector had been setup at position (0.5, 0.5) m and environment is set at y-position of 0.5. This mean, the end effector of the manipulator had been touched the environment from start. This setup is needed to make sure the force control algorithm get feedback force from environment from the beginning of the simulation, so that the force control algorithm can worked perfectly.

Force references were set at -80N for shoulder mono-articular muscle (l_{m1}) and 20N for elbow mono-articular muscle (l_{m2}) and biar-articular muscle (l_{m3}). The reason why l_{m1} is given with larger negative reference force (4:1 ratio) because it to make l_{m1} to extract faster so that end effector can maintain touched the environment (floor) as long as possible. All this force references (F_{ref}) were set at $t = 0.1sec$ for each muscles.

Figure 4.3 represent the result when reference forces had been set -80N for l_{m1} and 20N for l_{m2} and l_{m3} . From the Figure 4.3, there are 3 force that had been observed which is F_{lm1} (force applied at muscle l_{m1}), F_{lm2} (force applied at muscle l_{m2}) and F_{lm3} (force applied at muscle l_{m3}).

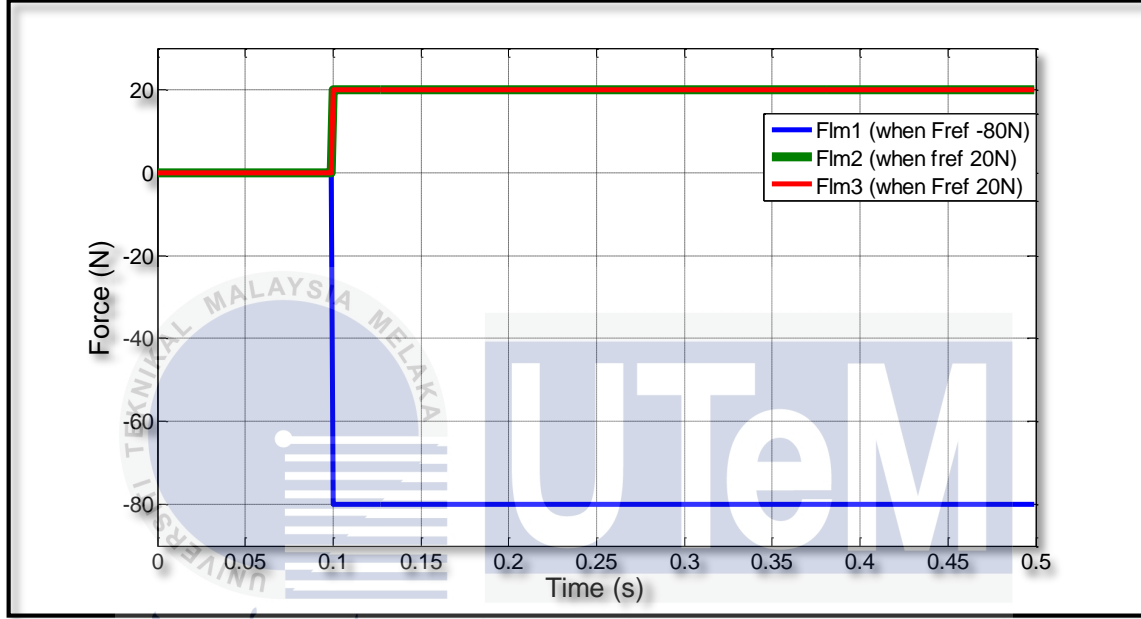


Figure 4.3: Sample of simulation 1 muscles force result

By take all data regarding force at muscle l_{m1} , l_{m2} and l_{m3} , force at end effector can be calculated. Equation (4.2) was used to calculate the end effector force.

$$\begin{bmatrix} F_{endx} \\ F_{endy} \end{bmatrix} = [J^T]^{-1} J_{lm}^T \begin{bmatrix} F_{lm1} \\ F_{lm2} \\ F_{lm3} \end{bmatrix} \quad (4.2)$$

Figure 4.4 shows the end effector force when reference forces had been set at -80N for l_{m1} and 20N for l_{m2} and l_{m3} . This simulation had been repeated with same condition but using a different force references command which is -160N,-240N,-360N and -400N for l_{m1} and 40N,60N,80N and 100N for l_{m2} and l_{m3} . All the Simulation result regarding muscles force were attached at Appendix A and all result regarding end effector force attached at Appendix B.

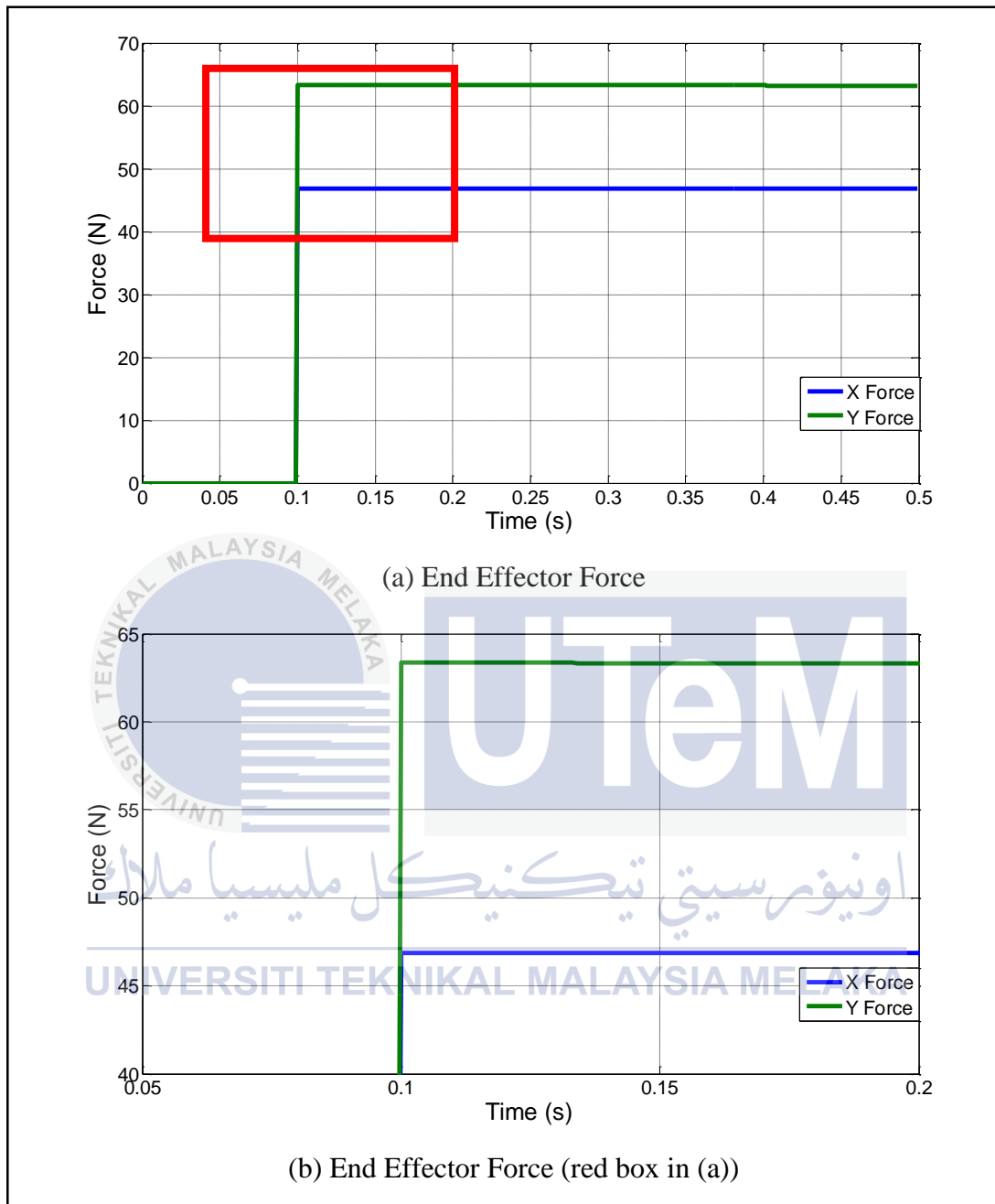


Figure 4.4: Sample of simulation 1 end effector force result

4.4.2 Comparison Between Same Type of Muscle With Different Type of Reference Forces.

All data regarding independent muscle control simulation were rearranged into the shoulder mono-articular muscle force (F_{lm1}) data, elbow mono-articular muscle force (F_{lm2}) data, bi-articular muscle force (F_{lm3}) data, end effector in x-direction force (F_{endx}) data and end effector in y-direction force (F_{endy}) data for comparison process.

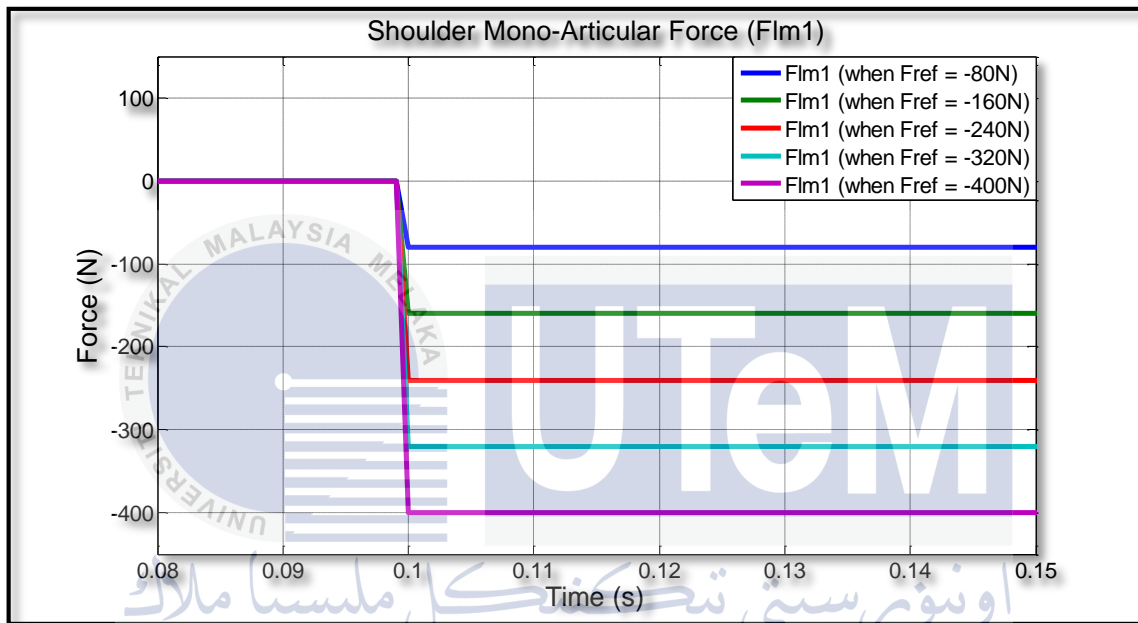


Figure 4.5: Simulation 1 all shoulder mono-articular muscle force (F_{lm1})

Figure 4.5 represent the force that applied to shoulder mono-articular (l_{m1}) with 5 different reference forces value which is -80N, -160N, -240N, -320N and -400N from $t = 0.08s$ until $t = 0.15s$. All shoulder mono-articular force (F_{lm1}) were 0 N before $t = 0.1s$ because the system had been set to give 0 Newton for $t < 0.1s$. When $t = 0.1s$, the system will start to give reference force for shoulder mono-articular muscle to follow. Even the shoulder mono-articular (l_{m1}) was given 5 different reference forces value, the settling time for the shoulder mono-articular (l_{m1}) is not change which is at $t = 0.1s$, and the force that applied at shoulder mono-articular muscle (l_{m1}) same as the reference forces that had been given. Full shoulder mono-articular muscle force (F_{lm1}) graph was attached at the Appendix C.

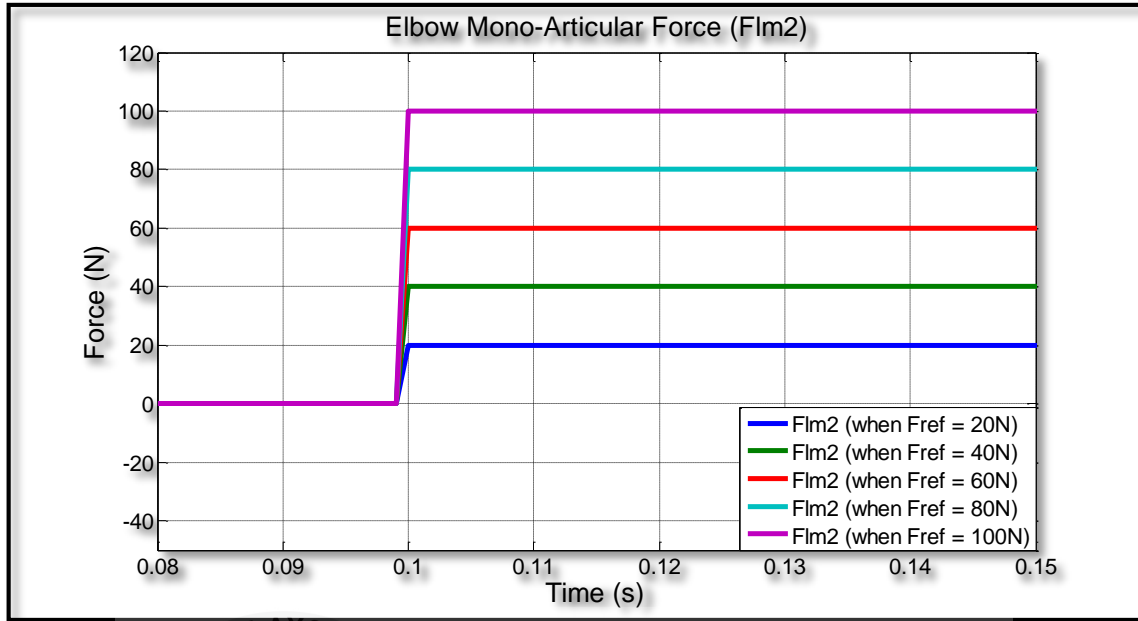


Figure 4.6: Simulation 1 all elbow mono-articular muscle force (F_{lm2})

Meanwhile, Figure 4.6 shown the force that applied to elbow mono-articular (l_{m2}) with 5 different reference forces value which is 20N, 40N, 60N, 80N and 100N from $t = 0.08s$ until $t = 0.15s$. All elbow mono-articular force (F_{lm2}) were 0 Newton when $t < 0.1s$ because the system had been set to give 0 Newton for $t < 0.1s$ and at $t = 0.1s$, the system will start to give reference force for elbow mono-articular muscle to follow. Although the elbow mono-articular (l_{m2}) was given 5 different reference forces value, the settling time for the elbow mono-articular (l_{m2}) is same which is at $t = 0.1s$. Other than that, force that applied at elbow mono-articular (l_{m2}) also same with the reference forces that had been given to elbow mono-articular muscle (l_{m2}). Full elbow mono-articular muscle force (F_{lm2}) graph was attached at the Appendix C.

For biar-articular muscle (l_{m3}), the settling time and the force applied to biar-articular muscle (l_{m3}) is same with elbow mono-articular (l_{m2}) because the reference forces that had given to the biar-articular muscle (l_{m3}) and elbow mono-articular (l_{m2}) were same which is 20N, 40N, 60N, 80N and 100N. Figure 4.7 shows the force that applied to biar-articular muscle from $t = 0.08s$ until $t = 0.15s$ and full biar-articular muscle force (F_{lm3}) graph was attached at the Appendix C.

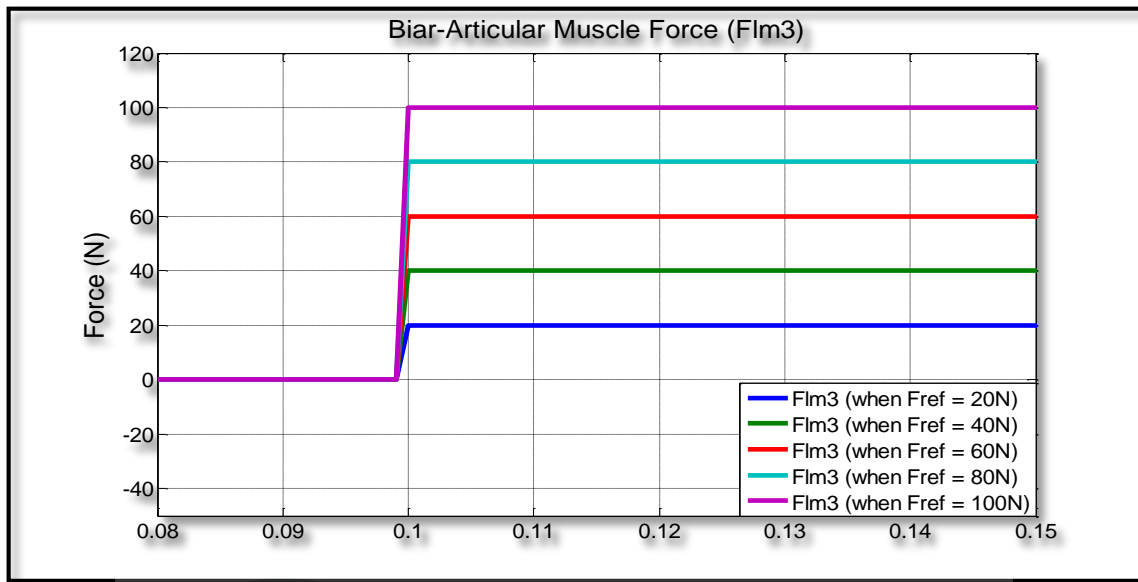


Figure 4.7: Simulation 1 all biar-articular muscle force (F_{lm3})

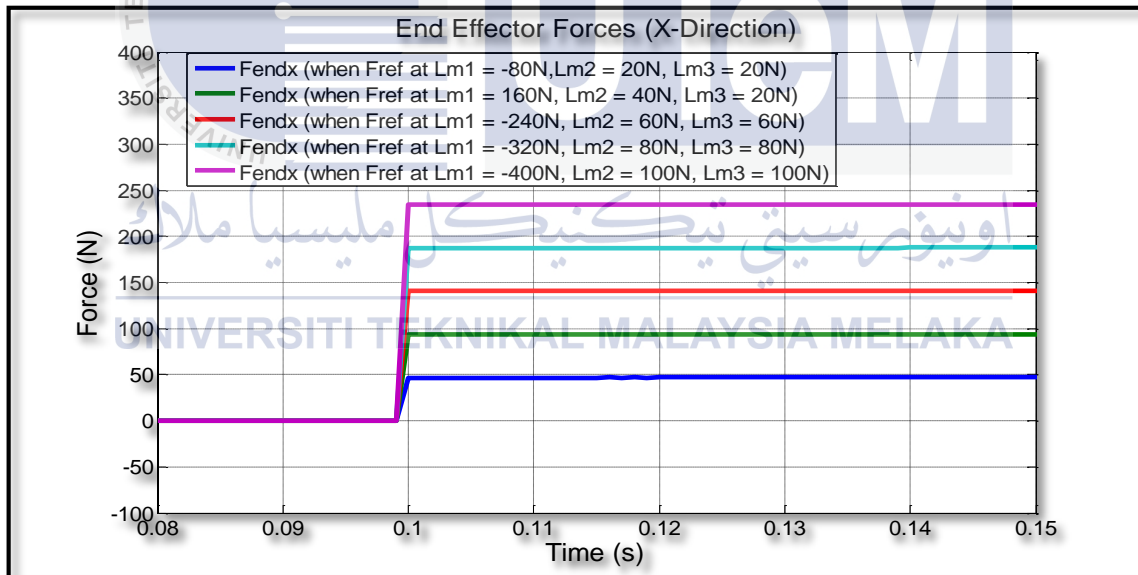


Figure 4.8: Simulation 1 all end effector force (X-direction)

Figure 4.8 represent the end effector force (F_{endx}) in x-direction when different reference force value had been applied at all muscles from $t = 0.08s$ until $t = 0.15s$. From the Figure 4.8, it shown if the larger value of references force had been applied to muscles, it will make end effector in x-direction force (F_{endx}) increase. Data regarding maximum and minimum value of end effector in x-direction force (F_{endx}) after $t = 0.1s$ had been shows in

Table 4.1 and full end effector in x-direction force (F_{endx}) graph was attached at the Appendix D.

Table 4.1: Simulation 1 maximum and minimum force at end effector (X-direction)

Reference Forces at Muscle (N)	Maximum Force (N)	Minimum Force (N)
$l_{m1} = -80$ $l_{m2} = 20$ $l_{m3} = 20$	4689×10^{-02} (at $t = 0.5\text{sec}$)	4687×10^{-02} (at $t = 0.1\text{sec}$)
$l_{m1} = -160$ $l_{m2} = 40$ $l_{m3} = 40$	9385×10^{-02} (at $t = 0.5\text{sec}$)	9376×10^{-02} (at $t = 0.1\text{sec}$)
$l_{m1} = -240$ $l_{m2} = 60$ $l_{m3} = 60$	1410×10^{-01} (at $t = 0.5\text{sec}$)	1406×10^{-01} (at $t = 0.1\text{sec}$)
$l_{m1} = -320$ $l_{m2} = 80$ $l_{m3} = 80$	1881×10^{-01} (at $t = 0.5\text{sec}$)	1875×10^{-01} (at $t = 0.1\text{sec}$)
$l_{m1} = -400$ $l_{m2} = 100$ $l_{m3} = 100$	2366×10^{-01} (at $t = 0.5\text{sec}$)	2344×10^{-01} (at $t = 0.1\text{sec}$)

Meanwhile, force that had been applied at end effector in y-direction force (F_{endy}), decrease if the larger value of references force had been applied to muscles. Data regarding maximum and minimum value of end effector in y-direction force (F_{endy}) after $t = 0.1\text{s}$ had been shows in Table 4.2. Furthermore, end effector force in y-direction data when different reference force value had been applied at all muscles from $t = 0.08\text{s}$ until $t = 0.15\text{s}$ is shows in Figure 4.9 and full end effector in y-direction force (F_{endy}) graph was attached at the Appendix D.

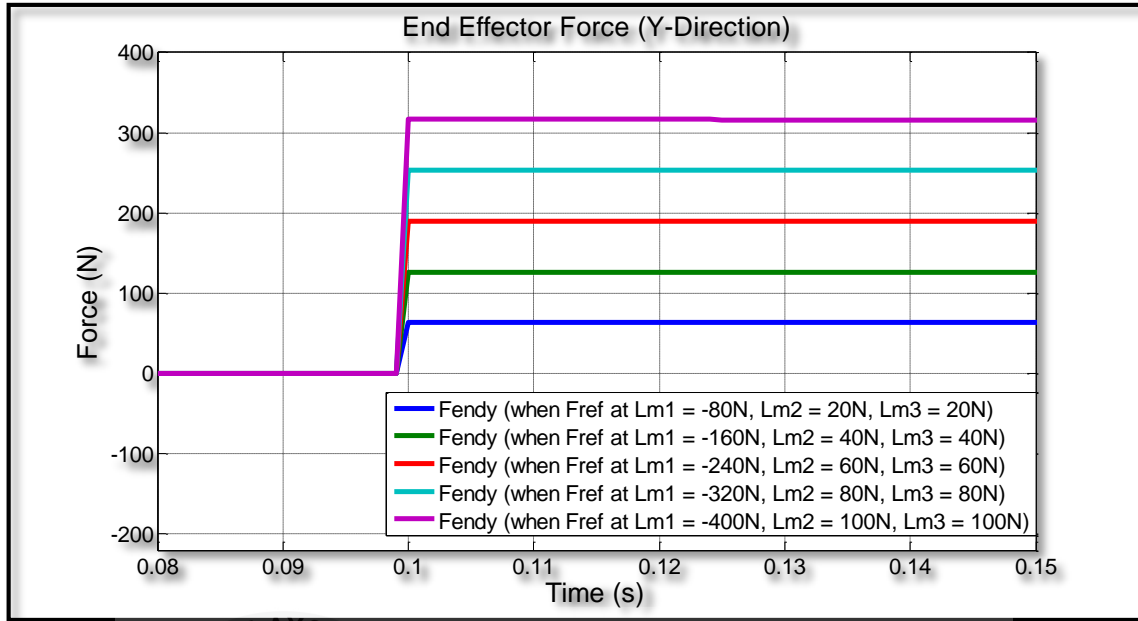


Figure 4.9: Simulation 1 all end effector forces (Y-direction)

Table 4.2: Simulation 1 maximum and minimum force at end effector (Y-direction)

Reference Forces at Muscle (N)	Maximum Force (N)	Minimum Force (N)
$l_{m1} = -80$ $l_{m2} = 20$ $l_{m3} = 20$	6337×10^{-02} (at $t = 0.1\text{sec}$)	6321×10^{-02} (at $t = 0.5\text{sec}$)
$l_{m1} = -160$ $l_{m2} = 40$ $l_{m3} = 40$	1267×10^{-01} (at $t = 0.1\text{sec}$)	1264×10^{-01} (at $t = 0.5\text{sec}$)
$l_{m1} = -240$ $l_{m2} = 60$ $l_{m3} = 60$	1901×10^{-01} (at $t = 0.1\text{sec}$)	1893×10^{-01} (at $t = 0.5\text{sec}$)
$l_{m1} = -320$ $l_{m2} = 80$ $l_{m3} = 80$	2535×10^{-01} (at $t = 0.1\text{sec}$)	2522×10^{-01} (at $t = 0.5\text{sec}$)
$l_{m1} = -400$ $l_{m2} = 100$ $l_{m3} = 100$	3169×10^{-01} (at $t = 0.1\text{sec}$)	3117×10^{-01} (at $t = 0.5\text{sec}$)

4.4.3 Synthesise of Data

Data synthesise process had been divided into two categories which is muscles and end effector categories where muscles categories will included shoulder mono-articular muscle force (F_{lm1}) data, elbow mono-articular muscle force (F_{lm2}) data and biar-articular muscle force (F_{lm3}) data. End effector in x-direction force (F_{endx}) data and end effector in y-direction force (F_{endy}) will be end effector categories and both categories been synthesized in term of settling time and accuracy for force tracking.

Table 4.3: Simulation 1 settling time (muscles)

Reference Forces at Muscle (N)	Shoulder Mono-Articular Muscle Force (second)	Elbow Mono-Articular Muscle Force (second)	Biar-Articular Muscle Force (second)
$l_{m1} = -80$ $l_{m2} = 20$ $l_{m3} = 20$	1×10^{-01}	1×10^{-01}	1×10^{-01}
$l_{m1} = -160$ $l_{m2} = 40$ $l_{m3} = 40$	1×10^{-01}	1×10^{-01}	1×10^{-01}
$l_{m1} = -240$ $l_{m2} = 60$ $l_{m3} = 60$	1×10^{-01}	1×10^{-01}	1×10^{-01}
$l_{m1} = -320$ $l_{m2} = 80$ $l_{m3} = 80$	1×10^{-01}	1×10^{-01}	1×10^{-01}
$l_{m1} = -400$ $l_{m2} = 100$ $l_{m3} = 100$	1×10^{-01}	1×10^{-01}	1×10^{-01}

Table 4.4: Simulation 1 settling time (end effector)

Reference Forces at Muscle (N)	End Effector Force in X-Direction (second)	End Effector Force in Y-Direction (second)
$l_{m1} = -80$ $l_{m2} = 20$ $l_{m3} = 20$	1×10^{-01}	1×10^{-01}
$l_{m1} = -160$ $l_{m2} = 40$ $l_{m3} = 40$	1×10^{-01}	1×10^{-01}
$l_{m1} = -240$ $l_{m2} = 60$ $l_{m3} = 60$	1×10^{-01}	1×10^{-01}
$l_{m1} = -320$ $l_{m2} = 80$ $l_{m3} = 80$	1×10^{-01}	1×10^{-01}
$l_{m1} = -400$ $l_{m2} = 100$ $l_{m3} = 100$	1×10^{-01}	1×10^{-01}

Table 4.5: Simulation 1 final force applied to muscles

Reference Forces at Muscle (N)	Shoulder Mono-Articular Muscle Force (N)	Elbow Mono-Articular Muscle Force (N)	Biar-Articular Muscle Force (N)
$l_{m1} = -80$ $l_{m2} = 20$ $l_{m3} = 20$	-80	20	20
$l_{m1} = -160$ $l_{m2} = 40$ $l_{m3} = 40$	-160	40	40
$l_{m1} = -240$ $l_{m2} = 60$ $l_{m3} = 60$	-240	60	60
$l_{m1} = -320$ $l_{m2} = 80$ $l_{m3} = 80$	-320	80	80
$l_{m1} = -400$ $l_{m2} = 100$ $l_{m3} = 100$	-400	100	100

4.4.4 Conclusion

The force control of independent muscles was successfully achieved but the force at end effector were fluctuated when every force references that had been given. The reason why end effector force fluctuated because the end effector position changed (slides). This phenomena happen because there are force in x-direction and y-direction for end effector.

Although force control of independent muscles was successfully achieved, to set the end effector force with specific force value is hard, because all 3 muscles force can effect end effector force. Furthermore, if the application required end effector force to work in one direction only, it difficult to achieve by using independent muscles control where this will required either complex mathematical calculation or complex force control algorithm.

Lastly, from the Simulation that had been done, it shows that if the larger force that had been given to the muscles, the end effector force also will increase.

4.5 Simulation 2 (End Effector Muscle Control)

4.5.1 Simulation Setup and Result

By using initial position for end effector at (0.5, 0.5) m and environment at y-position of 0.6, the muscle forces are indirectly controlled by the end effector forces in the cartesian domain. Initially, the end effector force in proper direction is given to ensure that the end effector hits the environment. After contacting with the environment, the force are controlled to maintain end effector force in the y-direction.

The force references (F_{ref}) for end effector in the y-direction and x-direction is given as 0 N for both direction when $t < 0.1s$. When $t \geq 0.1s$, force references for end effector in the y-direction ($F_{ref(endy)}$) is given as 20 N and force reference for end effector in x-direction

($F_{ref(endx)}$) is 0 N. This setup is used to ensure end effector hits the environment with only consisted one direction of force at end effector which is in y-direction.

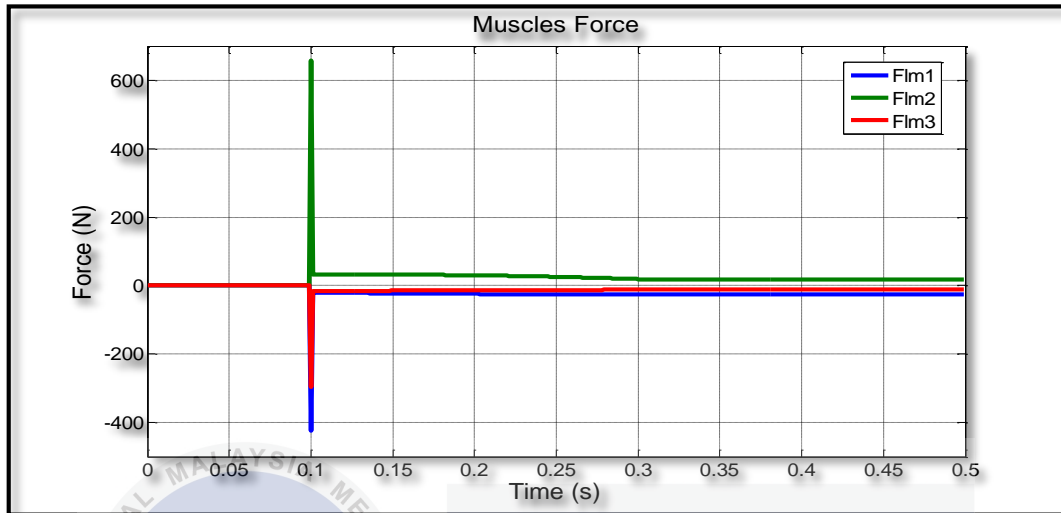


Figure 4.10: Sample of simulation 2 muscles force result

Figure 4.10 represent the force that applied at shoulder mono-articular muscle force (F_{lm1}), elbow mono-articular muscle force (F_{lm2}) and biar-articular muscle force (F_{lm3}) when end effector force in y-direction is given 20 N as force reference ($F_{ref(endy)}$) for $t \geq 0.1s$ and 0 N for $t \geq 0.1s$ as force reference ($F_{ref(endx)}$) for end effector force in x-direction. As the result, there are overshoot when force reference with some value was given to the system. The reason why all the force for shoulder mono-articular muscle (l_{m1}) and biar-articular muscle (l_{m3}) with negative value inside Figure 4.10 was due to extraction of the shoulder mono-articular muscle (l_{m1}) and biar-articular muscle (l_{m3}). This extraction is happen because positive force reference for end effector in y-direction ($F_{ref(endy)}$) is in downward direction.

By using Equation (4.2) and data from Figure 4.10, end effector in x-direction force (F_{endx}) and end effector in y-direction force (F_{endy}) can be calculated. All the data regarding end effector in x-direction force (F_{endx}) and end effector in y-direction force (F_{endy}) is shown in Figure 4.11.

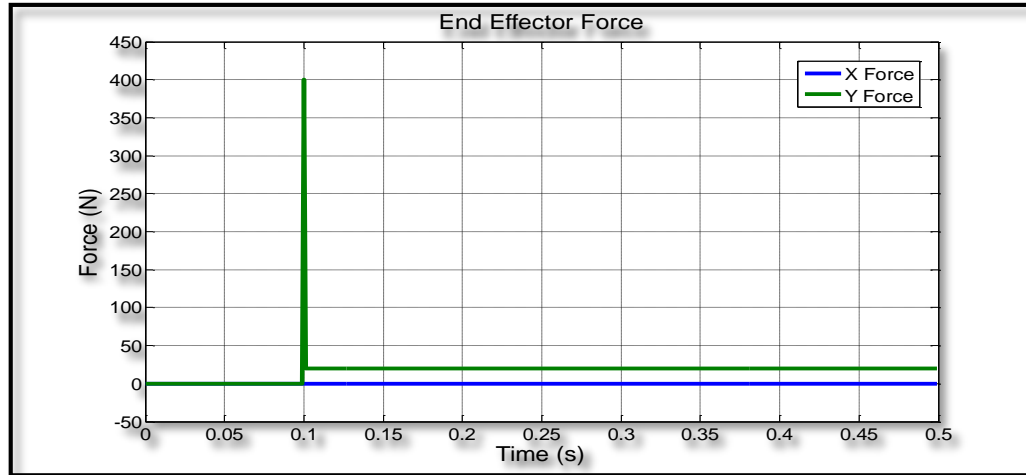


Figure 4.11: Sample of simulation 2 end effector force result

This simulation setup were repeated with different force reference (F_{ref}) value for the end effector in y-direction force (F_{endy}) which is 40N, 60N, 80N, and 100N. The purpose by doing this is to observe the performance of the system and manipulator behaviour. All the Simulation result regarding muscles force were attached at Appendix E and all result regarding end effector force attached at Appendix F.

Table 4.6: Simulation 2 maximum and minimum shoulder mono-articular muscle force (F_{lm1})

Reference Forces (N)	Maximum Force (N)	Minimum Force (N)
$F_{ref(endx)} = 0$ $F_{ref(endy)} = 20$	4241×10^{-01}	2120×10^{-02}
$F_{ref(endx)} = 0$ $F_{ref(endy)} = 40$	8482×10^{-01}	4241×10^{-02}
$F_{ref(endx)} = 0$ $F_{ref(endy)} = 60$	1272	6361×10^{-02}
$F_{ref(endx)} = 0$ $F_{ref(endy)} = 80$	1696	8482×10^{-02}
$F_{ref(endx)} = 0$ $F_{ref(endy)} = 100$	2121	1061×10^{-01}

Table 4.6 shown maximum and minimum forces that been applied to shoulder mono-articular muscle (l_{m1}) when a different value of force reference for end effector in y-direction

($F_{ref(endy)}$) is given to the system. Other than that, Table 4.6 also shows that if the larger value is given as force reference for end effector in y-direction ($F_{ref(endy)}$), it will make shoulder mono-articular muscle force (F_{lm1}) increased.

Table 4.7: Simulation 2 maximum and minimum elbow mono-articular muscle force (F_{lm2})

Reference Forces (N)	Maximum Force (N)	Minimum Force (N)
$F_{ref(endx)} = 0$ $F_{ref(endy)} = 20$	6588×10^{-01}	1691×10^{-02}
$F_{ref(endx)} = 0$ $F_{ref(endy)} = 40$	1318	3161×10^{-02}
$F_{ref(endx)} = 0$ $F_{ref(endy)} = 60$	1977	4409×10^{-02}
$F_{ref(endx)} = 0$ $F_{ref(endy)} = 80$	2635	5522×10^{-02}
$F_{ref(endx)} = 0$ $F_{ref(endy)} = 100$	3294	6654×10^{-02}

Table 4.7 shown maximum and minimum forces that been applied to elbow mono-articular muscle (l_{m2}) when a different value of force reference for end effector in y-direction ($F_{ref(endy)}$) is given to the system. The reason why all the force for elbow mono-articular muscle (l_{m2}) in positive value is due to extension of the elbow mono-articular muscle (l_{m2}). Elbow mono-articular muscle force (F_{lm2}) also increase if the force reference for end effector in y-direction ($F_{ref(endy)}$) increased.

Table 4.8: Simulation 2 maximum and minimum biar-articular muscle force (F_{lm3})

Reference Forces (N)	Maximum Force (N)	Minimum Force (N)
$F_{ref(endx)} = 0$ $F_{ref(endy)} = 20$	2957×10^{-01}	1125×10^{-02}
$F_{ref(endx)} = 0$ $F_{ref(endy)} = 40$	5915×10^{-01}	2327×10^{-02}
$F_{ref(endx)} = 0$ $F_{ref(endy)} = 60$	8872×10^{-01}	3562×10^{-02}
$F_{ref(endx)} = 0$ $F_{ref(endy)} = 80$	1183	4826×10^{-02}
$F_{ref(endx)} = 0$ $F_{ref(endy)} = 100$	1479	6073×10^{-02}

Table 4.8 shown maximum and minimum forces that been applied to biar-articular muscle (l_{m3}) when a different value of force reference for end effector in y-direction ($F_{ref(endy)}$) is given to the system. Biar-articular muscle force (F_{lm3}) also increase if the force reference for end effector in y-direction ($F_{ref(endy)}$) increased.

Table 4.9: Simulation 2 maximum and minimum end effector in X-direction force (F_{endx})

Reference Forces (N)	Maximum Force (N)	Minimum Force (N)
$F_{ref(endx)} = 0$ $F_{ref(endy)} = 20$	3020×10^{-05}	(-) 5620×10^{-05}
$F_{ref(endx)} = 0$ $F_{ref(endy)} = 40$	1164×10^{-04}	(-) 2571×10^{-04}
$F_{ref(endx)} = 0$ $F_{ref(endy)} = 60$	2565×10^{-04}	(-) 6031×10^{-04}
$F_{ref(endx)} = 0$ $F_{ref(endy)} = 80$	4536×10^{-04}	(-) 1103×10^{-03}
$F_{ref(endx)} = 0$ $F_{ref(endy)} = 100$	6879×10^{-04}	(-) 1734×10^{-03}

Table 4.9 shown the maximum and minimum end effector in x-direction force (F_{endx}) different value of force reference for end effector in y-direction ($F_{ref(endy)}$) is given to the

system. Although the system give 0 N force reference for end effector in x-direction ($F_{ref(endx)}$), there will had some value for end effector in x-direction force (F_{endx}) in the initial but when the time increased, end effector in x-direction force (F_{endx}) become stable and able to maintained the force at end effector at 0 N.

Table 4.10: Simulation 2 maximum and minimum end effector in Y-direction force (F_{endy})

Reference Forces (N)	Maximum Force (N)	Minimum Force (N)
$F_{ref(endx)} = 0$ $F_{ref(endy)} = 20$	400	1987×10^{-02}
$F_{ref(endx)} = 0$ $F_{ref(endy)} = 40$	800	3948×10^{-02}
$F_{ref(endx)} = 0$ $F_{ref(endy)} = 60$	1200	5887×10^{-02}
$F_{ref(endx)} = 0$ $F_{ref(endy)} = 80$	1600	7702×10^{-02}
$F_{ref(endx)} = 0$ $F_{ref(endy)} = 100$	2000	9699×10^{-02}

Table 4.10 shown the maximum and minimum end effector in y-direction force (F_{endy}) different value of force reference for end effector in y-direction ($F_{ref(endy)}$) is given to the system. Initially, there were overshoot for end effector in y-direction force (F_{endy}) but when the time increased, end effector in y-direction force (F_{endy}) become stable and able to maintained the force at end effector according to force reference for end effector in y-direction ($F_{ref(endy)}$).

4.5.2 Comparison Between Same Type of Muscle With Different Type of Reference Forces.

All data regarding end effector muscle control Simulation were rearranged into the shoulder mono-articular muscle force (F_{lm1}) data, elbow mono-articular muscle force (F_{lm2}) data, biar-articular muscle force (F_{lm3}) data, end effector in x-direction force (F_{endx}) data and end effector in y-direction force (F_{endy}) data for comparison process.

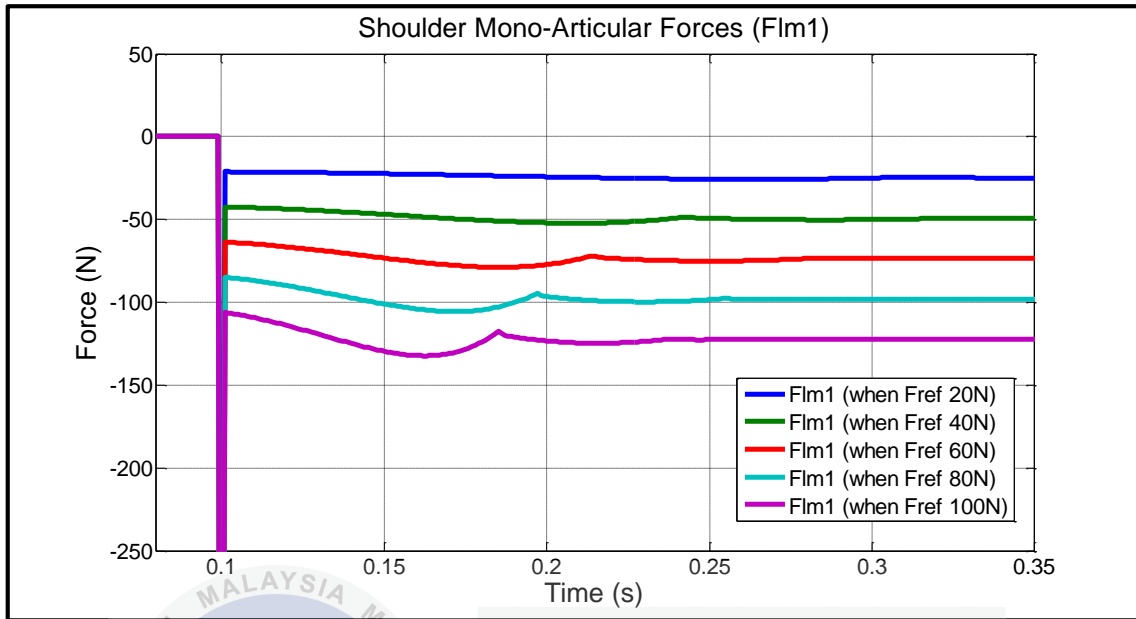


Figure 4.12: Simulation 2 all shoulder mono-articular muscle force (F_{lm1})

Figure 4.5 represent the force that applied to shoulder mono-articular muscles (l_{m1}) with 5 different reference forces value at end effector in y-direction ($F_{ref(endy)}$) which is 20N, 40N, 60N, 80N and 100N from $t = 0.08s$ until $t = 0.35s$. All shoulder mono-articular force (F_{lm1}) were 0 N before $t = 0.1s$ because the system had been set to give 0 Newton for $t < 0.1s$. When $t = 0.1s$, the system will start to give reference force reference forces for end effector in y-direction ($F_{ref(endy)}$). Although force reference was given to end effector, but musculoskeletal modelling were driven by all the muscles that attached to the modelling structure. So, by giving a reference force to end effector, this actually indirectly effect shoulder mono-articular muscle (l_{m1}). When $t = 0.1s$, force applied to shoulder mono-articular at maximum value due to inertia. Shoulder mono-articular muscle force (F_{lm1}) become stable after end effector collided with the environment. Table 4.11 shows stable shoulder mono-articular muscle force (F_{lm1}) and time when the end effector collide with the environment. Full shoulder mono-articular muscle force (F_{lm1}) graph was attached at the Appendix G.

Table 4.11 Simulation 2 settling time and final force value
for shoulder mono-articular muscle

Reference Forces (N)	Final Force Value (N)	Settling time (second)
$F_{ref}(endx) = 0$ $F_{ref}(endy) = 20$	2462×10^{-02}	311×10^{-03}
$F_{ref}(endx) = 0$ $F_{ref}(endy) = 40$	4912×10^{-02}	243×10^{-03}
$F_{ref}(endx) = 0$ $F_{ref}(endy) = 60$	7356×10^{-02}	215×10^{-03}
$F_{ref}(endx) = 0$ $F_{ref}(endy) = 80$	9799×10^{-02}	198×10^{-03}
$F_{ref}(endx) = 0$ $F_{ref}(endy) = 100$	1224×10^{-01}	185×10^{-03}

From Table 4.11, it shown that the increment of force references will increase the final force at shoulder mono-articular muscle and improved the settling time which mean end effector and environment collision occurred faster.

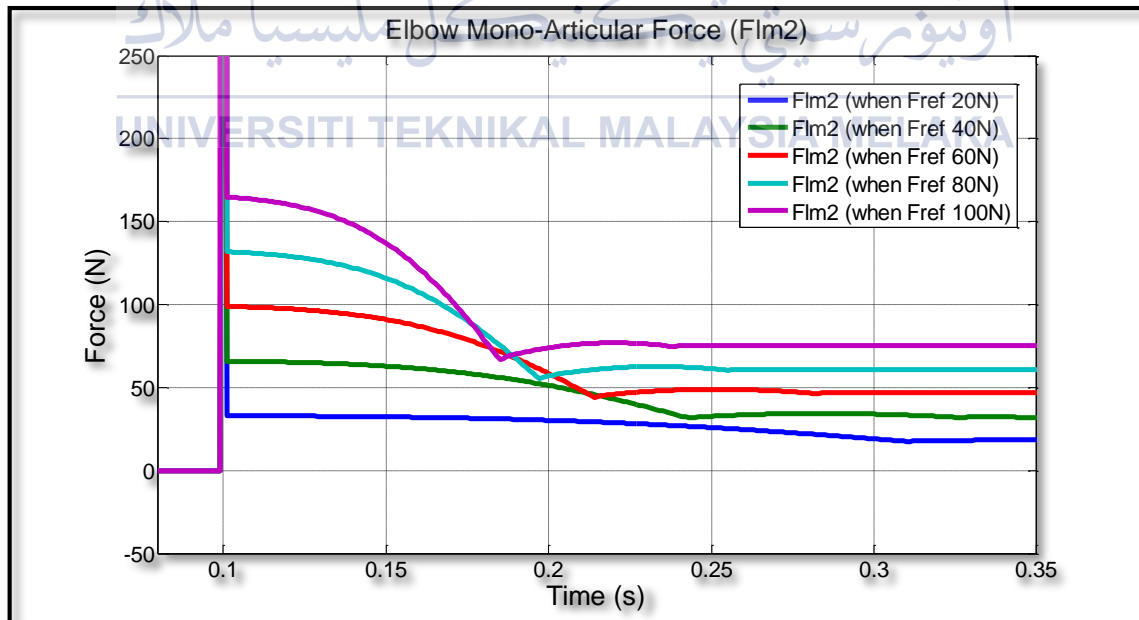


Figure 4.13: Simulation 2 all elbow mono-articular muscle force (F_{lm2})

Forces that been applied to elbow mono-articular muscle from $t = 0.08s$ until $t = 0.35s$ had been shows in Figure 4.13 where there are 5 elbow mono-articular muscle force (F_{lm2}) because this Simulation was repeated 5 times where 5 different reference forces value at end effector in y-direction ($F_{ref(endy)}$) which is 20N, 40N, 60N, 80N and 100N had been used. Basically all the settling time for elbow mono-articular muscle is same with shoulder mono-articular muscle. The different between elbow and shoulder mono-articular muscle is the force that applied at muscle and while shoulder mono-articular muscle extracted, elbow mono-articular extended. Full elbow mono-articular muscle force (F_{lm2}) graph was attached at the Appendix G.

Table 4.12: Simulation 2 settling time and final force value
for elbow mono-articular muscle

Reference Forces (N)	Final Force Value (N)	Settling time (second)
$F_{ref(endx)} = 0$ $F_{ref(endy)} = 20$	1693×10^{-02}	311×10^{-03}
$F_{ref(endx)} = 0$ $F_{ref(endy)} = 40$	3194×10^{-02}	243×10^{-03}
$F_{ref(endx)} = 0$ $F_{ref(endy)} = 60$	4650×10^{-02}	215×10^{-03}
$F_{ref(endx)} = 0$ $F_{ref(endy)} = 80$	6064×10^{-02}	198×10^{-03}
$F_{ref(endx)} = 0$ $F_{ref(endy)} = 100$	7478×10^{-01}	185×10^{-03}

From Table 4.12, it shown that the increment of force references will increase the final force at elbow mono-articular muscle and improved the settling time which mean end effector and environment collision occurred faster.

Figure 4.14 shows force that applied to biar-articular muscles (l_{m3}) with 5 different reference forces value at end effector in y-direction ($F_{ref(endy)}$) which is 20N, 40N, 60N, 80N and 100N from $t = 0.08s$ until $t = 0.35s$. All settling time for Biar-Articular Muscle Force

(F_{lm3}) were same with shoulder and elbow mono-articular muscle force but the force applied at biar-articular muscle is different from force that applied at shoulder and elbow mono-articular muscle. Full biar-articular muscle force (F_{lm3}) graph was attached at the Appendix G.

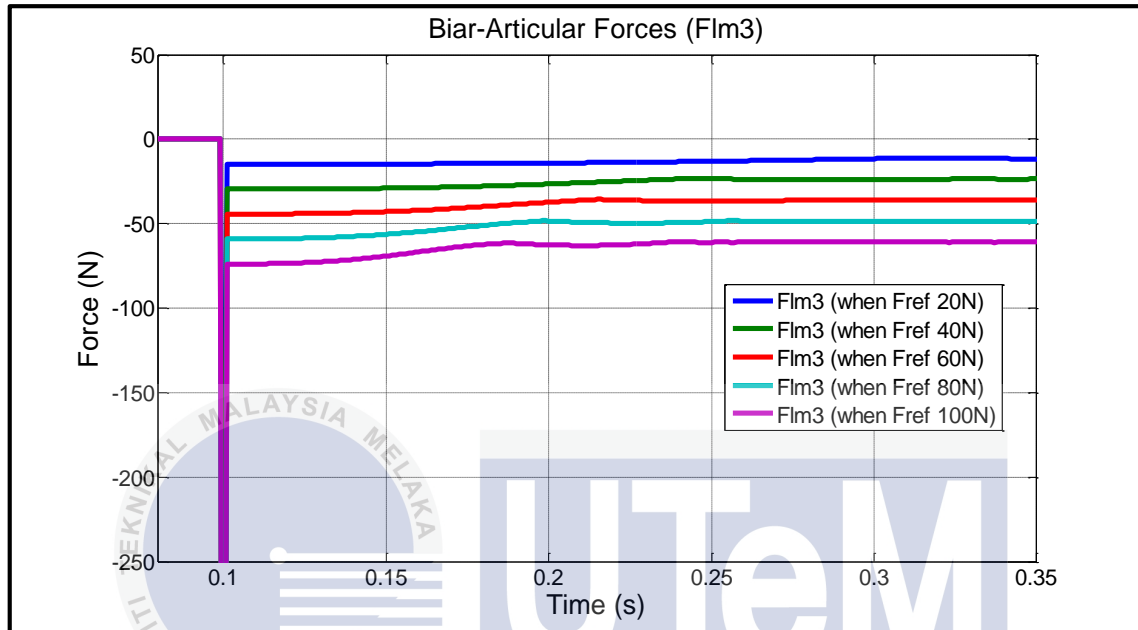


Figure 4.14: Simulation 2 all biar-articular muscle force (F_{lm3})

Table 4.13 represent the settling time and final force value that had been applied to biar-articular muscle. From the data, it's shown that the increment of force references will increase the final force at elbow mono-articular muscle and improved the settling time which mean end effector and environment collision occurred faster.

Table 4.13: Simulation 2 settling time and final force value
for biar-articular muscle

Reference Forces (N)	Final Force Value (N)	Settling time (second)
$F_{ref(endx)} = 0$ $F_{ref(endy)} = 20$	1154×10^{-02}	311×10^{-03}
$F_{ref(endx)} = 0$ $F_{ref(endy)} = 40$	2363×10^{-02}	243×10^{-03}
$F_{ref(endx)} = 0$ $F_{ref(endy)} = 60$	3593×10^{-02}	215×10^{-03}
$F_{ref(endx)} = 0$ $F_{ref(endy)} = 80$	4848×10^{-02}	198×10^{-03}
$F_{ref(endx)} = 0$ $F_{ref(endy)} = 100$	6105×10^{-02}	185×10^{-03}

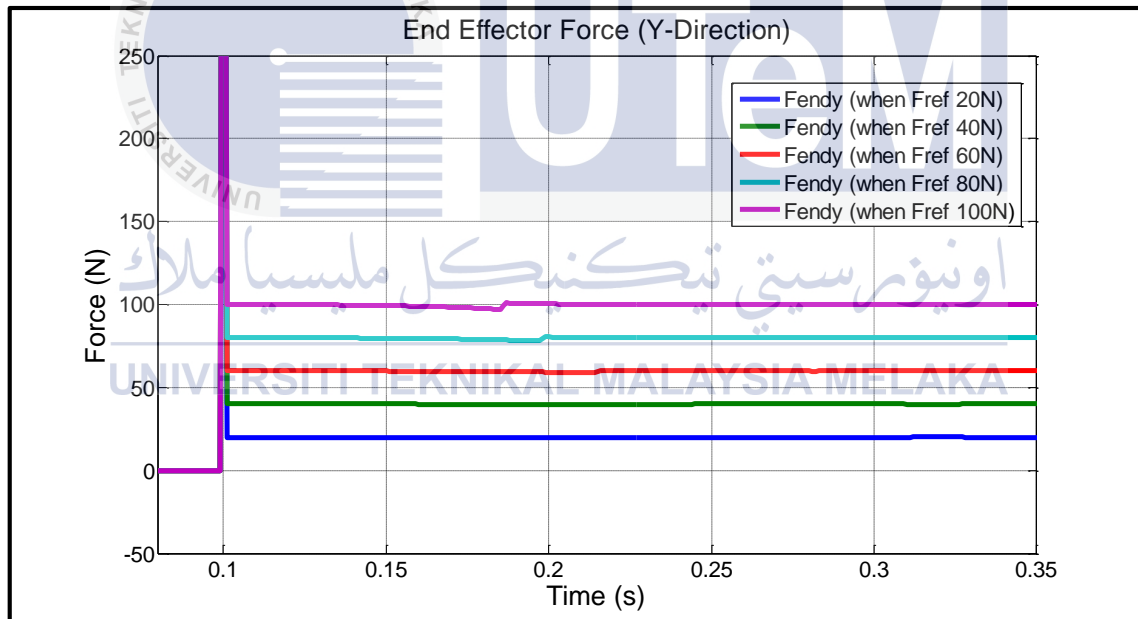


Figure 4.15: Simulation 2 all end effector forces (Y-direction)

Figure 4.15 shows force that applied to end effector in y-direction with 5 different reference forces value at end effector in y-direction ($F_{ref(endy)}$) which is 20N, 40N, 60N, 80N and 100N from $t = 0.08s$ until $t = 0.35s$. There were overshoots during $t = 0.1s$ due to the inertia but when the time increased, end effector in y-direction force (F_{endy}) become stable and

same as the reference force that had been given to the system. However, there were fluctuations during collision between end effector and environment (floor). After collision, end effector in y-direction force (F_{endy}) become stable again. This situation also applied for end effector in x-direction force (F_{endx}). Full end effector in y-direction force (F_{endy}) and end effector in x-direction force (F_{endx}) graph was attached at the Appendix H.

4.5.3 Conclusion

The force control of end effector muscles control was successfully achieved. By using this method, the end effector force can be controlled by user desired. The reason why end effector in y-direction force (F_{endy}) fluctuated because the impact from the collision make the end effector to bound back a little.

Although end effector force had been successfully controlled, there are one disadvantage by using this control method which is at the beginning force reference had been given to the system, there were overshoot force at all muscles. This happen due to inertia and the system make the end effector force immediately changed from 0 N to the desired reference force. Through this, it had possibility to damage the actuator that acted as muscle if the overshoot value to large.

Lastly, from this Simulation it concluded that if force references for end effector increased, it will increased the force that applied to the shoulder mono-articular muscle (l_{m1}) elbow mono-articular muscle (l_{m2}) and biar-articular muscle (l_{m3}) because all the muscles indirectly effected end effector force.

CHAPTER 5

CONCLUSION AND RECOMMENDATION

5.1 Introduction

This chapter will conclude the research finding and evaluation performance of the robot manipulator.

5.2 Conclusion

This research focusing on force control of musculoskeletal manipulator in the presence of environment contact. By using disturbance observers designed in workspace and muscle-space, force control were simulated in two different schemes which is independent muscle control and end effector muscle control.

Through independent muscle control scheme, force at all muscles was able to be controlled. Although all muscles force can be control, by using this scheme there are one major disadvantage which is the end effector force of the musculoskeletal manipulator can't be controlled specifically as desired by user. So, this make independent muscle control scheme only can be used by limited application.

Another force control scheme that had been tested was end effector force control. By using this scheme the end effector force was able to control specifically as desired by the user. This make end effector force control scheme suitable for any application in the industry. Even though this scheme suitable for any application, there are one disadvantage by using this scheme,

where at the initial condition, the large amount of force is required to make the end effector force same as desired by the user. This mean, linear actuator with high force capability is required for this scheme. If the linear actuator with low force capability had been used, there are chance for the actuator to damage or the end effector force not same as desired force by the user in the beginning.

5.3 Recommendation

For the recommendation, there are a lot improvement can be made in force control scheme. One of the improvement can be made is to combine the independent muscle control scheme with end effector control scheme. By combining this two scheme, it can prevent the muscles of the manipulator to damage and making end effector force able to be controlled perfectly according the user desired.

Other than that, it possible to add signal processing such as filter, amplifier and regulator to make force control scheme to work more precisely in term of force tracking. By adding all the signal processing to the force control scheme, the settling time and accuracy can be improve. By using this, there is possibility to overcome the overshoot problem in the beginning.

REFERENCES

- [1] - Y.S. Khong “Proton Tanjung Malim Plant - Building The Next Generation of Cars”
[online] Available at:
http://www.autoworld.com.my/v2/news/nb_details.asp?awReviewID=1824&awCatID=RT.ATC.CAR.FS [access 30 October 2013].
- [2] - “KUKA Company History” Available at: <http://www.kuka-robotics.com/en/company/group/milestones/> [access 04 November 2013].
- [3] - P. Bigras, M. Lambert, and C. Perron “Robust Cforce Controller for Industrial Robots: Optimal Design and Real-Time Implementation on a KUKA Robot” IEEE Transaction On Control System Technology, Vol. 20, No. 2, March 2012.
- [4] - X. Xin, “Swing-up and Stabilizing Control for Two-Link Underactuated Robot with Flexible Elbow Joint” Proceedings of the 30th Chinese Control Conference, July 2011.
- [5] - A.A. Ata. & H. Johar “Dynamic Simulation of Task Constrained of A Rigid-Flexible Manipulator” pp. 61 - 66, International Journal of Advanced Robotic Systems, Volume 1 Number 2, April 2004
- [6] - K. Tahara and H. Kino “Iterative Learning Scheme for a Redundant Musculoskeletal Arm: Task Space Learning with Joint and Muscle Redundancies”, 2010 International Conference on Broadband, Wireless Computing, Communication and Applications, Sept. 2010.
- [7] - H.Kino, S.Kikuchi, T.Yahiro and K.Tahara “ Basic Study of Biarticular Muscle’s Effect on Muscular Internal Force Control Based on Physiological Hypotheses”, 2009 IEEE International Conference on Robotics and Automation, May 2009.

- [8] - Y. Nakanishi, T. Izawa, T. Kurotobi and J. Urata, Kei Okada and Masayuki Inaba "Achievement of Complex Contact Motion with Environments by Musculoskeletal Humanoid using Humanlike Shock Absorption Strategy, 2012 IEEE/RSJ International Conference in Intelligent Robot and Systems, Oct 2012
- [9] - Y. Nakanishi, N. Ito, T. Shirai, M. Osada, T. Izawa, S. Ohta, J. Urata, K. Okada and M. Inaba "Design of Powerful and Flexible Musculoskeletal Arm by Using Nonlinear Spring Unit and Electromagnetic Clutch opening Mechanism" 2011 11th IEEE-IRS International Conference on Humanoid Robots Bled, Slovenia, Oct. 2011
- [10] - A. Z. Shukor and Y. Fujimoto "Force Control of Musculoskeletal Manipulator" 12th IEEE International Workshop on Advanced Motion Control, March 2012
- [11] - "Simulation Overview" [online] Available at: <http://msdn.microsoft.com/en-us/library/bb483076.aspx> [access 04 November 2013]
- [12] - "Why SolidWork?" [online] Available at: <http://www.solidworks.com/> [access 07 November 2013]
- [13] - "MATLAB Advantage for User" [online] Available at: <http://www.mathworks.com/> [access 07 November 2013]
- [14] - M. Gousasmi, M. Ouali, B. Fernini and M. Meghartria "Kinematic Modelling and Simulation of a 2-R Robot Using SolidWorks and Verification by MATLAB/Simulink" International Journal of Advanced Robotic Systems, Feb. 2008
- [15] - T. Wongratanaphisan and M. O. T. Cole "Robust Impedance Control of a Flexible Structure Mounted Manipulator Performing Contact Tasks", IEEE Transactions on Robotics, Vol.25, No.2 April 2009
- [16] - R. Kikuuwe, T. Yamamoto, and H. Fujimoto "A Guideline for Low-Force Robotic Guidance for Enhancing Human Performance of Positioning and Trajectory Tracking: It Should Be Stiff and Appropriately Slow", IEEE Transactions On Systems, Man and Cybernetics-Part A: System and Humans, Vol.38, No.4, July 2008
- [17] - Y. Bosheng, S. Bao, L. Zhengyi, X. Shuo, and T. Xiaoqi "A Study of Force and Position Tracking Control for Robot Contact with an Arbitrarily Inclined Plane", International Journal of Advanced Robotics Systems, Sept. 2009

- [18] - N. Zemiti, G. Morel, A. Micaelli, B. Cagneau, and D. Bellot “On The Force Control of Kinematically Defective Manipulators Interacting With an Unknown Environment”, IEEE transactions on Control Systems Technology, Vol.18, No.2, March 2010
- [19] - R. V. Patel, H. A. Talebi, J. Jayander, and F. Shadpey “ A Robust Position and Force Control Strategy for 7-DOF Redundant Manipulators”, IEEE/ASME Transactions on mechatronics, Vol.14, No.5, Oct.2009
- [20] - A. Z. Shukor and Y. Fujimoto “ Force Control of Musculoskeletal manipulator Driven By Spiral Motors” , DOI 10.7305/automatika 54-1.307, March 2013
- [21] - Lisa Nocks “The Robot: The Life Story of a Technology” [online] page 122, Available at:
http://books.google.com.my/books?id=urEaBTl3v1QC&pg=PA122&lpg=PA122&dq=percentage+of+robot+usage+at+malaysia&source=bl&ots=L9umisZja_&sig=Vhq36qOPpHlmMH9keENx9MKuAs&hl=en&sa=X&ei=3SCvUrykDOGpiAfuwoDgCw&sqi=2&redir_esc=y#v=onepage&q=percentage%20of%20robot%20usage%20at%20malaysia&f=false [access 04 December 2013].
- [22] - J. J. Craig, Introduction to Robotics Mechanics and Control, 3rd Edition, United State of America, Pearson Education. Inc, 2005.

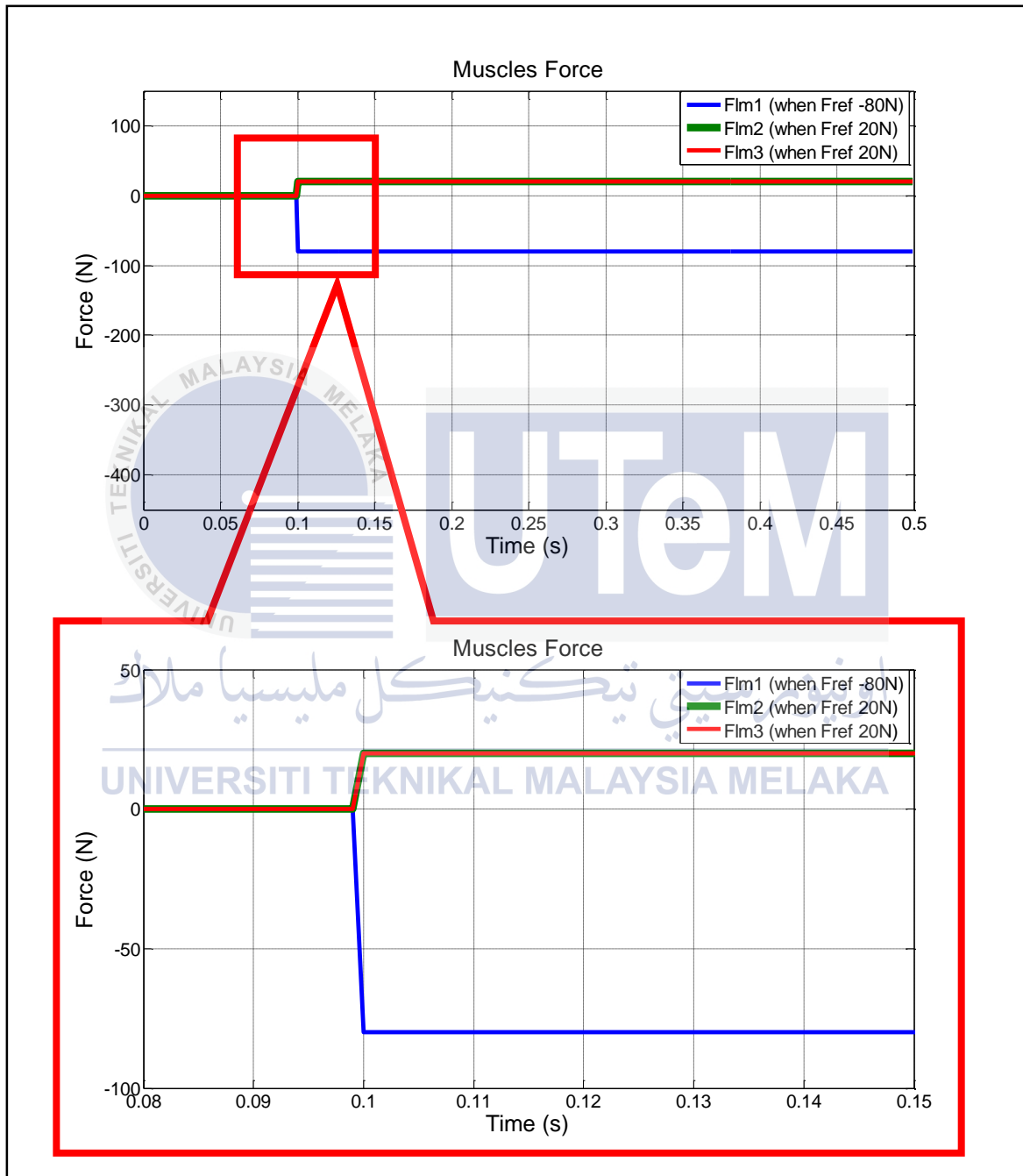
APPENDICES

- APPENDIX A - Simulation 1 muscle force results
- APPENDIX B - Simulation 1 end effector force results
- APPENDIX C - Simulation 1 muscle comparison results
- APPENDIX D - Simulation 1 end effector comparison results
- APPENDIX E - Simulation 2 muscle force results
- APPENDIX F - Simulation 2 end effector force results
- APPENDIX G - Simulation 2 muscle comparison results
- APPENDIX H - Simulation 2 end effector comparison results
- APPENDIX I - Two-link musculoskeletal manipulator modelling coding
- APPENDIX J - Force control algorithm coding

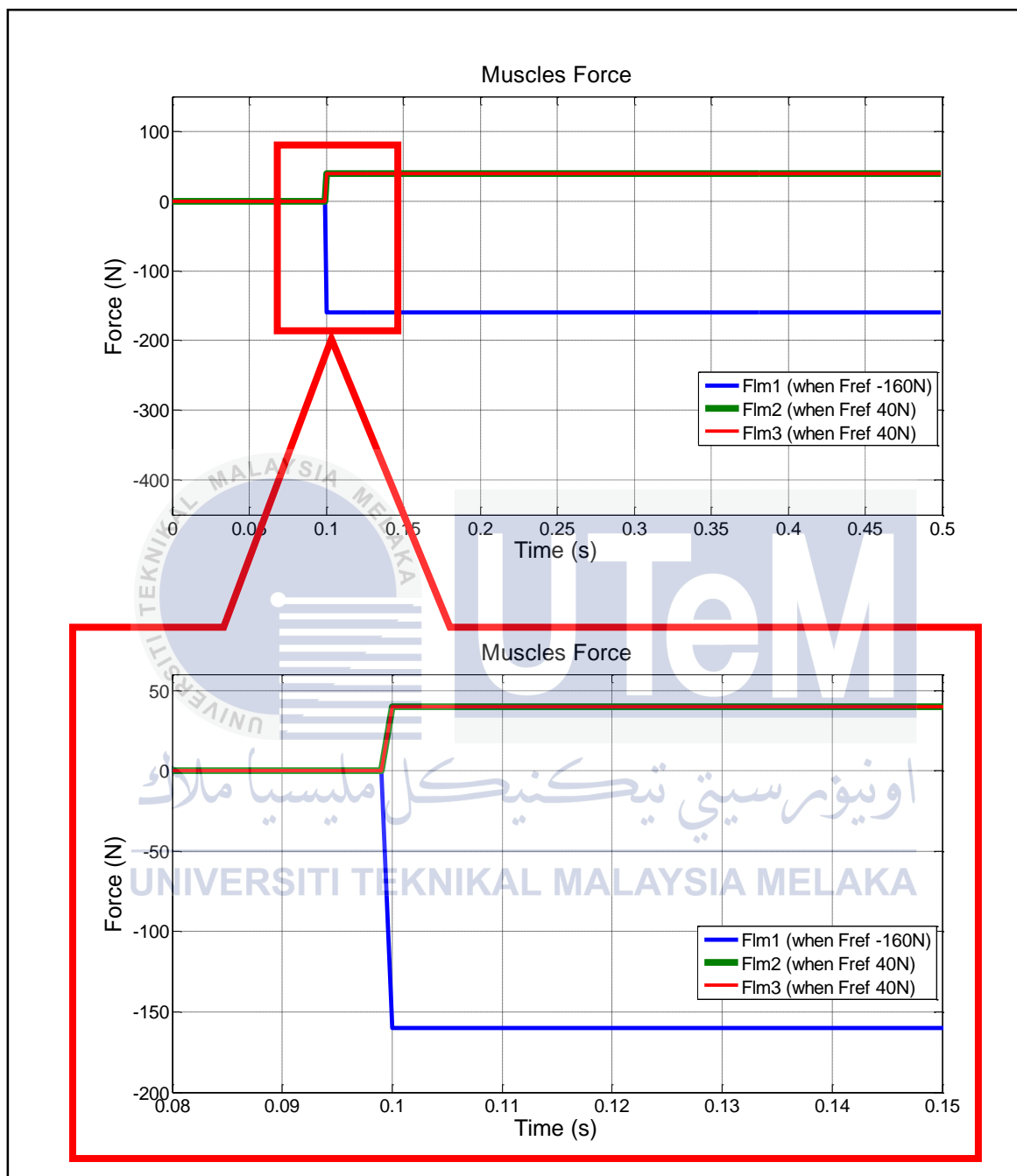
اونيورسيتي تيكنيكل مليسيا ملاك

UNIVERSITI TEKNIKAL MALAYSIA MELAKA

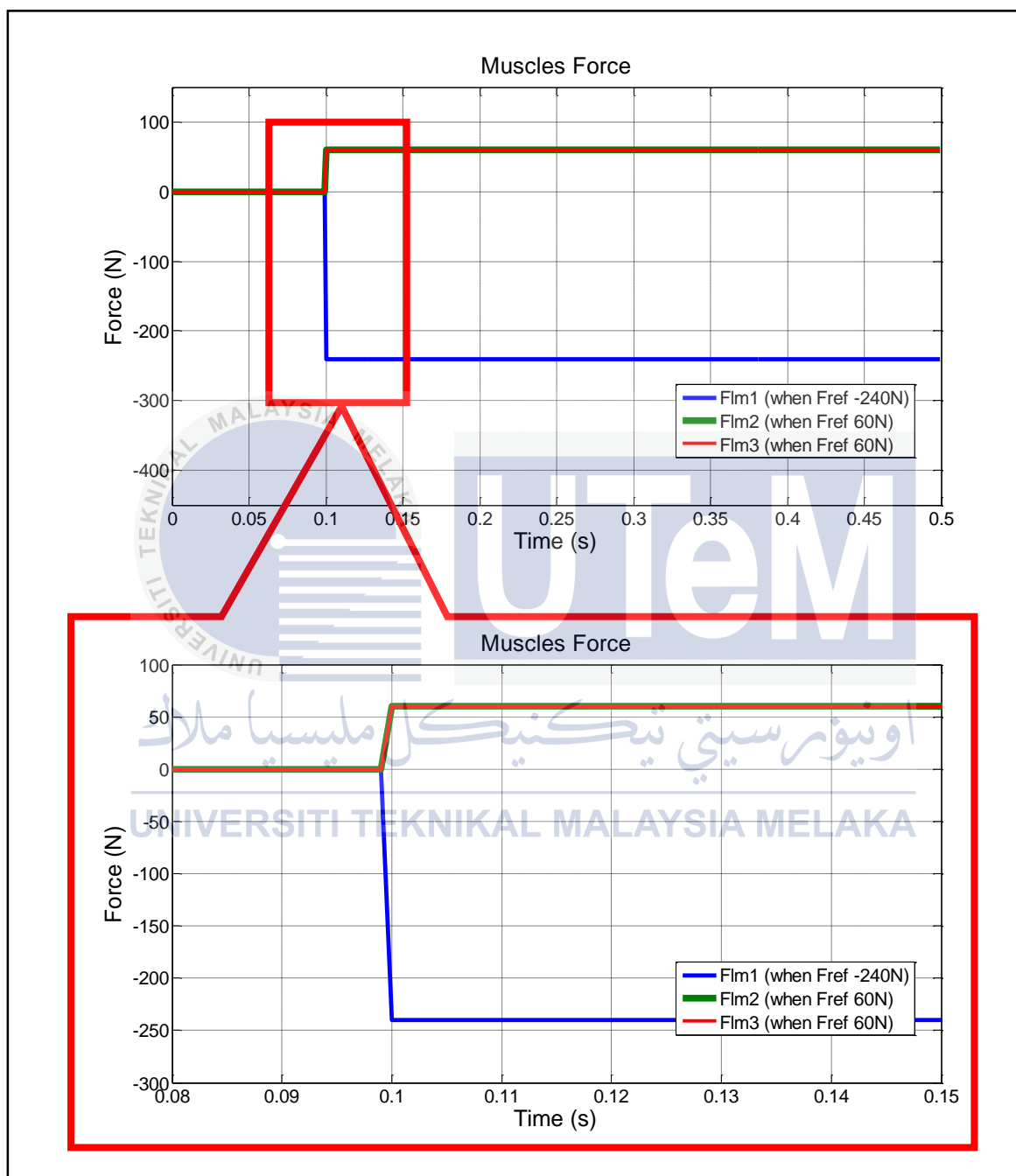
APPENDIX A



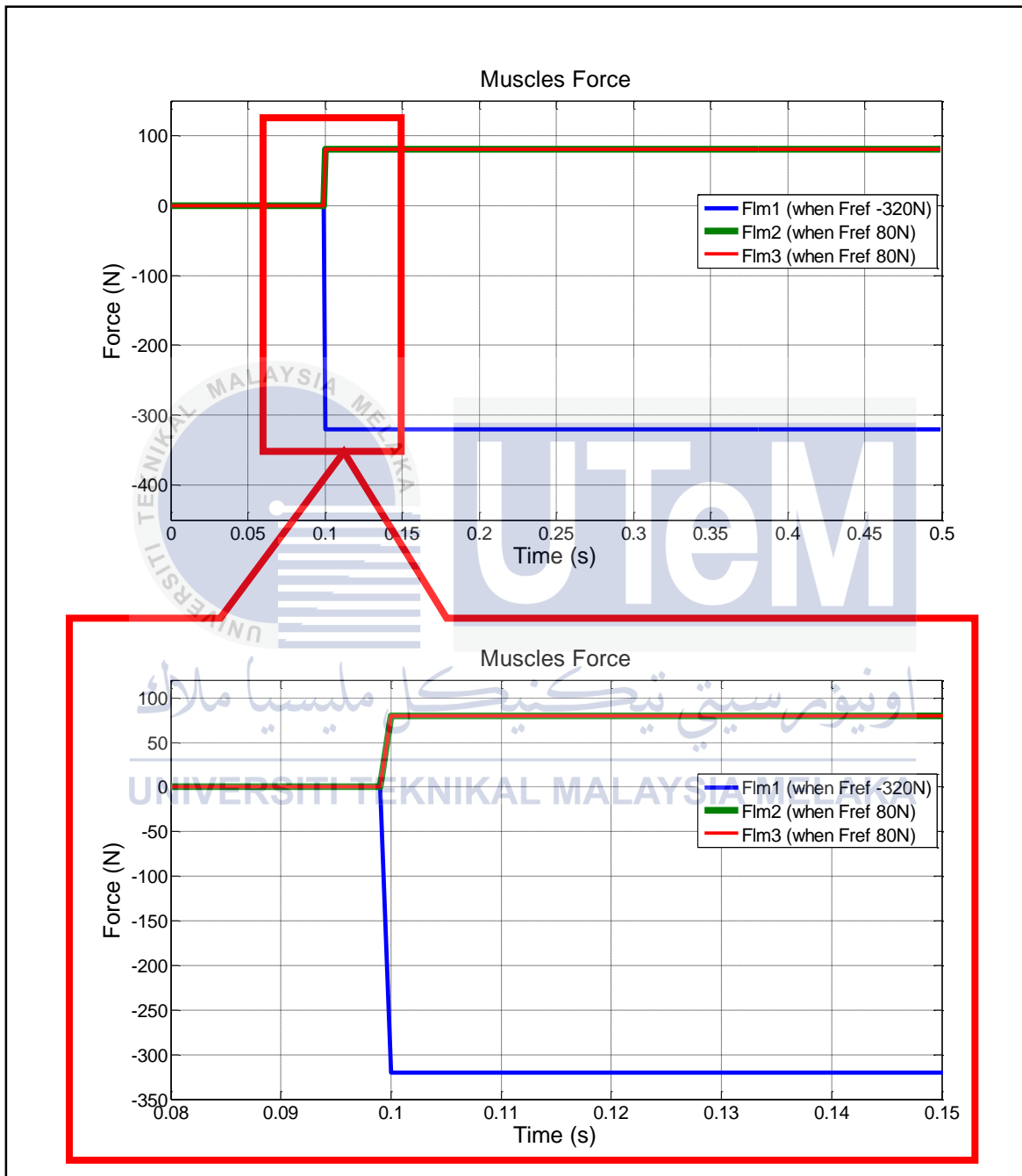
Muscles Force When Force References -80N and 20N



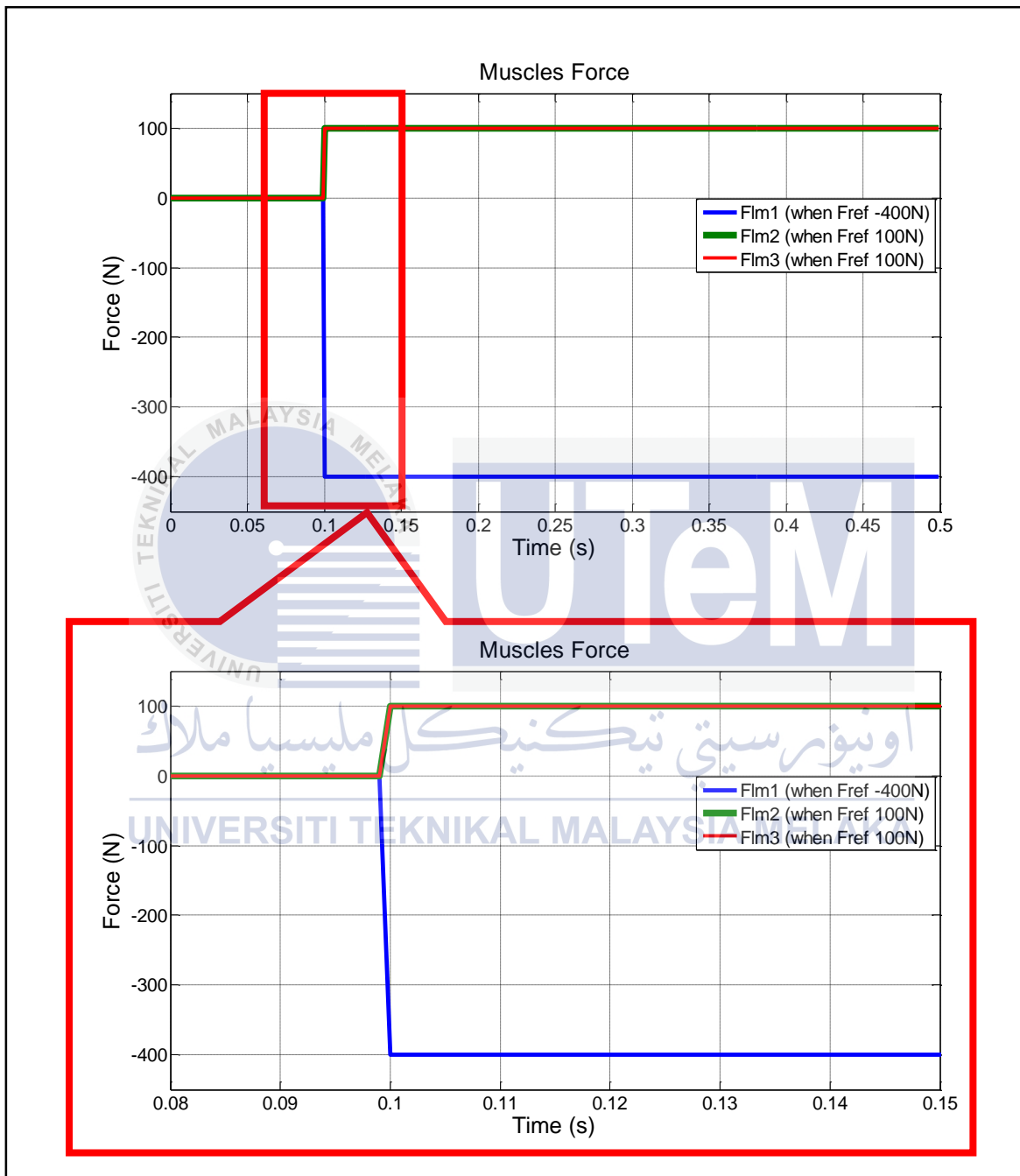
Muscles Force When Force References -160N and 40N



Muscles Force When Force References -240N and 60N

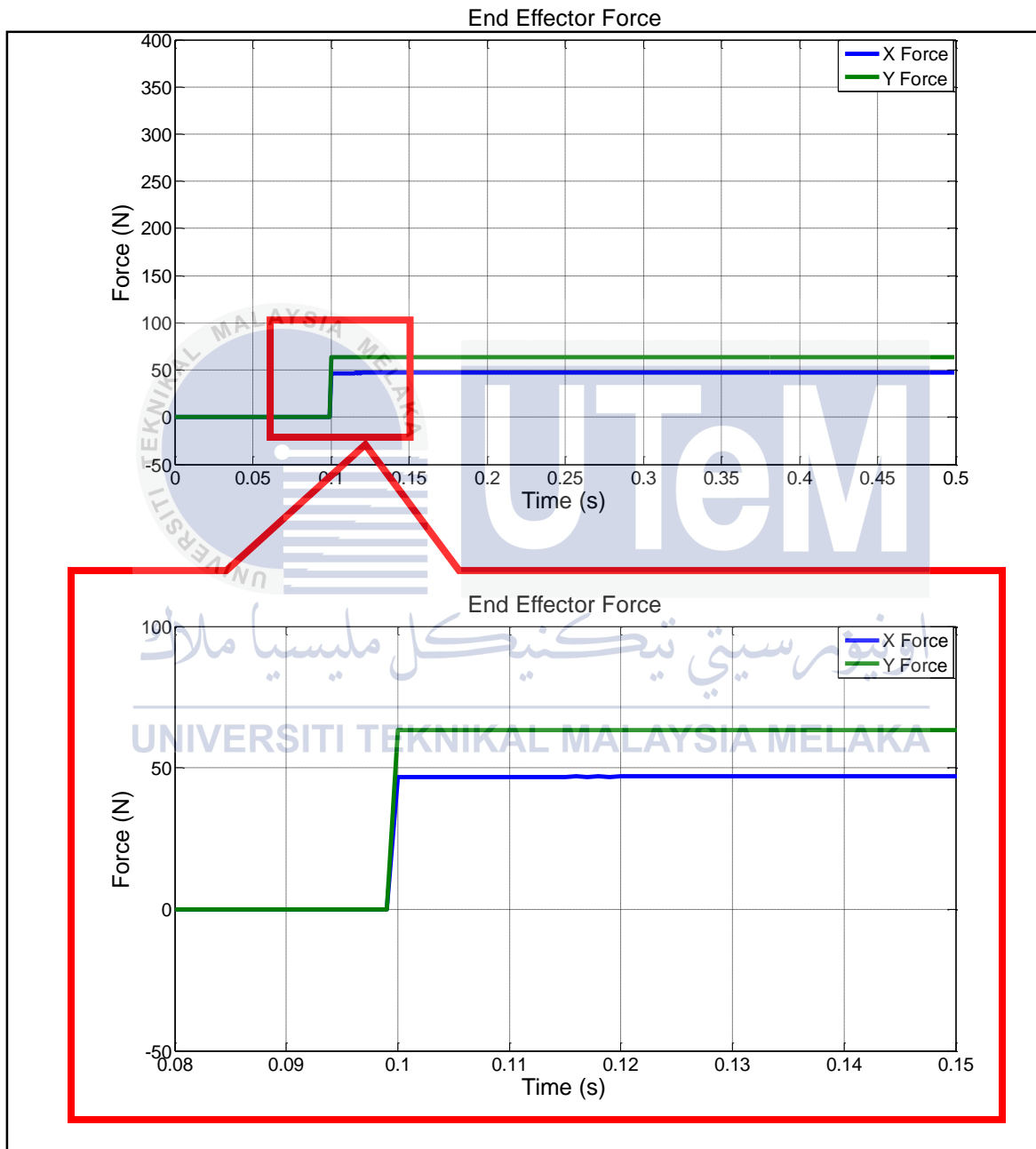


Muscles Force When Force References -320N and 80N

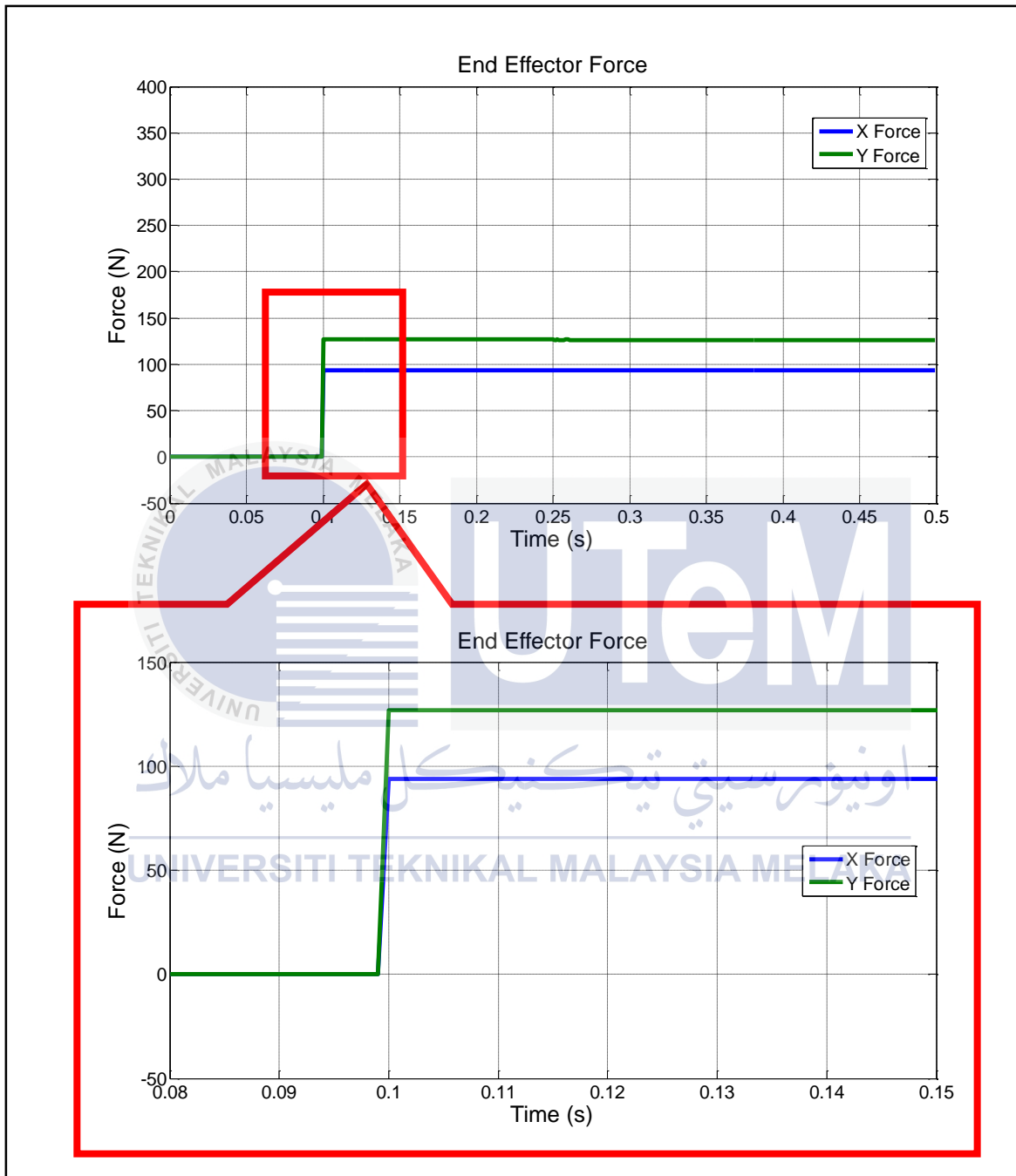


Muscles Force When Force References -400N and 100N

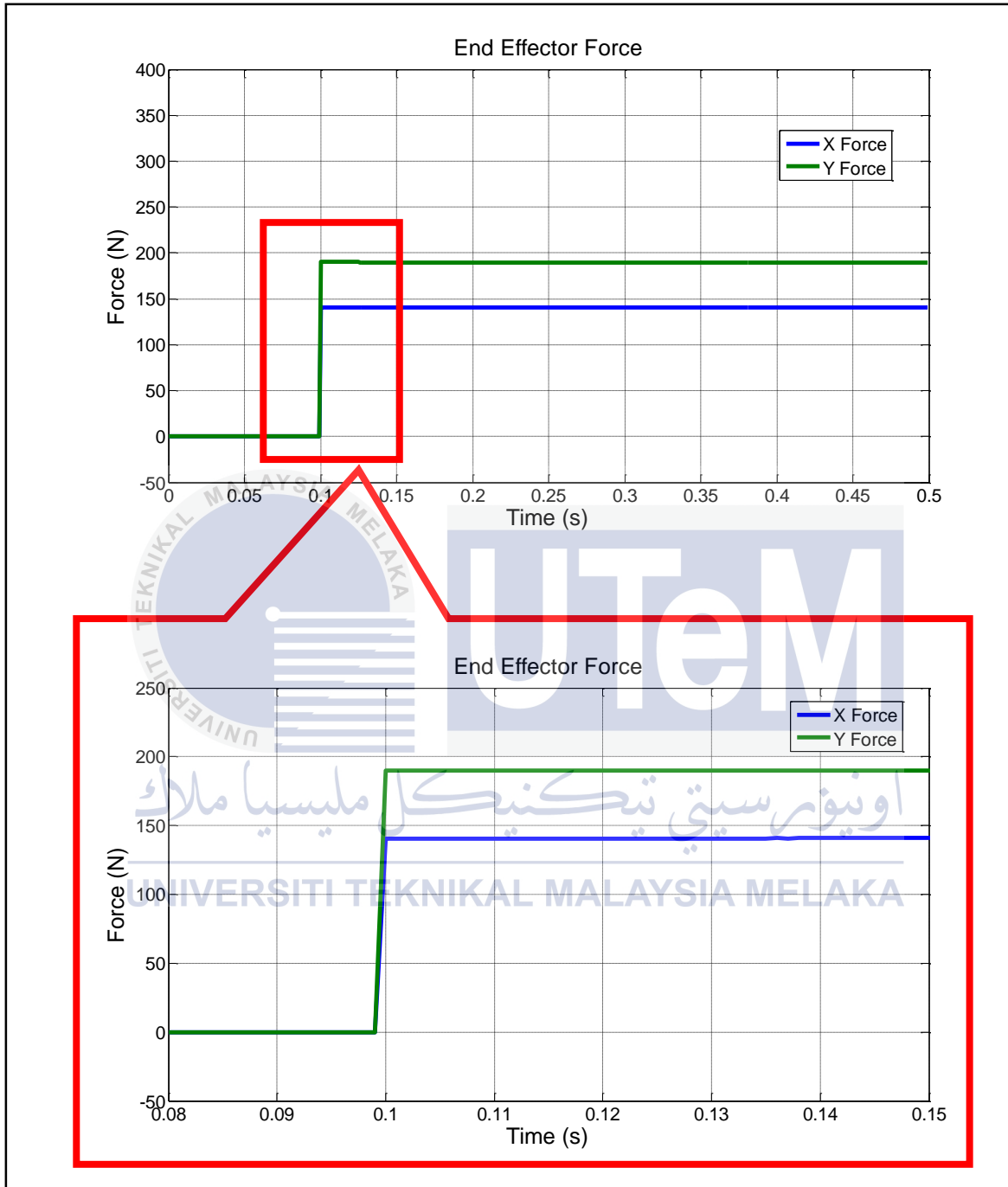
APPENDIX B



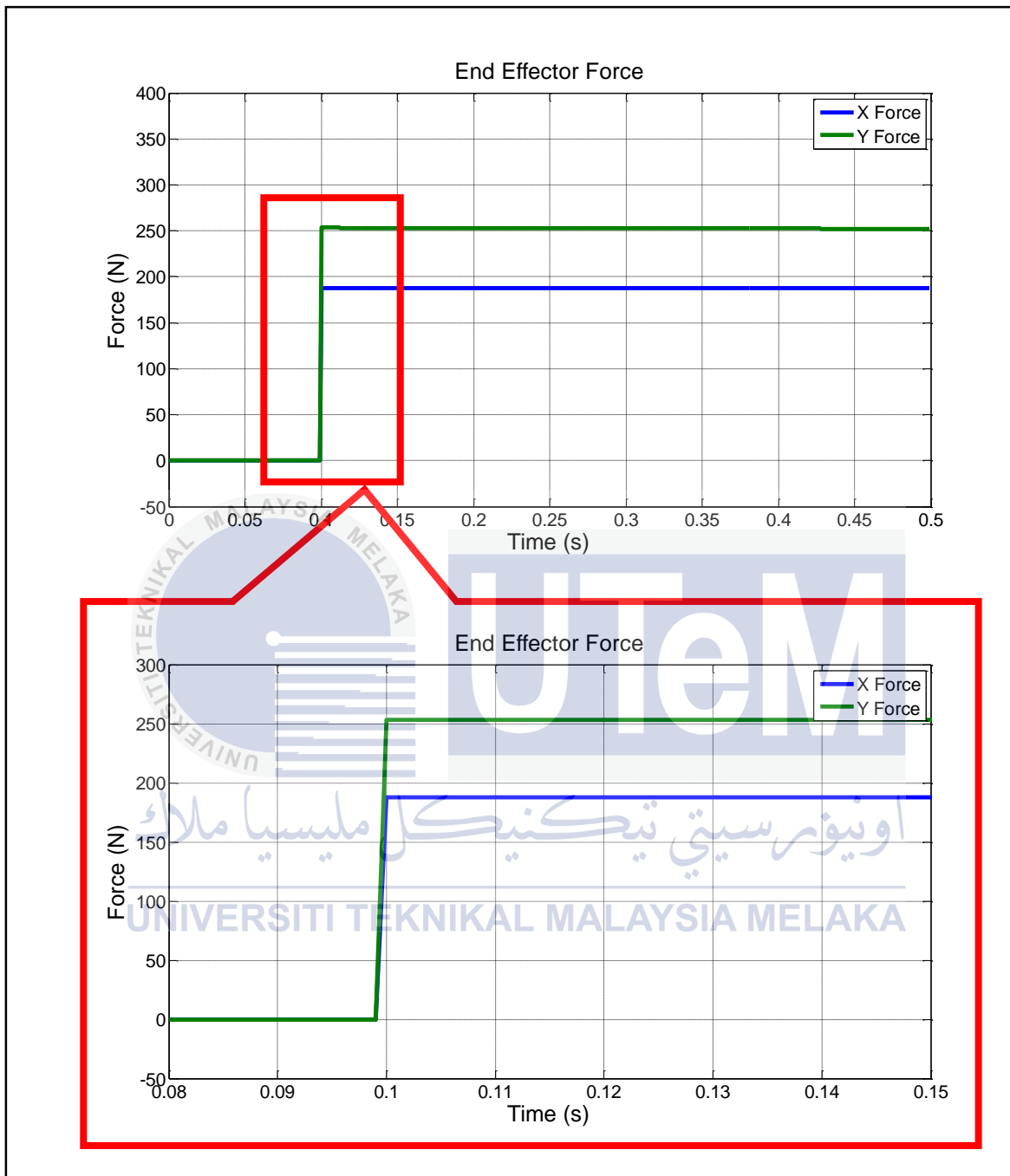
End Effector Force When Force References -80N and 20N



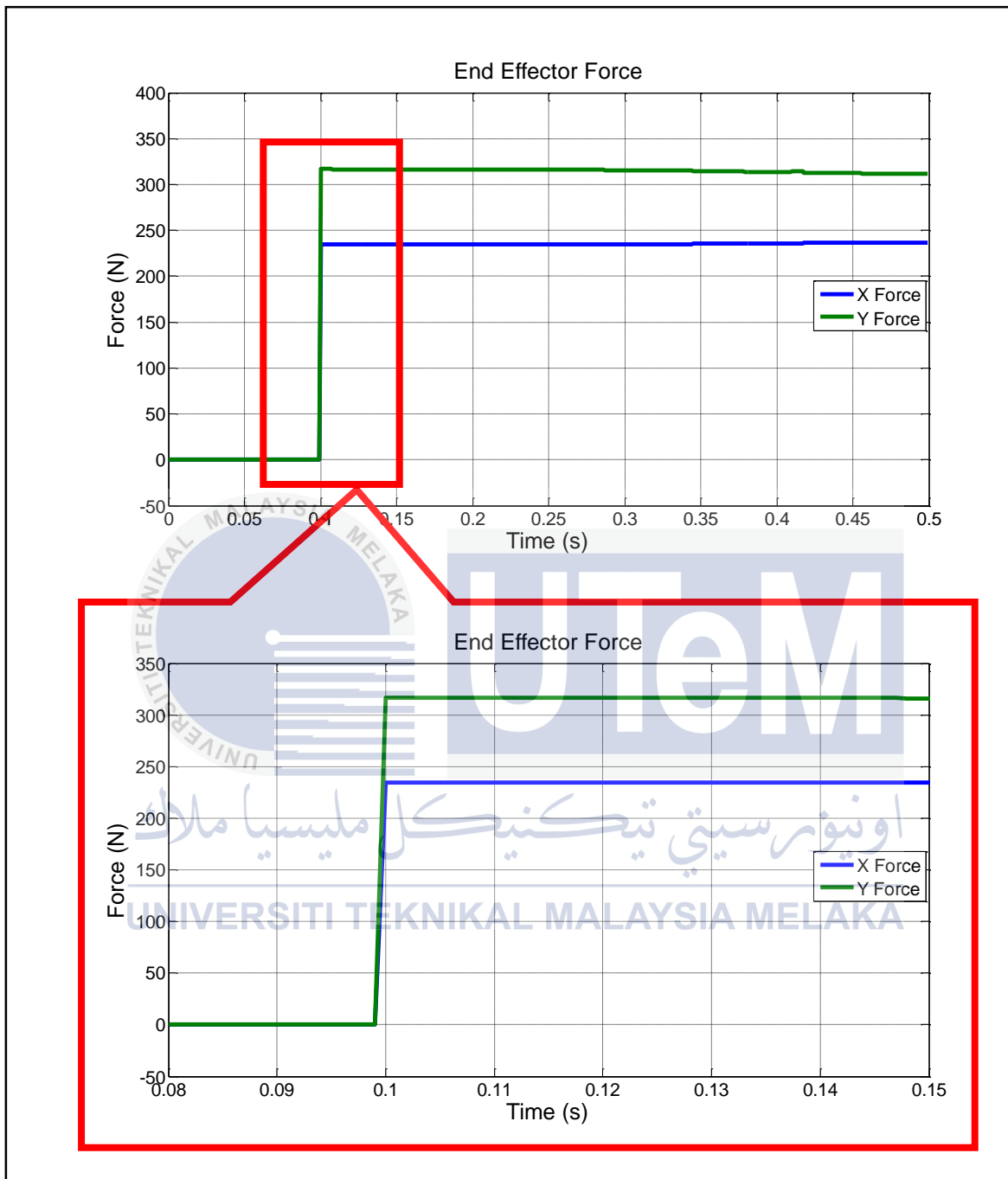
End Effector Force When Force References -160N and 40N



End Effector Force When Force References -240N and 60N

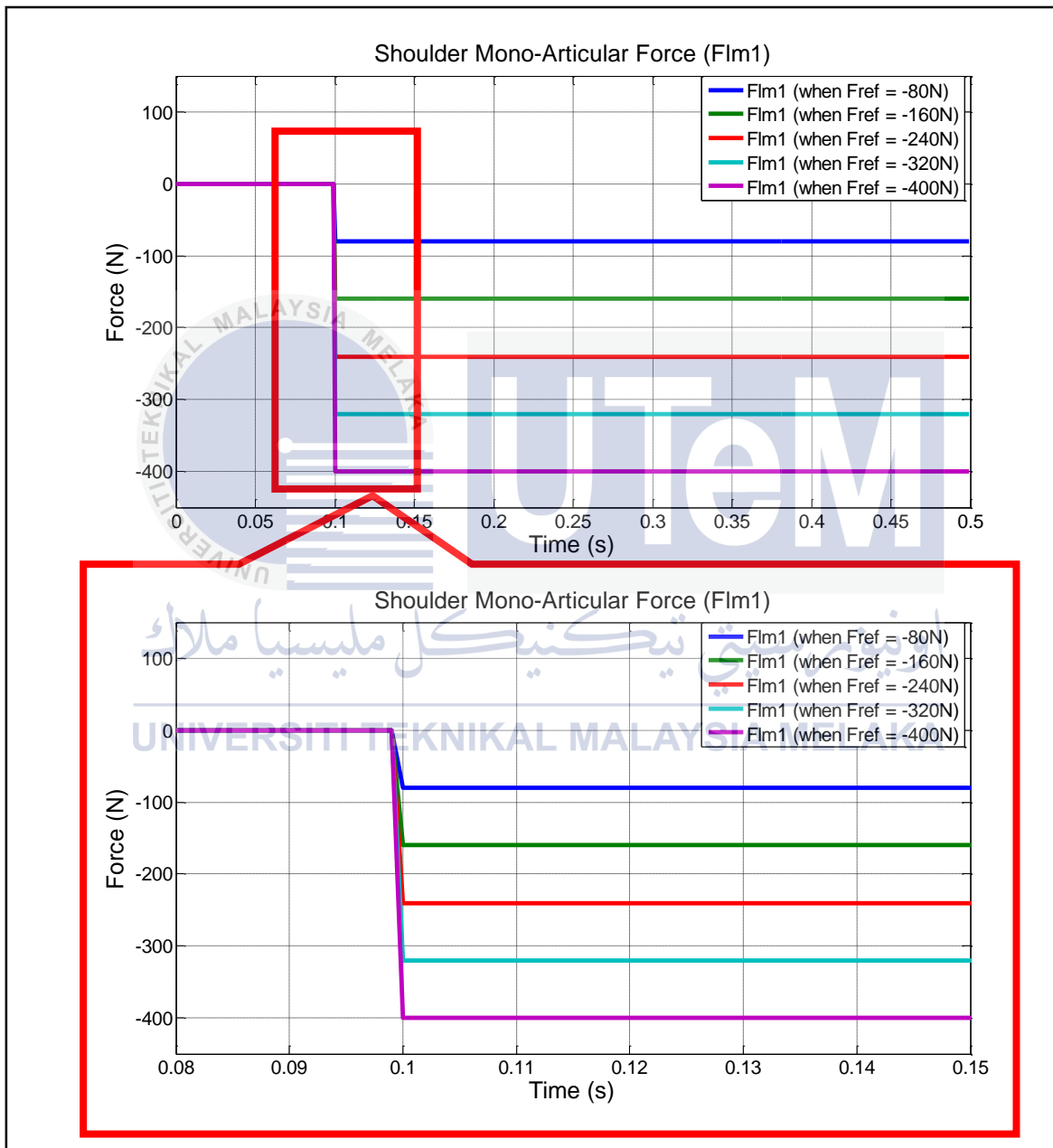


End Effector Force When Force References -320N and 80N

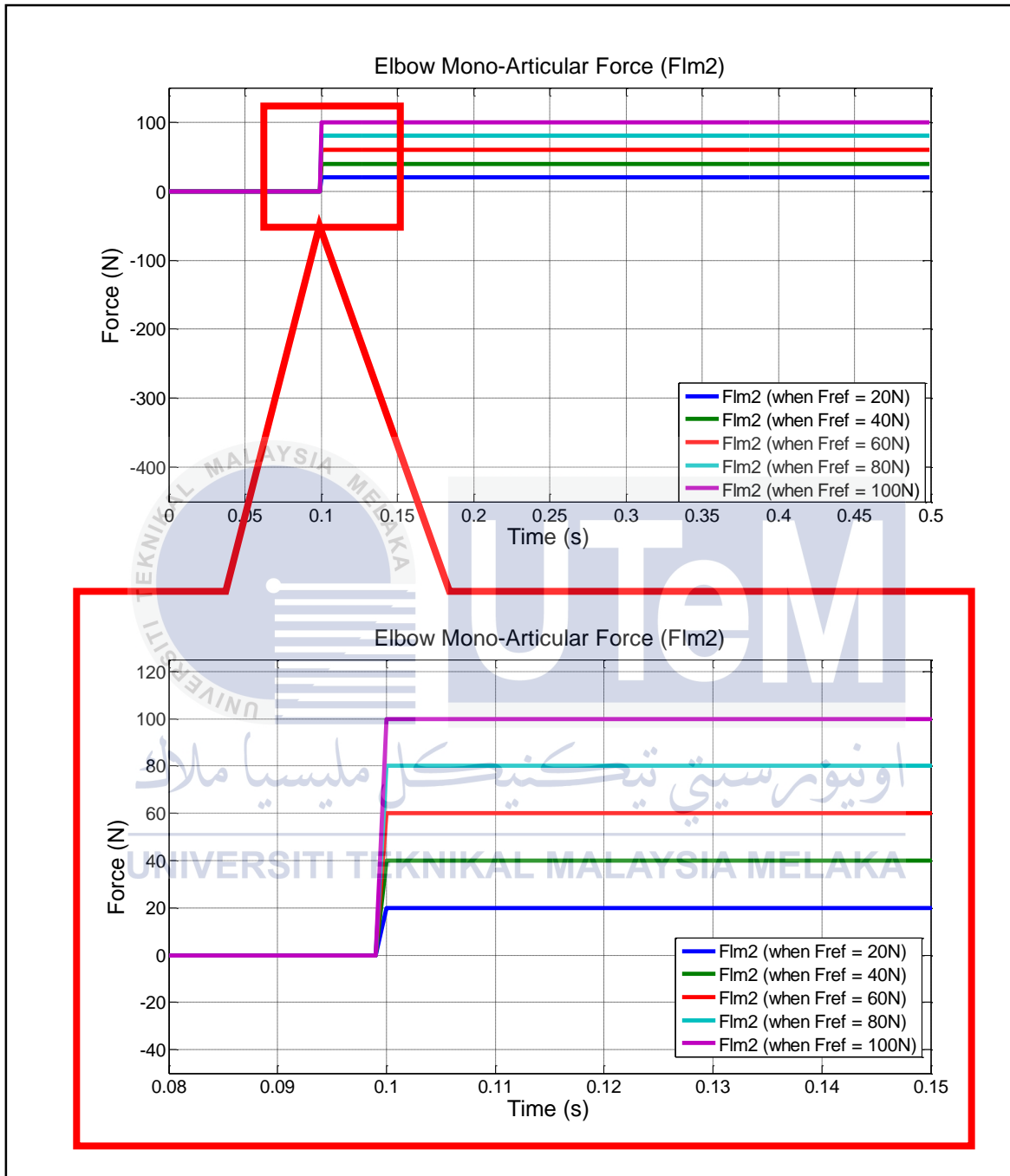


End Effector Force When Force References -400N and 100N

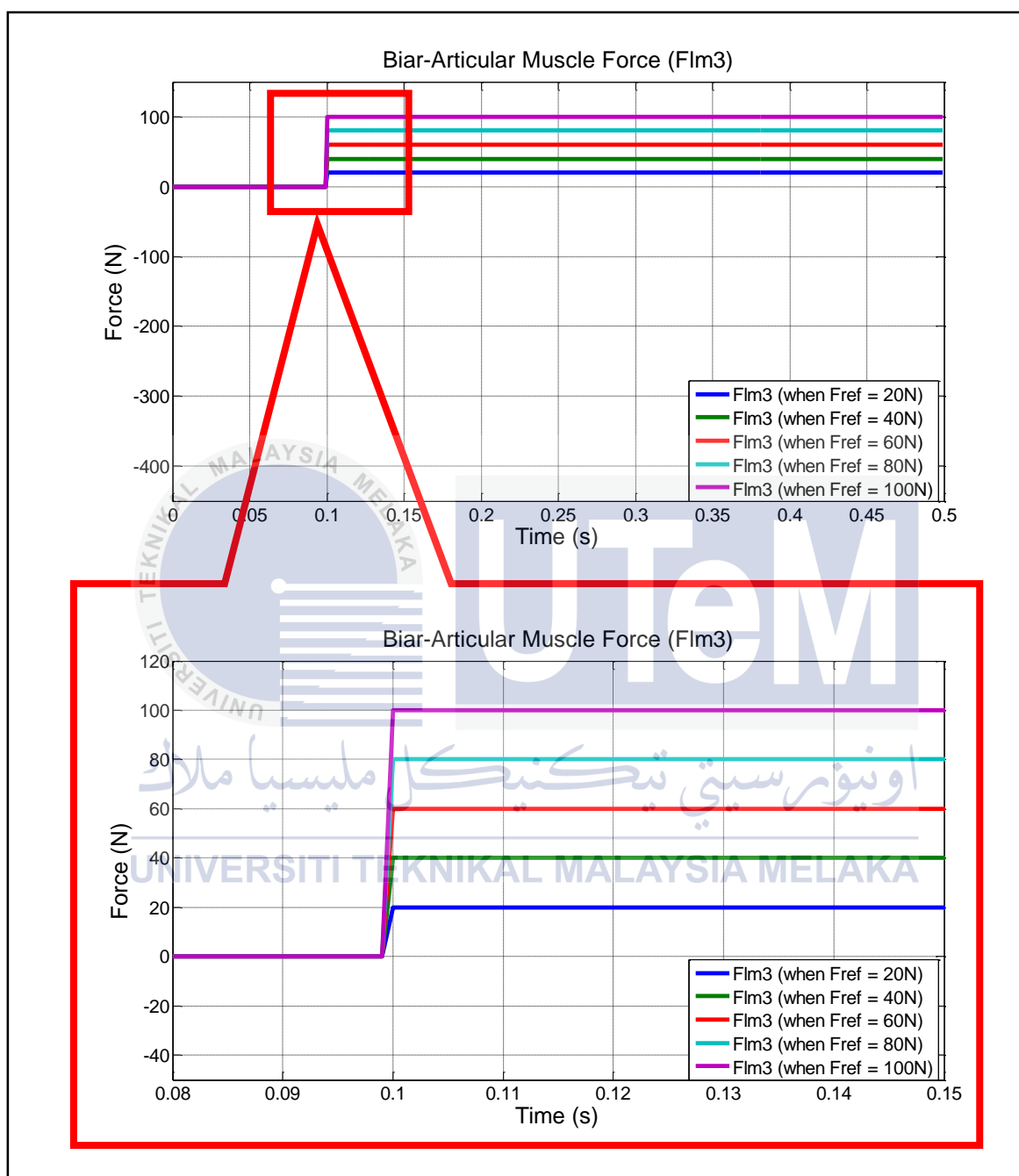
APPENDIX C



All shoulder mono-articular force data

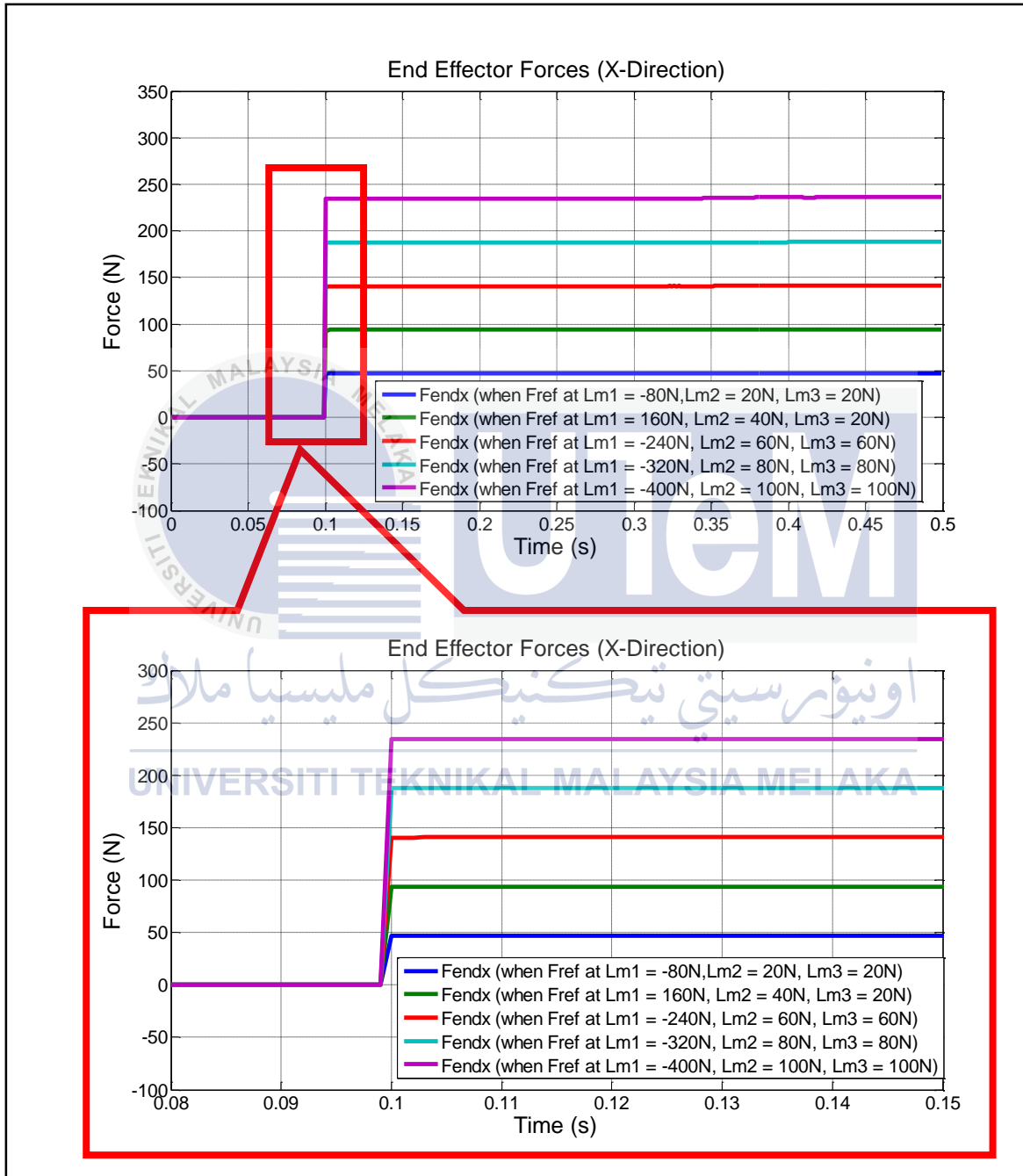


All elbow mono-articular force data

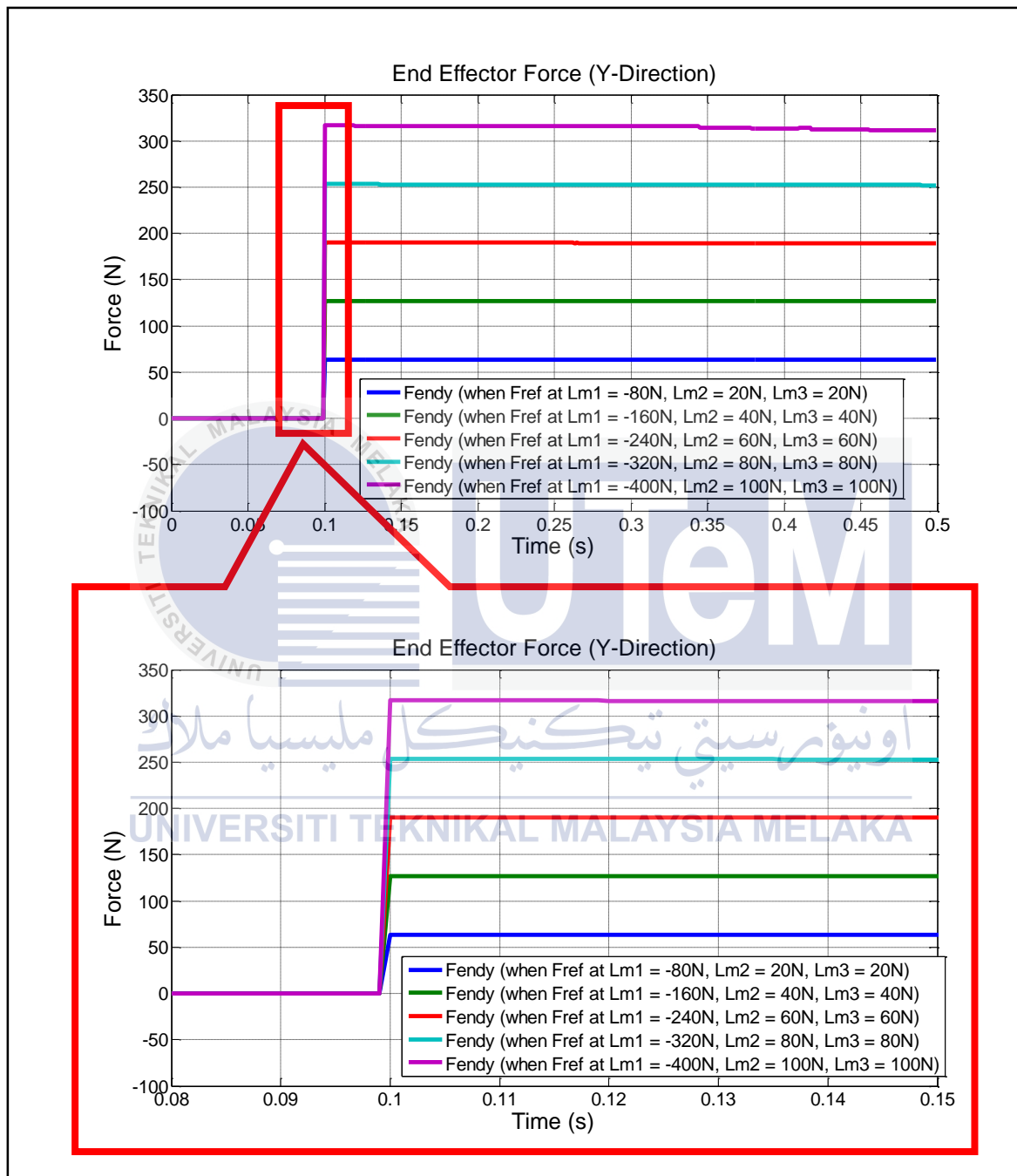


All biar-articular force data

APPENDIX D

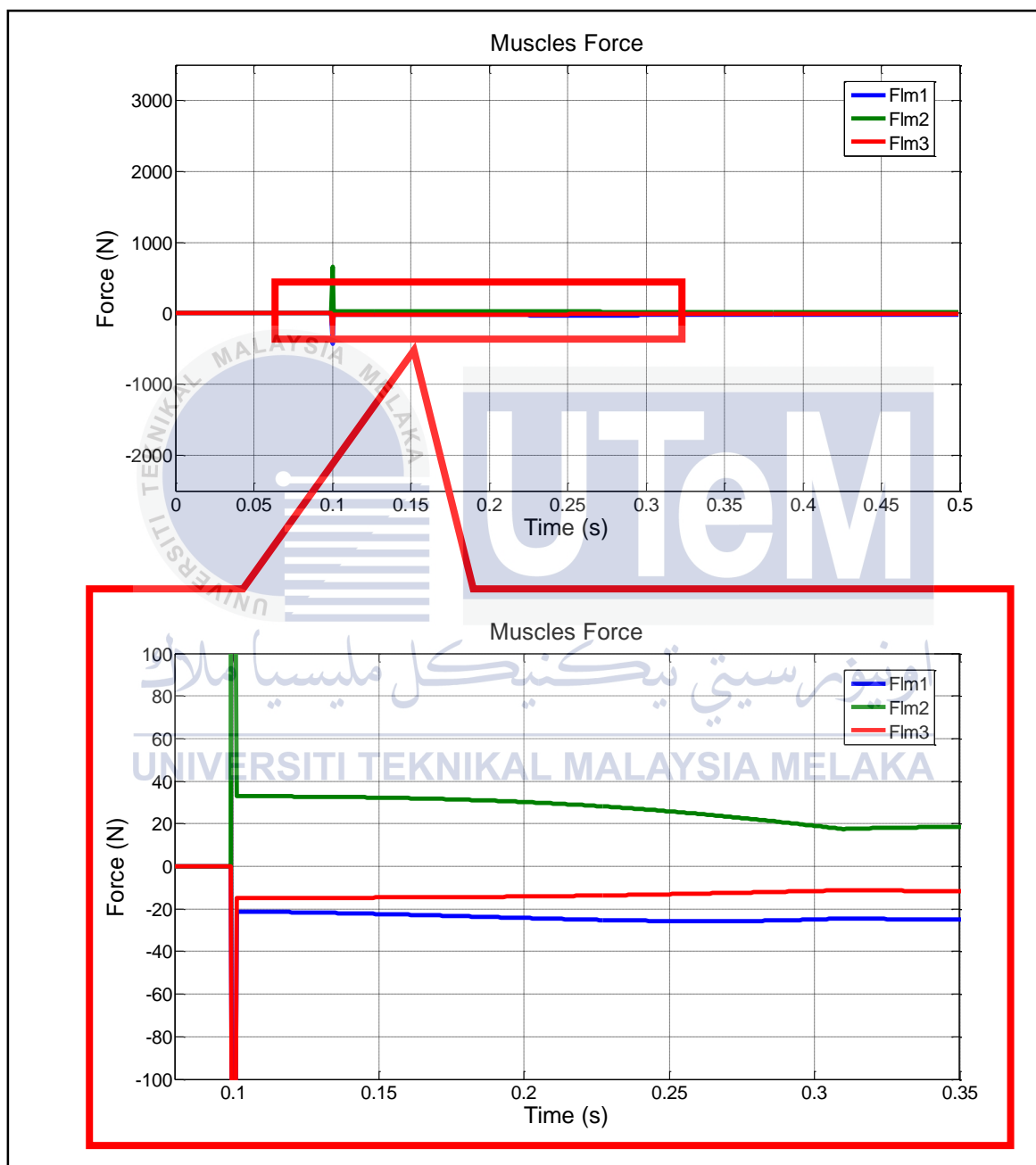


All end effector in x-direction force data

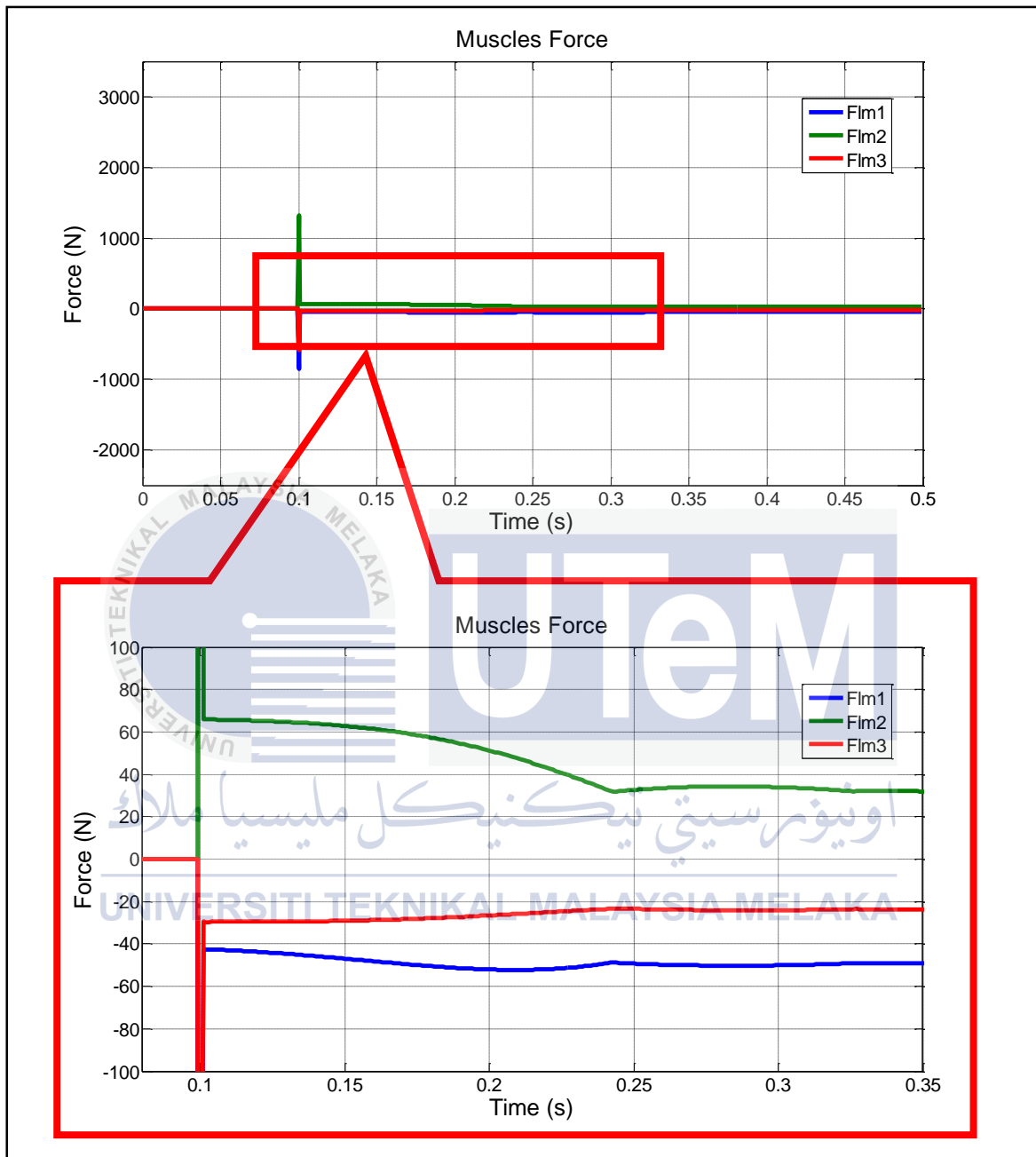


All end effector in y-direction force data

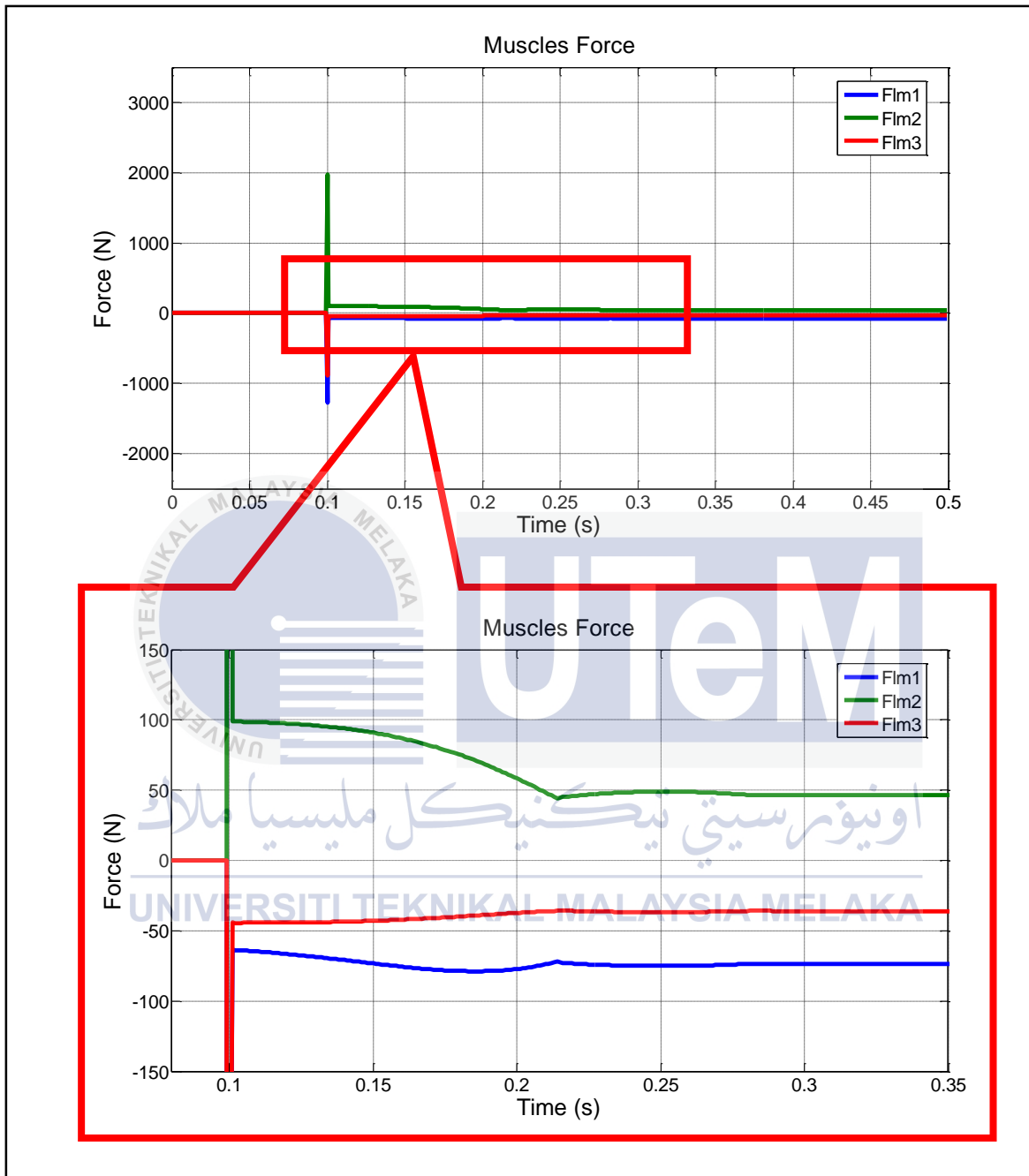
APPENDIX E



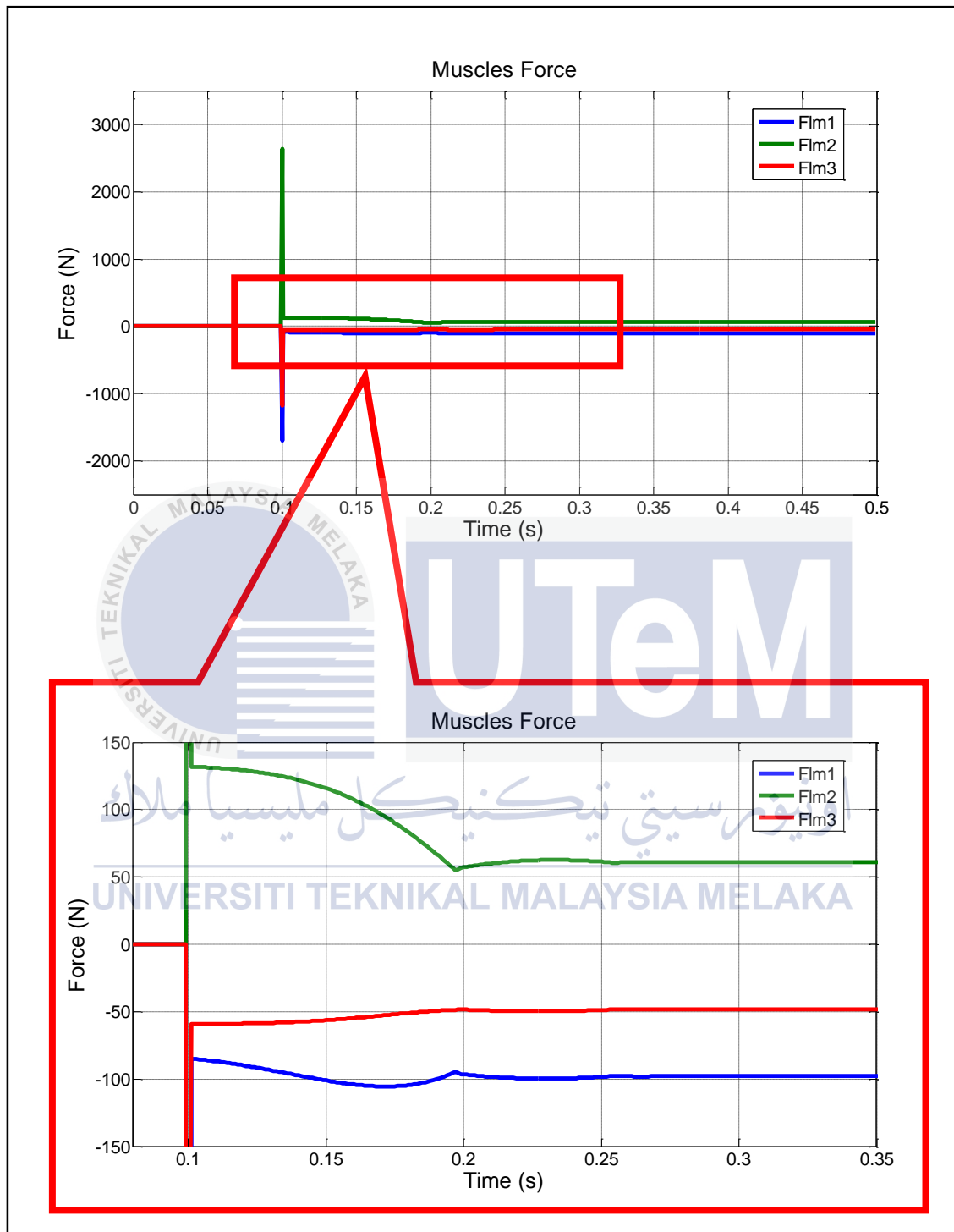
Muscles force when force reference 20N



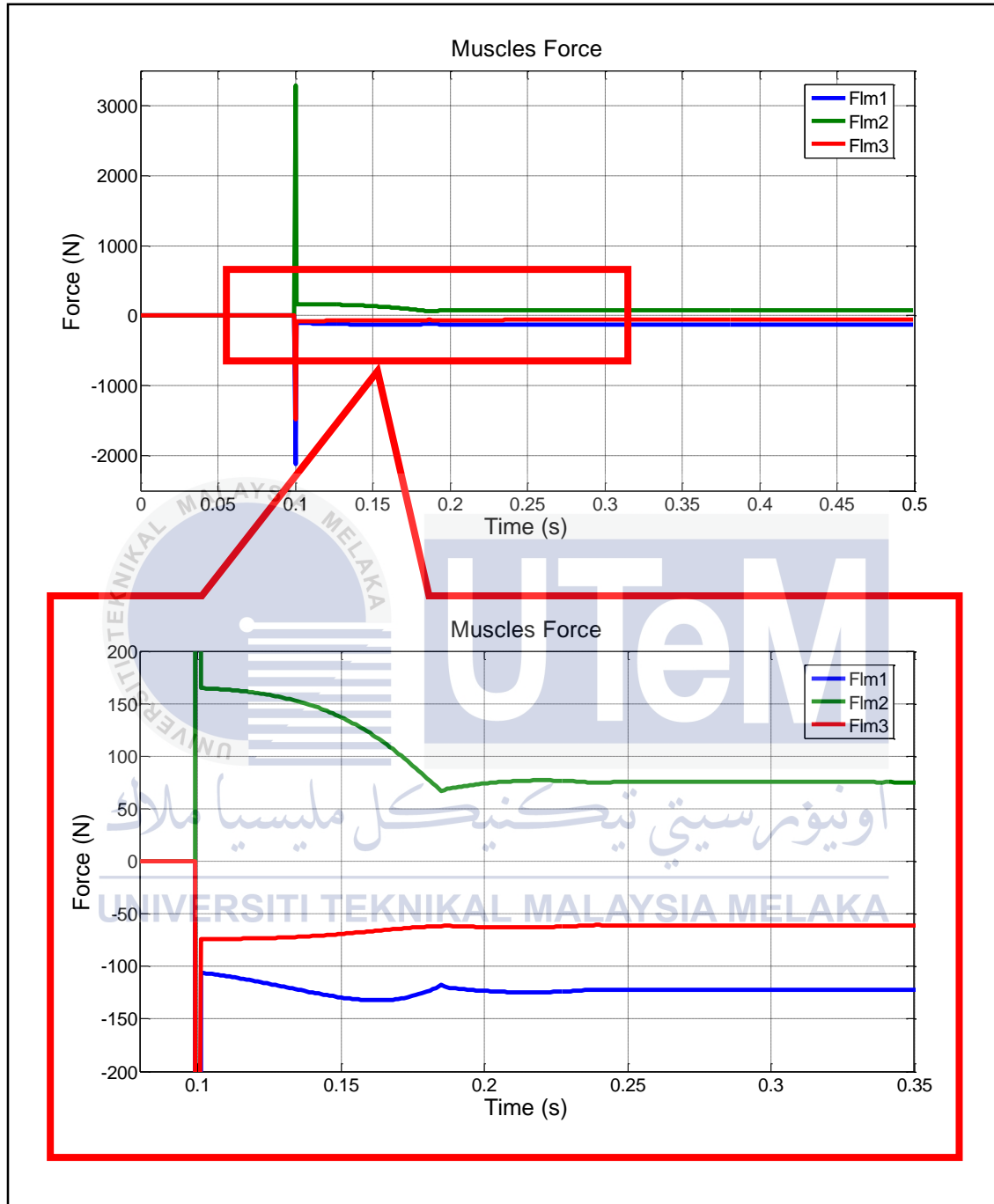
Muscles force when force reference 40N



Muscles force when force reference 60N

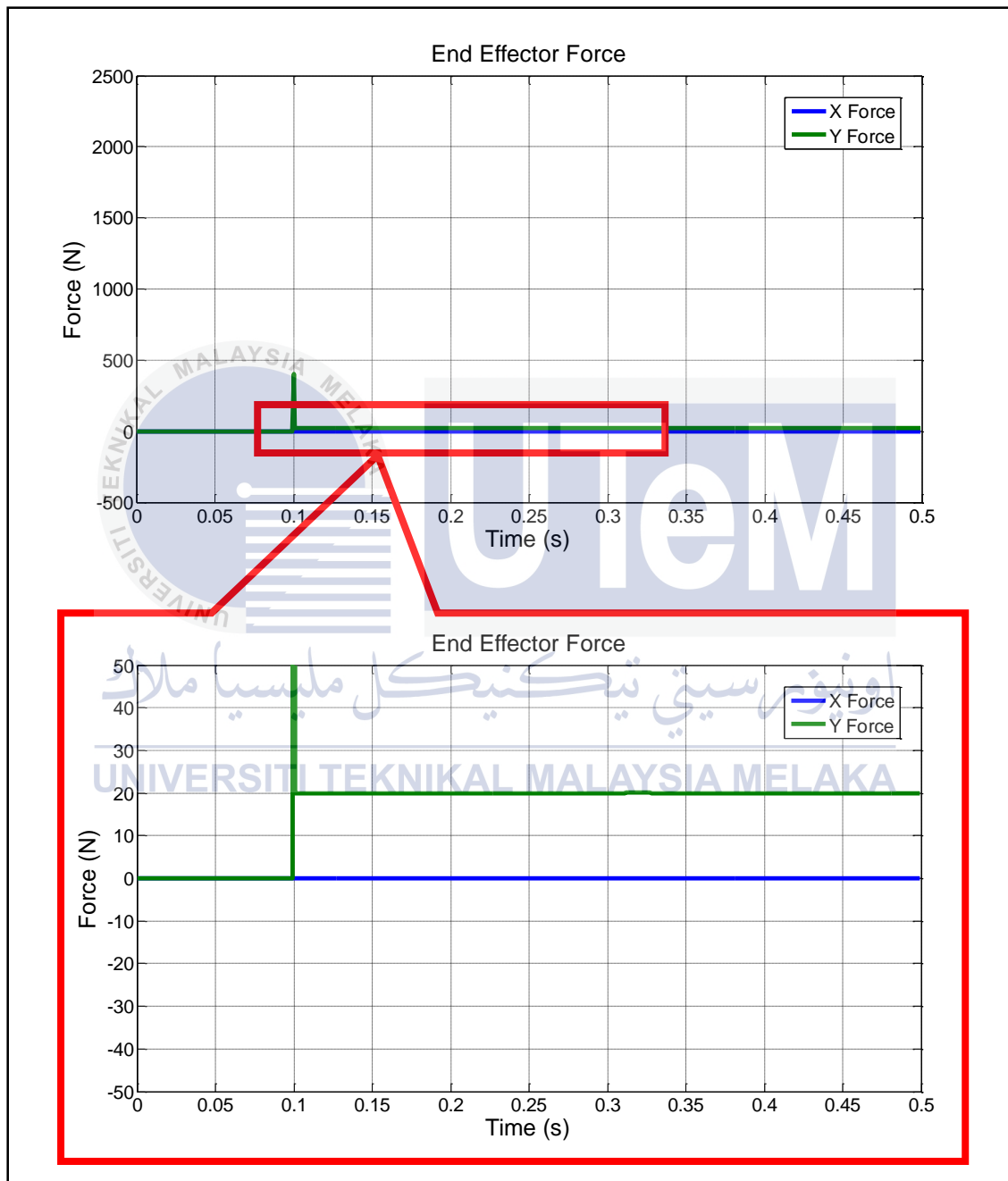


Muscles force when force reference 80N

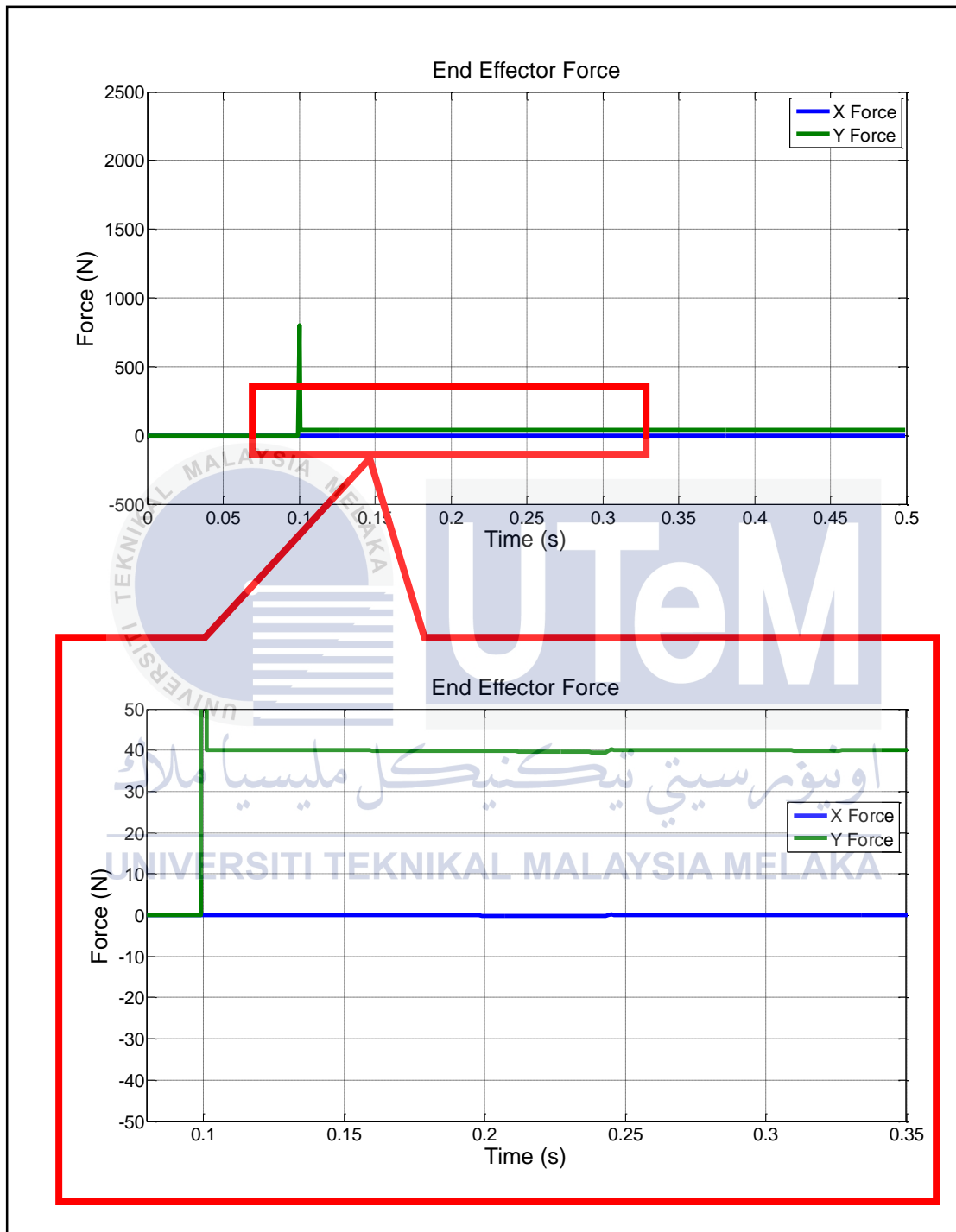


Muscles force when force reference 100N

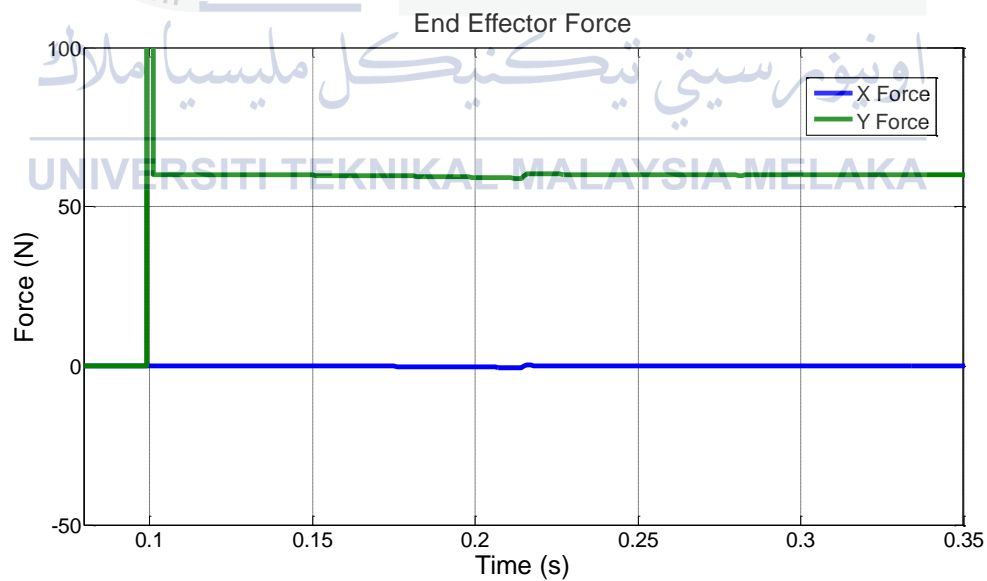
APPENDIX F



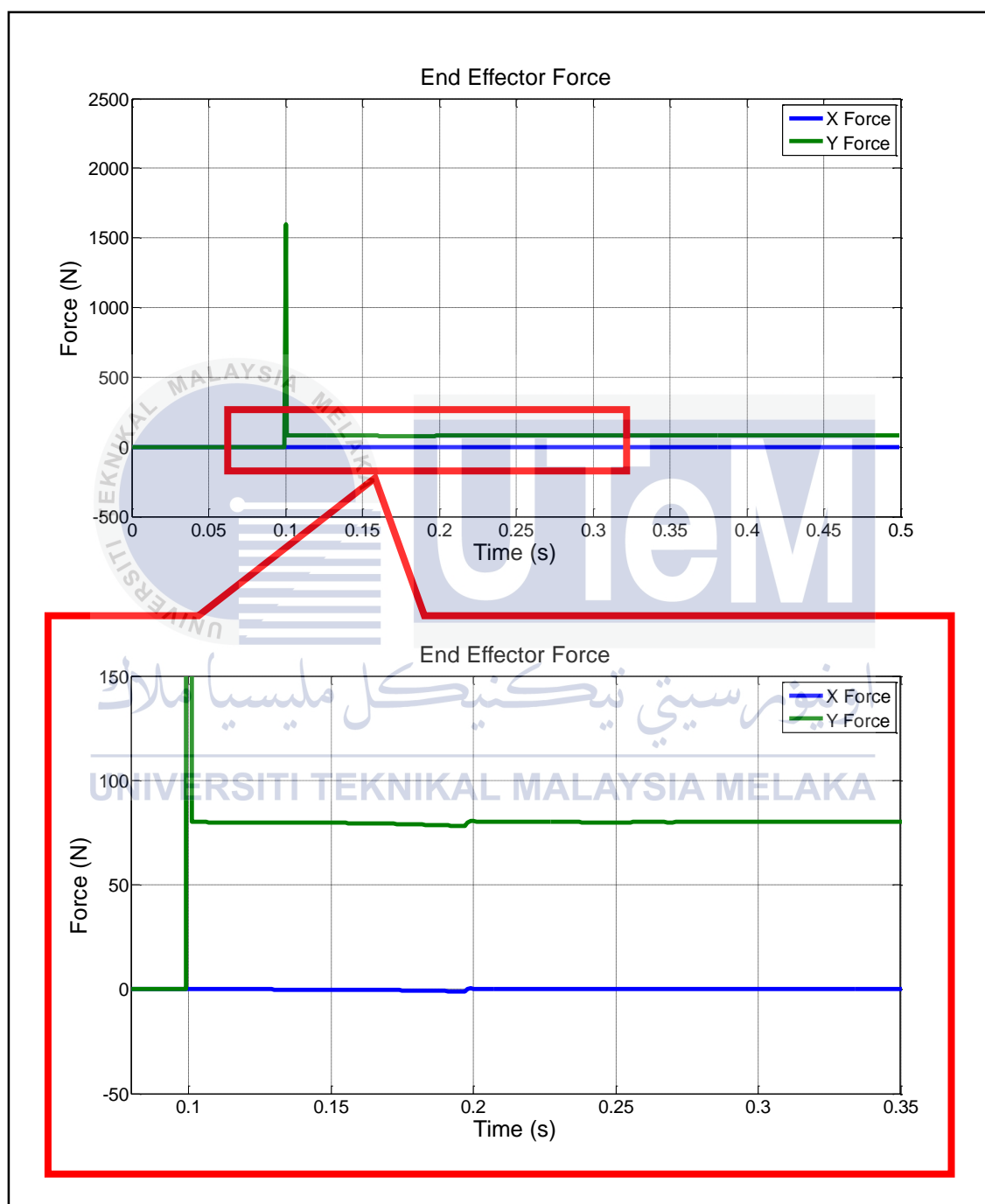
End Effector Force When Force References 20N



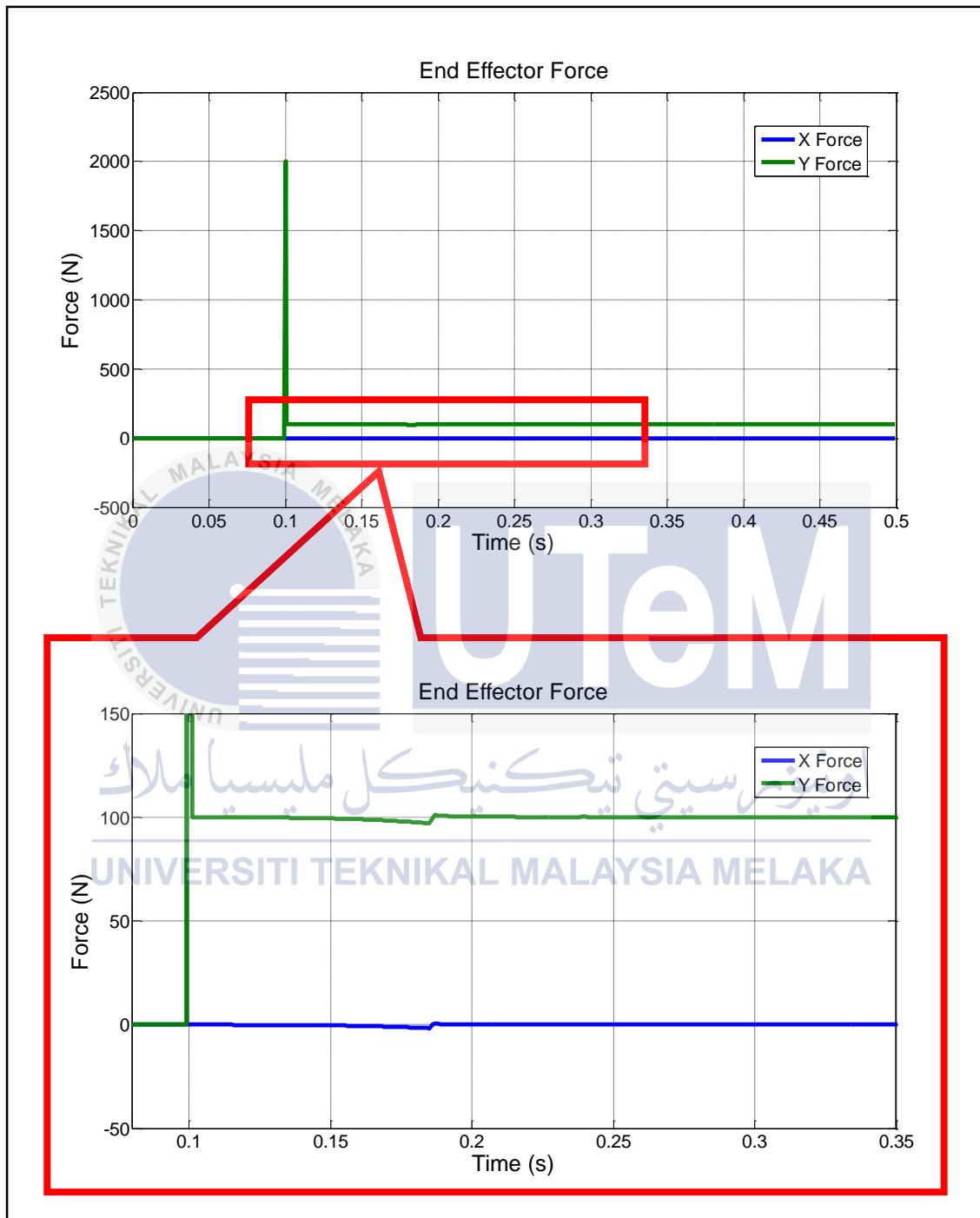
End Effector Force When Force References 40N



End Effector Force When Force References 60N

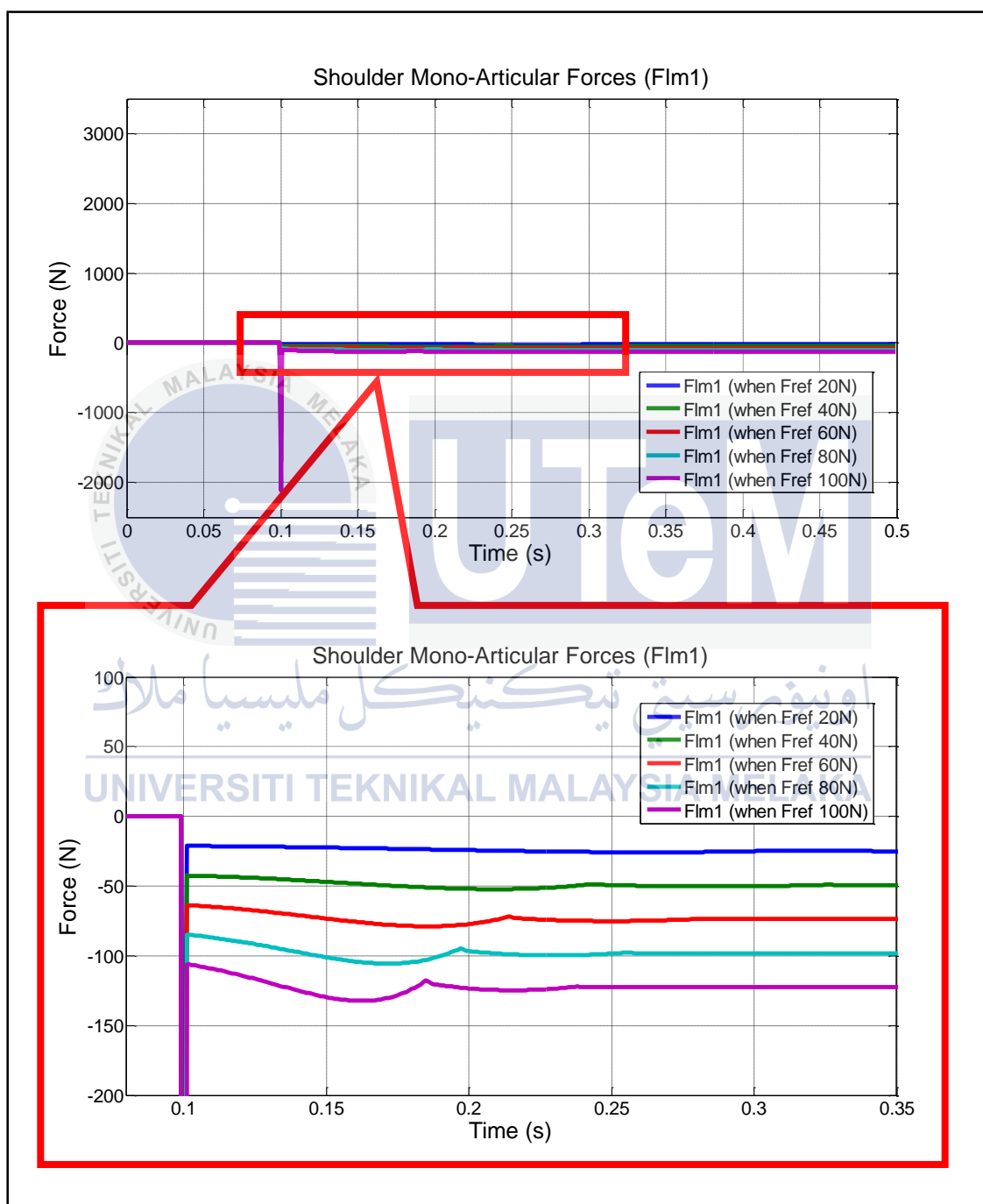


End Effector Force When Force References 80N

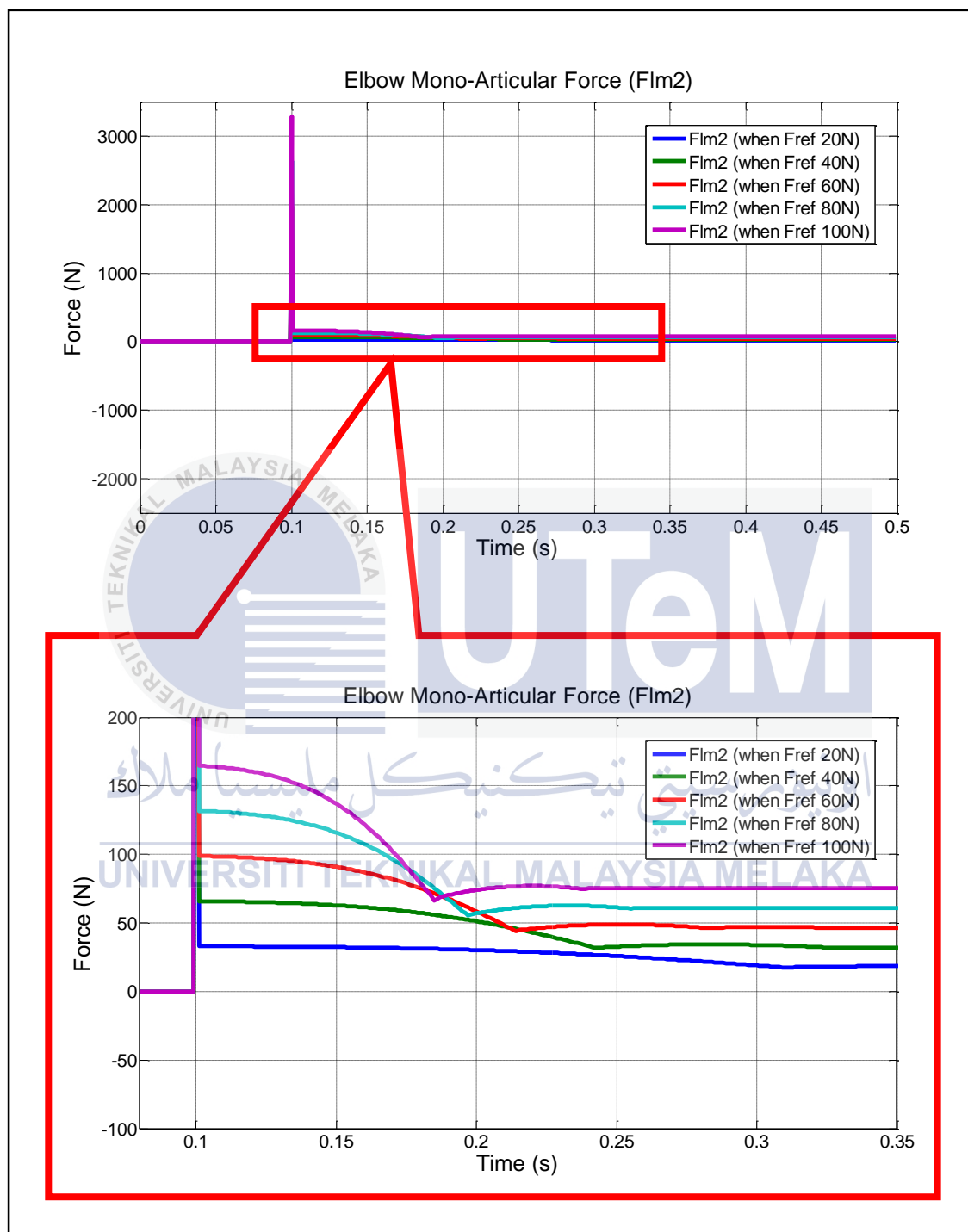


End Effector Force When Force References 100N

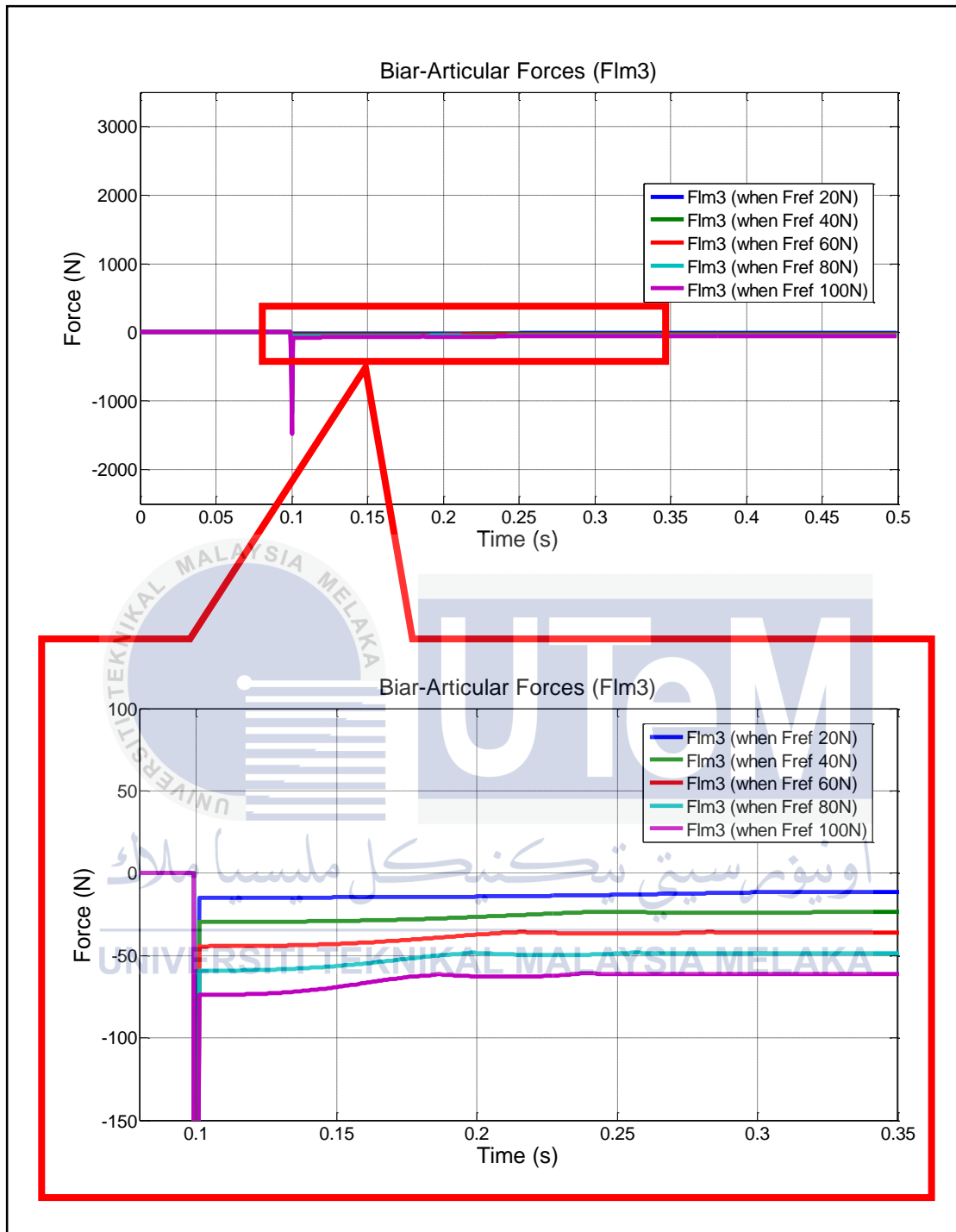
APPENDIX G



All shoulder mono-articular muscles force

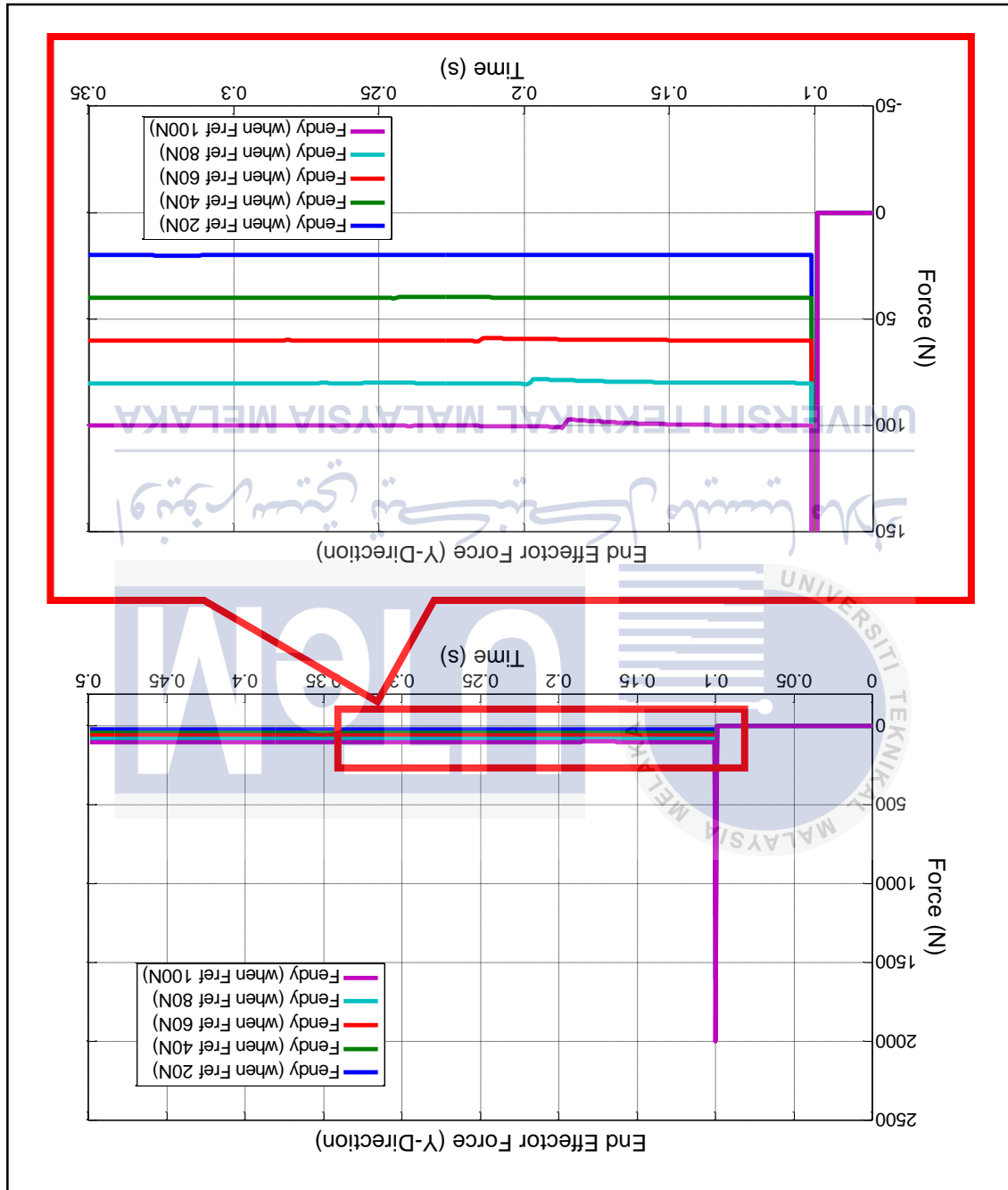


All elbow mono-articular muscles force



All biar-articular muscles force

APPENDIX H



All end effector in y-direction force

APPENDIX I

```

#include <math.h>
#include "environment.prm"
#include "time.prm"

/***** robot parameters *****/
#define DISTANCE (0.2)
#define L1X (0.3) /*base*/
#define L1Y (0.3)
#define L1Z (0.1)

#define L2X (0.0) /*biart*/
#define L2Y (0.0)
#define L2Z (0.0)
#define L3X (0.05)
#define L3Y (2.5*DISTANCE)
#define L3Z (0.05)
#define L4X (0.02)
#define L4Y (0.02)
#define L4Z (2.5*DISTANCE)

#define L5X (0.0) /*mono1*/
#define L5Y (0.0)
#define L5Z (0.0)
#define L6X (0.05)
#define L6Y (DISTANCE)
#define L6Z (0.05)
#define L7X (0.02)
#define L7Y (0.02)
#define L7Z (DISTANCE)

#define L8X (0.05) /*link1*/
#define L8Y (2.0*DISTANCE)
#define L8Z (0.05)
#define L9X (0.05) /*link2*/
#define L9Y (2.0*DISTANCE)
#define L9Z (0.05)

```

```

#define L11X (0.05)
#define L11Y (DISTANCE)
#define L11Z (0.05)
#define L12X (0.02)
#define L12Y (0.02)
#define L12Z (DISTANCE)

num_of_links = 12;
num_of_children = {3,1,1,0,1,1,0,2,0,1,1,0};
linear_flag = {0,0,1,0,0,1,0,0,0,0,1};
num_of_closed_loops = 3;
num_of_closed_points = {2,1,1,1,1,1,1,2,2,1,1,1};
closed_flag = {{0},{0},{0},{-1},{0},{0},{-2},{2},{3,1},{0},{0},{-3}};
p_closed = {
  {{0.0, 0.0, 0.0}}, {{0.0, 0.0, 0.0}}, {{0.0, 0.0, 0.0}}, {{0.0, 0.0, L4Z}}, {{0.0, 0.0,
  0.0}}, {{0.0, 0.0, 0.0}}, {{0.0, 0.0, L7Z}}, {{ 1/2*L8Y, 0.0, 0.0}}, {{ L9Y/2,0.0,
  0.0}}, {{ 3*L9Y/4,0.0, 0.0}}, {{0.0, 0.0, 0.0}}, {{0.0, 0.0, 0.0}}, {{0.0, 0.0, L12Z}}
};

/* angles */
phi = {
  1*M_PI/2.0,
  0*M_PI/2.0,
  3*M_PI/2.0,
  1*M_PI/2.0,
  0*M_PI/2.0,
  3*M_PI/2.0,
  1*M_PI/2.0,
  0*M_PI/2.0,
  0*M_PI/2.0,
  0*M_PI/2.0,
  0*M_PI/2.0,
  3*M_PI/2.0
};

alpha = {
  0*M_PI/2.0,
  -1*M_PI/2.0,
  3*M_PI/2.0,
  0*M_PI/2.0,
  -1*M_PI/2.0,
  3*M_PI/2.0,
  -1*M_PI/2.0,
  0*M_PI/2.0,
  3*M_PI/2.0,
  1*M_PI/2.0,
  3*M_PI/2.0
};

```

```

/* lengthes */
a = {-0.2, 0.0, 0.0, -0.1, 0.0, 0.0, 0.1, L8Y, 1/2*L8Y, 0.0, 0.0};
d = {L1Z/2, 0.0, 0.0, 0*L1Z/2, 0.0, 0.0, 0*L1Z/2, 0.0, 0.0, 0.0, 0.0};

/* initial state of robot */
dq = {0.0, 0.0, 0.0, 0.0, 0.0, 0.0, 0.0, 0.0, 0.0, 0.0, 0.0};
q = {
0.0,                //virt. joint

28*M_PI/180.0,      //biart,
0.35,              //biart mover length (range?),

0.0,                //virt. joint

8*M_PI/180.0,       //mono1,
0.19,              //mono1 length (range?),

17*M_PI/180.0,      //link1
56*M_PI/180.0,      //link2

0*M_PI/4.0,         //virt. joint

28*M_PI/180.0,      //mono2
0.15                //mono2 length

/* masses */
#define M1 (100000000.0)
#define M2 (0.0)
#define M3 (0.45)
#define M4 (0.45)

#define M5 (0.0)
#define M6 (0.3)
#define M7 (0.3)

#define M8 (0.5)
#define M9 (0.5)

#define M10 (0.0)
#define M11 (0.3)
#define M12 (0.3)

```

```

/* link[i]'s center of gravity in its coordinates */
s_hat = {
    {0.0, -0.225, -0.225},
    {0.0, 0.0, 0.0},
    {L3Y/2.0, 0.0, 0.0},
    {0.0, 0.0, L4Z/2},
    {0.0, 0.0, 0.0},
    {L6Y/2.0, 0.0, 0.0},
    {0.0, 0.0, L7Z/2},
    { L8Y/2.0, 0.0, 0.0},
    { L9Y/2.0, 0.0, 0.0},
    {0.0, 0.0, 0.0},
    {L11Y/2, 0.0, 0.0},
    {0.0, 0.0,L12Z/2.0}
};

/* contact points */
num_of_contacts = {20, 16, 16, 16, 16, 16, 16, 16, 16, 16, 16, 16};
c_hat = {
    {
        {L1X/2.0, -L1Y/2.0, L1Z/2.0},//1
        {-L1X/2.0, -L1Y/2.0, L1Z/2.0},//2
        {-L1X/2.0, -L1Y/2.0, -L1Z/2.0},//3
        {L1X/2.0, -L1Y/2.0, -L1Z/2.0},//4
        {L1X/2.0, L1Y/2.0, L1Z/2.0},//5
        {-L1X/2.0, L1Y/2.0, L1Z/2.0},//6
        {-L1X/2.0, L1Y/2.0, -L1Z/2.0},//7
        {L1X/2.0, L1Y/2.0, -L1Z/2.0},//8
        {-L1X/2.0, -L1Y*2.0, L1Z/2.0},//9
        {L1X/2.0, -L1Y*2.0, L1Z/2.0},//10
        {-L1X/2.0, -L1Y/2.0, -L1Z*6.0},//11
        {L1X/2.0, -L1Y/2.0, -L1Z*6.0},//12
        {-L1X/2.0, -L1Y*2.0, -L1Z*6.0},//13
        {L1X/2.0, -L1Y*2.0, -L1Z*6.0},//14
        {0, L1Y/2.0, L1Z/2.0},//15
        {0, L1Y/2.0, -L1Z/2.0},//16
        {0, -L1Y/2.0, -L1Z/2.0},//17
        {0, -L1Y/2.0, -L1Z*6.0},//18
        {0, -L1Y*2.0, -L1Z*6.0},//19
        {0, -L1Y*2.0, L1Z/2.0},//20
    },

```



```
{
  {L2X/2.0, -L2Y/2.0, L2Z/2.0},//1
  {-L2X/2.0, -L2Y/2.0, L2Z/2.0},//2
  {-L2X/2.0, -L2Y/2.0, -L2Z/2.0},//3
  {L2X/2.0, -L2Y/2.0, -L2Z/2.0},//4
  {L2X/2.0, L2Y/2.0, L2Z/2.0},//5
  {-L2X/2.0, L2Y/2.0, L2Z/2.0},//6
  {-L2X/2.0, L2Y/2.0, -L2Z/2.0},//7
  {L2X/2.0, L2Y/2.0, -L2Z/2.0},//8
  {0, -L2Y/2.0, L2Z/2.0},//9
  {-L2X/2.0, -L2Y/2.0, 0},//10
  {0, -L2Y/2.0, -L2Z/2.0},//11
  {L2X/2.0, -L2Y/2.0, 0},//12
  {0, L2Y/2.0, L2Z/2.0},//13
  {-L2X/2.0, L2Y/2.0, 0},//14
  {0, L2Y/2.0, -L2Z/2.0},//15
  {L2X/2.0, L2Y/2.0, 0},//16
},
```

```
{
  {L3Y, L3X/2.0, L3Z/2.0},//1
  {L3Y, L3X/2.0, -L3Z/2.0},//2
  {L3Y, -L3X/2.0, -L3Z/2.0},//3
  {L3Y, -L3X/2.0, L3Z/2.0},//4
  {0, L3X/2.0, L3Z/2.0},//5
  {0, L3X/2.0, -L3Z/2.0},//6
  {0, -L3X/2.0, -L3Z/2.0},//7
  {0, -L3X/2.0, L3Z/2.0},//8
  {L3Y, 0, L3Z/2.0},//9
  {L3Y, L3X/2.0, 0},//10
  {L3Y, 0, -L3Z/2.0},//11
  {L3Y, -L3X/2.0, 0},//12
  {0, 0, L3Z/2.0},//13
  {0, L3X/2.0, 0},//14
  {0, 0, -L3Z/2.0},//15
  {0, -L3X/2.0, 0},//16
},
```



اونیورسیتی تکنیکل

UNIVERSITI TEKNIKAL MALAYSIA MELAKA

```
{
{-L4X/2.0, -L4Y/2.0, L4Z},//1
{-L4X/2.0, L4Y/2.0, L4Z},//2
{L4X/2.0, L4Y/2.0, L4Z},//3
{L4X/2.0, -L4Y/2.0, L4Z},//4
{-L4X/2.0, -L4Y/2.0, 0.0},//5
{-L4X/2.0, L4Y/2.0, 0.0},//6
{L4X/2.0, L4Y/2.0, 0.0},//7
{L4X/2.0, -L4Y/2.0, 0.0},//8
{0.0, -L4Y/2.0, L4Z},//9
{-L4X/2.0, -L4Y/2.0, L4Z/2.0},//10
{0.0, -L4Y/2.0, 0.0},//11
{L4X/2.0, -L4Y/2.0, L4Z/2.0},//12
{0.0, L4Y/2.0, L4Z},//13
{-L4X/2.0, L4Y/2.0, L4Z/2.0},//14
{0.0, L4Y/2.0, 0.0},//15
{L4X/2.0, L4Y/2.0, L4Z/2.0},//16
},
```

```
{
{L5X/2.0, -L5Y/2.0, L5Z/2.0},//1
{-L5X/2.0, -L5Y/2.0, L5Z/2.0},//2
{-L5X/2.0, -L5Y/2.0, -L5Z/2.0},//3
{L5X/2.0, -L5Y/2.0, -L5Z/2.0},//4
{L5X/2.0, L5Y/2.0, L5Z/2.0},//5
{-L5X/2.0, L5Y/2.0, L5Z/2.0},//6
{-L5X/2.0, L5Y/2.0, -L5Z/2.0},//7
{L5X/2.0, L5Y/2.0, -L5Z/2.0},//8
{0, -L5Y/2.0, L5Z/2.0},//9
{-L5X/2.0, -L5Y/2.0, 0},//10
{0, -L5Y/2.0, -L5Z/2.0},//11
{L5X/2.0, -L5Y/2.0, 0},//12
{0, L5Y/2.0, L5Z/2.0},//13
{-L5X/2.0, L5Y/2.0, 0},//14
{0, L5Y/2.0, -L5Z/2.0},//15
{L5X/2.0, L5Y/2.0, 0},//16
},
```

```

{
  {L6Y, L6X/2.0, L6Z/2.0},//1
  {L6Y, L6X/2.0, -L6Z/2.0},//2
  {L6Y, -L6X/2.0, -L6Z/2.0},//3
  {L6Y, -L6X/2.0, L6Z/2.0},//4
  {0, L6X/2.0, L6Z/2.0},//5
  {0, L6X/2.0, -L6Z/2.0},//6
  {0, -L6X/2.0, -L6Z/2.0},//7
  {0, -L6X/2.0, L6Z/2.0},//8
  {L6Y, 0, L6Z/2.0},//9
  {L6Y, L6X/2.0, 0},//10
  {L6Y, 0, -L6Z/2.0},//11
  {L6Y, -L6X/2.0, 0},//12
  {0, 0, L6Z/2.0},//13
  {0, L6X/2.0, 0},//14
  {0, 0, -L6Z/2.0},//15
  {0, -L6X/2.0, 0},//16
},
{
  {-L7X/2.0, -L7Y/2.0, L7Z},//1
  {-L7X/2.0, L7Y/2.0, L7Z},//2
  {L7X/2.0, L7Y/2.0, L7Z},//3
  {L7X/2.0, -L7Y/2.0, L7Z},//4
  {-L7X/2.0, -L7Y/2.0, 0.0},//5
  {-L7X/2.0, L7Y/2.0, 0.0},//6
  {L7X/2.0, L7Y/2.0, 0.0},//7
  {L7X/2.0, -L7Y/2.0, 0.0},//8
  {0.0, -L7Y/2.0, L7Z},//9
  {-L7X/2.0, -L7Y/2.0, L7Z/2.0},//10
  {0.0, -L7Y/2.0, 0.0},//11
  {L7X/2.0, -L7Y/2.0, L7Z/2.0},//12
  {0.0, L7Y/2.0, L7Z},//13
  {-L7X/2.0, L7Y/2.0, L7Z/2.0},//14
  {0.0, L7Y/2.0, 0.0},//15
  {L7X/2.0, L7Y/2.0, L7Z/2.0},//16
},

```



اونیورسیتی تکنیک

UNIVERSITI TEKNIKAL MALAYSIA MELAKA

```

{
  {L8Y, L8X/2.0, L8Z/2.0},//1
  {L8Y, L8X/2.0, -L8Z/2.0},//2
  {L8Y, -L8X/2.0, -L8Z/2.0},//3
  {L8Y, -L8X/2.0, L8Z/2.0},//4
  {0, L8X/2.0, L8Z/2.0},//5
  {0, L8X/2.0, -L8Z/2.0},//6
  {0, -L8X/2.0, -L8Z/2.0},//7
  {0, -L8X/2.0, L8Z/2.0},//8
  {L8Y, 0, L8Z/2.0},//9
  {L8Y, L8X/2.0, 0},//10
  {L8Y, 0, -L8Z/2.0},//11
  {L8Y, -L8X/2.0, 0},//12
  {0, 0, L8Z/2.0},//13
  {0, L8X/2.0, 0},//14
  {0, 0, -L8Z/2.0},//15
  {0, -L8X/2.0, 0},//16
},

```

```

{
  {L9Y, L9X/2.0, L9Z/2.0},//1
  {L9Y, L9X/2.0, -L9Z/2.0},//2
  {L9Y, -L9X/2.0, -L9Z/2.0},//3
  {L9Y, -L9X/2.0, L9Z/2.0},//4
  {0, L9X/2.0, L9Z/2.0},//5
  {0, L9X/2.0, -L9Z/2.0},//6
  {0, -L9X/2.0, -L9Z/2.0},//7
  {0, -L9X/2.0, L9Z/2.0},//8
  {L9Y, 0, L9Z/2.0},//9
  {L9Y, L9X/2.0, 0},//10
  {L9Y, 0, -L9Z/2.0},//11
  {L9Y, -L9X/2.0, 0},//12
  {0, 0, L9Z/2.0},//13
  {0, L9X/2.0, 0},//14
  {0, 0, -L9Z/2.0},//15
  {0, -L9X/2.0, 0},//16
},

```



اونیورسیتی تکنیک

TEKNIKAL MALAYSIA MELAKA

```

{
{L10X/2.0, -L10Y/2.0, L10Z/2.0},//1
{-L10X/2.0, -L10Y/2.0, L10Z/2.0},//2
{-L10X/2.0, -L10Y/2.0, -L10Z/2.0},//3
{L10X/2.0, -L10Y/2.0, -L10Z/2.0},//4
{L10X/2.0, L10Y/2.0, L10Z/2.0},//5
{-L10X/2.0, L10Y/2.0, L10Z/2.0},//6
{-L10X/2.0, L10Y/2.0, -L10Z/2.0},//7
{L10X/2.0, L10Y/2.0, -L10Z/2.0},//8
{0, -L10Y/2.0, L10Z/2.0},//9
{-L10X/2.0, -L10Y/2.0, 0},//10
{0, -L10Y/2.0, -L10Z/2.0},//11
{L10X/2.0, -L10Y/2.0, 0},//12
{0, L10Y/2.0, L10Z/2.0},//13
{-L10X/2.0, L10Y/2.0, 0},//14
{0, L10Y/2.0, -L10Z/2.0},//15
{L10X/2.0, L10Y/2.0, 0},//16
},

```

```

{
{L11Y, L11X/2.0, L11Z/2.0},//1
{L11Y, L11X/2.0, -L11Z/2.0},//2
{L11Y, -L11X/2.0, -L11Z/2.0},//3
{L11Y, -L11X/2.0, L11Z/2.0},//4
{0, L11X/2.0, L11Z/2.0},//5
{0, L11X/2.0, -L11Z/2.0},//6
{0, -L11X/2.0, -L11Z/2.0},//7
{0, -L11X/2.0, L11Z/2.0},//8
{L11Y, 0, L11Z/2.0},//9
{L11Y, L11X/2.0, 0},//10
{L11Y, 0, -L11Z/2.0},//11
{L11Y, -L11X/2.0, 0},//12
{0, 0, L11Z/2.0},//13
{0, L11X/2.0, 0},//14
{0, 0, -L11Z/2.0},//15
{0, -L11X/2.0, 0},//16
},

```



اونیورسیتی تکنیکل

TEKNIKAL MALAYSIA MELAKA

```

{
  {-L12X/2.0, -L12Y/2.0, L12Z},//1
  {-L12X/2.0, L12Y/2.0, L12Z},//2
  {L12X/2.0, L12Y/2.0, L12Z},//3
  {L12X/2.0, -L12Y/2.0, L12Z},//4
  {-L12X/2.0, -L12Y/2.0, 0.0},//5
  {-L12X/2.0, L12Y/2.0, 0.0},//6
  {L12X/2.0, L12Y/2.0, 0.0},//7
  {L12X/2.0, -L12Y/2.0, 0.0},//8
  {0.0, -L12Y/2.0, L12Z},//9
  {-L12X/2.0, -L12Y/2.0, L12Z/2.0},//10
  {0.0, -L12Y/2.0, 0.0},//11
  {L12X/2.0, -L12Y/2.0, L12Z/2.0},//12
  {0.0, L12Y/2.0, L12Z},//13
  {-L12X/2.0, L12Y/2.0, L12Z/2.0},//14
  {0.0, L12Y/2.0, 0.0},//15
  {L12X/2.0, L12Y/2.0, L12Z/2.0},//16
}

};

/***** polygon data *****/
num_of_polygons = {8,6,6,6,6,6,6,6,6,6};
num_of_points = 6;
polygon = {
  {
    {-L1X/2.0, -L1Y*2.0, L1Z/2.0}, {0, -L1Y*2.0, L1Z/2.0},
    {L1X/2.0, -L1Y*2.0, L1Z/2.0}, {L1X/2.0, -L1Y*2.0, -L1Z*6.0},
    {0, -L1Y*2.0, -L1Z*6.0}, {-L1X/2.0, -L1Y*2.0, -L1Z*6.0}},

    //9,20,10,14,19,13 (1)
  }
}

```

{ {-L1X/2.0, L1Y/2.0, L1Z/2.0}, {L1X/2.0, L1Y/2.0, L1Z/2.0},
 {L1X/2.0, -L1Y/2.0, L1Z/2.0}, {L1X/2.0, -L1Y*2.0, L1Z/2.0},
 {-L1X/2.0, -L1Y*2.0, L1Z/2.0}, {-L1X/2.0, -L1Y/2.0, L1Z/2.0}},

//6,5,1,10,9,2 (2)

{ {-L1X/2.0, L1Y/2.0, -L1Z/2.0}, {0, L1Y/2.0, -L1Z/2.0},
 {L1X/2.0, L1Y/2.0, -L1Z/2.0}, {L1X/2.0, L1Y/2.0, L1Z/2.0},
 {0, L1Y/2.0, L1Z/2.0}, {-L1X/2.0, L1Y/2.0, L1Z/2.0}},

//7,16,8,5,15,6 (3)

{ {-L1X/2.0, -L1Y/2.0, -L1Z/2.0}, {0, -L1Y/2.0, -L1Z/2.0},
 {L1X/2.0, -L1Y/2.0, -L1Z/2.0}, {L1X/2.0, L1Y/2.0, -L1Z/2.0},
 {0, L1Y/2.0, -L1Z/2.0}, {-L1X/2.0, L1Y/2.0, -L1Z/2.0}},

//3,17,4,8,16,7 (4)

{ {-L1X/2.0, -L1Y/2.0, -L1Z*6.0}, {0, -L1Y/2.0, -L1Z*6.0},
 {L1X/2.0, -L1Y/2.0, -L1Z*6.0}, {L1X/2.0, -L1Y/2.0, -L1Z/2.0},
 {0, -L1Y/2.0, -L1Z/2.0}, {-L1X/2.0, -L1Y/2.0, -L1Z/2.0}},

//11,18,12,4,17,3 (5)

{ {-L1X/2.0, -L1Y*2.0, -L1Z*6.0}, {0, -L1Y*2.0, -L1Z*6.0},
 {L1X/2.0, -L1Y*2.0, -L1Z*6.0}, {L1X/2.0, -L1Y/2.0, -L1Z*6.0},
 {0, -L1Y/2.0, -L1Z*6.0}, {-L1X/2.0, -L1Y/2.0, -L1Z*6.0}},

//13,19,14,12,18,11 (6)

{ {-L1X/2.0, L1Y/2.0, L1Z/2.0}, {-L1X/2.0, L1Y/2.0, -L1Z/2.0},
 {-L1X/2.0, -L1Y/2.0, -L1Z/2.0}, {-L1X/2.0, -L1Y/2.0, -L1Z*6.0},
 {-L1X/2.0, -L1Y*2.0, -L1Z*6.0}, {-L1X/2.0, -L1Y*2.0, L1Z/2.0}},

//6,7,3,11,13,9 (7)

{L1X/2.0, L1Y/2.0, L1Z/2.0}, {L1X/2.0, L1Y/2.0, -L1Z/2.0},
 {L1X/2.0, -L1Y/2.0, -L1Z/2.0}, {L1X/2.0, -L1Y/2.0, -L1Z*6.0},
 {L1X/2.0, -L1Y*2.0, -L1Z*6.0}, {L1X/2.0, -L1Y*2.0, L1Z/2.0}}

//5,8,4,12,14,10 (8)
 },

{
 {{L2X/2.0, -L2Y/2.0, L2Z/2.0}, {0, -L2Y/2.0, L2Z/2.0},
 {-L2X/2.0, -L2Y/2.0, L2Z/2.0}, {-L2X/2.0, -L2Y/2.0, -L2Z/2.0},
 {0, -L2Y/2.0, -L2Z/2.0}, {L2X/2.0, -L2Y/2.0, -L2Z/2.0}}},

//1,9,2,3,11,4 (1)

{{L2X/2.0, -L2Y/2.0, L2Z/2.0}, {0, -L2Y/2.0, L2Z/2.0},
 {-L2X/2.0, -L2Y/2.0, L2Z/2.0}, {-L2X/2.0, L2Y/2.0, L2Z/2.0},
 {0, L2Y/2.0, L2Z/2.0}, {L2X/2.0, L2Y/2.0, L2Z/2.0}}},

//1,9,2,6,13,5 (2)

{{L2X/2.0, L2Y/2.0, L2Z/2.0}, {0, L2Y/2.0, L2Z/2.0},
 {-L2X/2.0, L2Y/2.0, L2Z/2.0}, {-L2X/2.0, L2Y/2.0, -L2Z/2.0},
 {0, L2Y/2.0, -L2Z/2.0}, {L2X/2.0, L2Y/2.0, -L2Z/2.0}}},

//5,13,6,7,15,8 (3)

{{-L2X/2.0, -L2Y/2.0, -L2Z/2.0}, {0, -L2Y/2.0, -L2Z/2.0},
 {L2X/2.0, -L2Y/2.0, -L2Z/2.0}, {L2X/2.0, L2Y/2.0, -L2Z/2.0},
 {0, L2Y/2.0, -L2Z/2.0}, {-L2X/2.0, L2Y/2.0, -L2Z/2.0}}},

//3,11,4,8,15,7 (4)

{{-L2X/2.0, -L2Y/2.0, L2Z/2.0}, {-L2X/2.0, -L2Y/2.0, 0},
 {-L2X/2.0, -L2Y/2.0, -L2Z/2.0}, {-L2X/2.0, L2Y/2.0, -L2Z/2.0},
 {-L2X/2.0, L2Y/2.0, 0}, {-L2X/2.0, L2Y/2.0, L2Z/2.0}}},

//2,10,3,7,14,6 (5)

{ {L2X/2.0, -L2Y/2.0, L2Z/2.0}, {L2X/2.0, -L2Y/2.0, 0},
 {L2X/2.0, -L2Y/2.0, -L2Z/2.0}, {L2X/2.0, L2Y/2.0, -L2Z/2.0},
 {L2X/2.0, L2Y/2.0, 0}, {L2X/2.0, L2Y/2.0, L2Z/2.0} }

//1,12,4,8,16,5 (6)
 },

{
 {0, L3X/2.0, L3Z/2.0}, {0, L3X/2.0, -L3Z/2.0},
 {0, 0, -L3Z/2.0}, {0, -L3X/2.0, -L3Z/2.0},
 {0, -L3X/2.0, L3Z/2.0}, {0, 0, L3Z/2.0} },

//5,6,15,7,8,13 (1)

{ {L3Y, L3X/2.0, L3Z/2.0}, {L3Y, 0, L3Z/2.0},
 {L3Y, -L3X/2.0, L3Z/2.0}, {0, -L3X/2.0, L3Z/2.0},
 {0, 0, L3Z/2.0}, {0, L3X/2.0, L3Z/2.0} },

//1,9,4,8,13,5 (2)

{ {L3Y, L3X/2.0, L3Z/2.0}, {L3Y, L3X/2.0, -L3Z/2.0},
 {L3Y, 0, -L3Z/2.0}, {L3Y, -L3X/2.0, -L3Z/2.0},
 {L3Y, -L3X/2.0, L3Z/2.0}, {L3Y, 0, L3Z/2.0} },

//1,2,11,3,4,9 (3)

{ {L3Y, L3X/2.0, -L3Z/2.0}, {L3Y, 0, -L3Z/2.0},
 {L3Y, -L3X/2.0, -L3Z/2.0}, {0, -L3X/2.0, -L3Z/2.0},
 {0, 0, -L3Z/2.0}, {0, L3X/2.0, -L3Z/2.0} },

//2,11,3,7,15,6 (4)

{ {L3Y, -L3X/2.0, -L3Z/2.0}, {L3Y, L3X/2.0, 0},
 {L3Y, -L3X/2.0, L3Z/2.0}, {0, -L3X/2.0, L3Z/2.0},
 {0, L3X/2.0, 0}, {0, -L3X/2.0, -L3Z/2.0} },

//3,10,4,8,14,7 (5)

APPENDIX J

```

/***** All Declaration Degarding Muscle 01 *****/
static double lm1, flm1ref, flm1reac, flm1act, lm1temp, lm1vel, ke1;

/***** All Declaration Degarding Muscle 02 *****/
static double lm2, flm2ref, flm2reac, flm2act, lm2temp, lm2vel, ke2;

/***** All Declaration Degarding Muscle 03 *****/
static double lm3, flm3ref, flm3reac, flm3act, lm3temp, lm3vel, ke3;

/***** All Declaration Degarding End Effector *****/
static double fxref, fyref, fxreac, fyreac;
static double Mnx, gx, tmp1i1, tmp1i2=0.0, tmp1=0.0, tmp1o=0.0;
static double Mny, gy, tmp1i3, tmp1i4=0.0, tmp2=0.0, tmp2o=0.0;
static double xref, yref, xrefvel, yrefvel;

/***** All Declaration Degarding Manipulator (Link) *****/
static double a1, a2;
static double x1, y1, x2, y2;
static double q1r, q2r;
static double q1rr, q2rr;

/***** All Declaration Degarding Manipulator (Muscle) *****/
static double a1, a2, b11, b12, c11, c12;
static double d1, d2, d3;

/***** All Declaration Degarding Link Jacobian *****/
static double J1c11, J1c12, J1c21, J1c22; // Jacobian
static double J2c11, J2c12, J2c21, J2c22; // Jacobian Transpose
static double J3c11, J3c12, J3c21, J3c22, detJ3c;
static double J4c11, J4c12, J4c21, J4c22, detJ4c;

```

```

/***** All Declaration Degarding Muscle Jacobian *****/
static double J1m11, J1m12, J1m21, J1m22, J1m31, J1m32; // Jacobian
static double J2m11, J2m12, J2m13, J2m21, J2m22, J2m23; // Jacobian Transpose
static double J3m11, J3m12, J3m21, J3m22;
static double J4m11, J4m12, J4m21, J4m22, detJ4m;
static double J5m11, J5m12, J5m21, J5m22, J5m31, J5m32;
static double J6m11, J6m12, J6m13, J6m21, J6m22, J6m23, J6m31, J6m32, J6m33;
static double J7m11, J7m12, J7m13, J7m21, J7m22, J7m23, J7m31, J7m32, J7m33;
static double J8m11, J8m12, J8m13, J8m21, J8m22, J8m23, J8m31, J8m32, J8m33;
static double J9m11, J9m12, J9m13, J9m21, J9m22, J9m23, J9m31, J9m32, J9m33;
static double J10m11, J10m12, J10m13, J10m21, J10m22, J10m23, J10m31,
J10m32, J10m33;
static double det01, det02, det03, detJ10m;
static double J11m11, J11m12, J11m13, J11m21, J11m22, J11m23;

if (u == NULL) u = (double*)calloc(n, sizeof(double));

/***** Manipulator Data *****/
a1=0.2; a2=0.2; b1=0.2; b2=0.2; c1=0.3; c2=0.3;
d1=0.2; d2=0.2; d3=0.5;
a1=0.4; a2=0.4;

/***** Angles of Manipulator *****/
x1 = (q[5]+0.2)*(q[5]+0.2) - (a1*a1) - (a2*a2);
y1 = 2*a1*a2;
x2 = (q[10]+0.2)*(q[10]+0.2) - (b1*b1) - (b2*b2);
y2 = 2*b1*b2;
q1r = acos (x1/y1);
q2r = acos (x2/y2);

/***** End Effector Force and Coordinates References *****/
if (t<0.1) fxref = 0.0;
if (t>0.1) fxref = 0.0;

if (t<0.1) fyref = 0.0;
if (t>0.1) fyref = 100.0;

```

```

ref    = (a1*cos(q1r)) + (a2*cos(q1r+q2r));
yref   = (a1*sin(q1r)) + (a2*sin(q1r+q2r));

lm1    = sqrt(a1*a1 + a2*a2 + 2*a1*a2*cos(q1r)) - d1;
lm2    = sqrt(b1*b1 + b2*b2 + 2*b1*b2*cos(q2r)) - d2;
lm3    =
sqrt(c1*c1+c2*c2+a1*a1+2*c1*a1*cos(q1r)+2*c2*a1*cos(q2r)+2*c1*c2*cos(q1r+q2r))-d3;

/***** Jacobian Equation (Muscle) *****/
J1m11 = (-a1*a2*sin(q1r))/lm1;
J1m12 = 0.0;
J1m21 = 0.0;
J1m22 = (-b1*b2*sin(q2r))/lm2;
J1m31 = ((-c1*a1*sin(q1r))- (c1*c2*sin(q1r+q2r)))/lm3;
J1m32 = ((-c2*a1*sin(q2r))- (c1*c2*sin(q1r+q2r)))/lm3;

/***** Jacobian Transpose Equation (Muscle) *****/
J2m11 = (-a1*a2*sin(q1r))/lm1;
J2m12 = 0.0;
J2m13 = ((-c1*a1*sin(q1r))- (c1*c2*sin(q1r+q2r)))/lm3;
J2m21 = 0.0;
J2m22 = (-b1*b2*sin(q2r))/lm2;
J2m23 = ((-c2*a1*sin(q2r))- (c1*c2*sin(q1r+q2r)))/lm3;

/***** J2m*J1m (Muscle) *****/
J3m11 = (J2m11*J1m11) + (J2m12*J1m21) + (J2m13*J1m31);
J3m12 = (J2m11*J1m12) + (J2m12*J1m22) + (J2m13*J1m32);
J3m21 = (J2m21*J1m11) + (J2m22*J1m21) + (J2m23*J1m31);
J3m22 = (J2m21*J1m12) + (J2m22*J1m22) + (J2m23*J1m32);

/***** Inverse (J1m*J2m) (Muscle) *****/
detJ4m = (1/((J3m11*J3m22)-(J3m12*J3m21)));
J4m11 = detJ4m*(J3m22);
J4m12 = detJ4m*(-J3m12);
J4m21 = detJ4m*(-J3m21);
J4m22 = detJ4m*(J3m11);

```

```

lm1temp      = lm1;
lm1vel = (lm1-lm1temp)/t_control;

lm2temp      = lm2;
lm2vel = (lm2-lm2temp)/t_control;

lm3temp      = lm3;
lm3vel = (lm3-lm3temp)/t_control;

q1rr  = (J11m11*lm1vel) + (J11m12*lm2vel) + (J11m13*lm3vel);
q2rr  = (J11m21*lm1vel) + (J11m22*lm2vel) + (J11m23*lm3vel);
xrefvel = (J1c11*q1rr) + (J1c12*q2rr);
yrefvel = (J1c21*q1rr) + (J1c22*q2rr);

/***** Disturbance Force *****/
fxreac = (((J4c11*J2m11) + (J4c12*J2m21)) * u[5]) + (((J4c11*J2m12) +
(J4c12*J2m22)) * u[10]) + (((J4c11*J2m13) + (J4c12*J2m23)) *
u[2]);

fyreac = (((J4c21*J2m11) + (J4c22*J2m21)) * u[5]) + (((J4c21*J2m12) +
(J4c22*J2m22)) * u[10]) + (((J4c21*J2m13) + (J4c22*J2m23)) *
u[2]);

Mnx=2.0;
gx=0.05;

tmp1i1=fxreac+Mnx*gx*xrefvel;
tmp1i2=tmp1i1+gx*(tmp1i1-tmp1i2);
tmp1=tmp1i2;
tmp1o=tmp1i2-Mnx*gx*xrefvel;

```

Mny=2.0;

gy=0.05;

tmp1i3=fyreact+Mny*gy*yrefvel;

tmp1i4=tmp2+gy*(tmp1i3-tmp1i4);

tmp2=tmp1i4;

tmp2o=tmp1i4-Mny*gy*yrefvel;

/***** All Equation Regarding Muscle 01 *****/

flm1ref= (((J5m11*J2c11) + (J5m12*J2c21)) * (fxref)) + (((J5m11*J2c12) + (J5m12*J2c22)) * (fyref));

flm1react= (((J5m11*J2c11) + (J5m12*J2c21)) * (tmp1o)) + (((J5m11*J2c12) + (J5m12*J2c22)) * (tmp2o));

flm1act = flm1react;

ke1=20.0;

u[5]=ke1*(flm1ref - flm1react) + flm1act;

/***** All Equation Regarding Muscle 02 *****/

flm2ref= (((J5m21*J2c11) + (J5m22*J2c21)) * (fxref)) + (((J5m21*J2c12) + (J5m22*J2c22)) * (fyref));

flm2react= (((J5m21*J2c11) + (J5m22*J2c21)) * (tmp1o)) + (((J5m21*J2c12) + (J5m22*J2c22)) * (tmp2o));

flm2act = flm2react;

ke2=20.0;

u[10]=ke2*(flm2ref - flm2react) + flm2act;

/***** All Equation Regarding Muscle 03 *****/

flm3ref= (((J5m31*J2c11) + (J5m32*J2c21)) * (fxref)) + (((J5m31*J2c12) + (J5m32*J2c22)) * (fyref));

flm3react= (((J5m31*J2c11) + (J5m32*J2c21)) * (tmp1o)) + (((J5m31*J2c12) + (J5m32*J2c22)) * (tmp2o));

flm3act = flm3react;

```
ke3=20.0;  
u[2]=ke3*(flm3ref - flm3reac) + flm3act;  
  
t = t + t_control; //time increase  
  
return u;  
  
}
```



اونيورسيتي تیکنیکل ملیسیا ملاک

UNIVERSITI TEKNIKAL MALAYSIA MELAKA